

SOIL MATRIC SUCTION AND ACTIVE ZONE
DEPTH IN OKLAHOMA

By

ER YUE

Bachelor of Science in Meteorology
Nanjing University of Information Science and Technology
Nanjing, Jiangsu, China
2009

Master of Science in Geography
Oklahoma State University
Stillwater, OK
2011

Submitted to the Faculty of the
Graduate College of the
Oklahoma State University
in partial fulfillment of
the requirements for
the Degree of
DOCTOR OF PHILOSOPHY
May, 2017

SOIL MATRIC SUCTION AND ACTIVE ZONE
DEPTH IN OKLAHOMA

Dissertation Approved:

Dr. John Veenstra

Dissertation Adviser

Dr. Avdhesh Tyagi

Dr. Xiaoming Yang

Dr. Tyson Ochsner

ACKNOWLEDGEMENTS

I would like to express my sincere appreciation to my advisor, Dr. John Veenstra, for his continuous help, valuable guidance, and encouragement during the whole process of this work. It was a rewarding experience to work under Dr. John Veenstra's supervision.

I wish to thank Dr. Avdhesh Tyagi for helping me understand the concepts on groundwater hydrology. I would like to extend my gratitude to Dr. Xiaoming Yang, who provided me financial support as well as the guidance on geotechnical engineering. I am particularly grateful to Dr. Tyson Ochsner for providing insightful inputs and suggestions while reviewing this work.

I also wish to thank SoilVision Systems Ltd. for the software support.

Last but not least, I would like to thank my parents and my husband. They have always been supportive and encouraged me to pursue my dreams. This work would not have been possible without them.

Name: ER YUE

Date of Degree: May, 2017

Title of Study: SOIL MATRIC SUCTION AND ACTIVE ZONE DEPTH IN
OKLAHOMA

Major Field: CIVIL ENGINEERING

Abstract: Soil matric suction is an important parameter in unsaturated soils. The shrink-swell properties of expansive soils is controlled by soil matric suction. Matric suction variations cause volume change in expansive soils, which further causes damages to pavements and foundations. This research makes use of field measurements of matric suction obtained from the Oklahoma Mesonet and the Department of Energy's Atmospheric Radiation Measurement network to estimate active zone depth. The long-term matric suction measurement indicated a seasonal pattern of matric suction variation. The shallower depth of soil is more sensitive to the climatic conditions. Two methodologies, empirical equation and numerical analysis, were used to calculate the active zone depth in Oklahoma. The active zone depth is approximately 0.5 to 4 m depending on the soil properties and climatic conditions. The diffusion coefficient and saturated hydraulic conductivity are the two important parameters controlling the active zone depth.

TABLE OF CONTENTS

Chapter	Page
I. INTRODUCTION.....	1
1.1 Background.....	1
1.2 Problem Statement.....	3
1.3 Objectives.....	5
1.4 Methodology.....	7
1.5 Outline.....	8
II. LITERATURE REVIEW.....	10
2.1 Expansive Soils.....	10
2.2 Soil Suction.....	13
2.2.1 Total Suction, Matric Suction, and Osmotic Suction.....	14
2.2.2 Matric Suction Profile and Active Zone.....	16
2.3 Models for Soil Moisture Flow.....	18
2.3.1 Seasonal Variation of Matric Suction.....	19
2.3.2 Soil Water Characteristic Curve.....	22
2.3.3 Numerical Model.....	25
2.4 Diffusion Coefficient.....	27
2.4.1 Diffusion Coefficient from Laboratory Test.....	28
2.4.2 Diffusion Coefficient from Field Estimates.....	31
2.5 Thermal Conductivity Sensor.....	32
2.5.1 Overview of Thermal Conductivity Sensors.....	33
2.5.2 Thermal Conductivity Sensors used by the Oklahoma Mesonet.....	33
2.6 Application of Soil Suction in Engineering Practice.....	36
2.6.1 Crack Analysis.....	37
2.6.2 Slab-On-Ground Foundation.....	37
2.7 Summary.....	40
III. MATRIC SUCTION FROM FIELD MEASUREMENT.....	42
3.1 The Oklahoma Mesonet.....	42
3.2 The DOE ARM Network.....	44
3.3 Climate in Oklahoma.....	47

Chapter	Page
3.4 Oklahoma Expansive Soils	56
3.5 Thermal Conductivity Sensor Installation at Oklahoma Mesonet	53
3.6 Soil Matric Suction derived from ΔT_{ref}	56
IV. DEPTH OF ACTIVE ZONE FROM FIELD DATA	65
4.1 Evapotranspiration of Oklahoma	66
4.1.1 Data and ASCE-PM Method	68
4.1.2 Spatial Distribution of Evapotranspiration	74
4.2 Seasonal Variation of Matric Suction	75
4.2.1 Dry Period	78
4.2.2 Wet Period	83
4.2.3 Average Period	87
4.2.4 Summary	91
4.3 Determination of Diffusion Coefficient	92
4.4 Determination of Active Zone Depth	99
V. NUMERICAL MODELING	104
5.1 Model Description	104
5.1.1 Unsaturated Transient-State Seepage Theory	106
5.1.2 Model Geometry and Boundary Conditions	107
5.1.3 Model Parameters	108
5.2 Modeling Procedure	112
5.3 Modeling Results	113
VI. RESULTS AND DISCUSSION	119
6.1 Comparison between Two Methodologies	119
6.2 Field Measurement for Validation	120
6.2.1 Validation by the Data from the Oklahoma Mesonet	120
6.2.2 Validation by the Data from the ARM Network	125
VII. CONCLUSIONS	130
7.1 Summary	130
7.2 Recommendations for Future Research	132
REFERENCES	134
APPENDICES	141
Appendix A	141
Appendix B	146
Appendix C	149
Appendix D	152

Chapter	Page
Appendix E	156
Appendix F.....	156

LIST OF TABLES

Table	Page
Table 3.1 Sensors' depth at ARM sites.....	46
Table 3.2 Expansive soil classification.....	50
Table 4.1 Relationship between frequent number and potential active zone depth.....	77
Table 4.2 Active zone depth predicted by McKeen and Johnson (1990).....	100
Table 4.3 Active zone depth predicted by El-Garhy and Wray (2004).....	101
Table 5.1 Model parameters	109
Table 5.2 Average values of van Genuchten SWCC parameters for major soil textures	118
Table 6.1 Active zone depth compared with the Mesonet measurement	125
Table 6.2 Active zone depth compared with the ARM measurement	129

LIST OF FIGURES

Figure	Page
Figure 1.1 Moisture content in active zone with and without moisture barrier	4
Figure 1.2 Research methodology	8
Figure 2.1 Relative abundance of expansive soils in Oklahoma	12
Figure 2.2 Theoretical suction profile for a fairly uniform soil	17
Figure 2.3 Seasonal suction variation at soil surface	20
Figure 2.4 Theoretical seasonal suction change in a semi-arid climate	21
Figure 2.5 Fitting function to field suction data	22
Figure 2.6 Typical SWCC for a silty soil	24
Figure 2.7 Geometry of a spherical particle for unsaturated soil	27
Figure 2.8 Test for measuring diffusion coefficient	30
Figure 2.9 The Campbell Scientific 229-L sensor	35
Figure 2.10 Temperature rise vs. heating time of 229-L sensor	36
Figure 2.11 Soil-structure interaction mode	39
Figure 3.1 Map of the Mesonet stations	43
Figure 3.2 Selected Mesonet Stations with Station ID	44
Figure 3.3 Selected ARM sites	46
Figure 3.4 Oklahoma climatic divisions	47
Figure 3.5 Temperature and precipitation in Oklahoma	49
Figure 3.6 Soil information from the USDA web soil survey	51
Figure 3.7 Oklahoma expansive soils	53
Figure 3.8 Vertical profile of moisture sensors	55
Figure 3.9 Daily ΔT_{ref} and monthly precipitation in Stillwater from March to September 2011	56
Figure 3.10 Matric suction profile vs precipitation in Stillwater	60
Figure 3.11 Temporal matric suction variation vs precipitation in Stillwater	64
Figure 4.1 Evapotranspiration vs. matric suction in 2009	73
Figure 4.2 Spatial distribution of average annual evapotranspiration in Oklahoma	74
Figure 4.3 Spatial distribution of daily evapotranspiration in Oklahoma	75
Figure 4.4 Sample curve fitting in Origin software	76
Figure 4.5 Statewide annual total precipitation	78
Figure 4.6 Stations selected to calculate the active zone depth for the dry period	79
Figure 4.7 Curve fitting for dry period	82
Figure 4.8 Spatial distribution of equilibrium matric suction during dry period	83
Figure 4.9 Stations selected to calculate the active zone depth for wet period	84
Figure 4.10 Curve fitting for wet period	86

Figure 4.11 Spatial distribution of equilibrium matric suction during wet period	87
Figure 4.12 Stations selected to calculate the active zone depth for average period...	88
Figure 4.13 Curve fitting for average period	90
Figure 4.14 Spatial distribution of equilibrium matric suction during average period	90
Figure 4.15 Field measurement of matric suction	95
Figure 4.16 Spatial distribution of diffusion coefficient.....	98
Figure 4.17 Spatial distribution of active zone depth	103
Figure 5.1 Model geometry.....	108
Figure 5.2 Spatial distribution of saturated hydraulic conductivity.....	111
Figure 5.3 SWCC for NRMN station	114
Figure 5.4 Matric suction distribution for NRMN station	114
Figure 5.5 Matric suction profile for NRMN station.....	115
Figure 5.6 SWCC for GOOD station.....	115
Figure 5.7 Matric suction distribution for GOOD station	116
Figure 5.8 Matric suction profile for GOOD station	116
Figure 5.9 Spatial distribution of active zone depth during dry period	117
Figure 6.1 Spatial distribution of the 10 selected Mesonet stations	121
Figure 6.2 Matric suction profile for ARNE station.....	122
Figure 6.3 Matric suction profile for LANE station	124
Figure 6.4 Matric suction profile for Byron.....	127
Figure 6.5 Matric suction profile for Cordell.....	128

CHAPTER I

INTRODUCTION

1.1 Background

Environmental conditions have a significant effect on both unsaturated and saturated soils. The moisture flow between the atmosphere and the soil surface is a significant part of many soil mechanics and geotechnical engineering problems (Fredlund et al. 2012). Soil moisture impacts soil surface energy fluxes, such as infiltration and evaporation. Moisture enters the soil surface as liquid by infiltration, and leaves from the soil surface as vapor by evaporation. The variation of moisture content in soil is highly related to environmental factors, such as temperature, precipitation, as well as soil properties, such as soil types, Atterberg limits, and soil suction. Improving the understanding of environmental interactions with soils can provide solutions to a variety of geotechnical engineering problems. Many constructions of pavements and foundations cannot be designed without evaluating the moisture fluxes at the soil surface (Wilson et al. 1997). The movement of water significantly influences soil profile, especially expansive soil profile. A well-planned soil and environmental investigation is a virtual prerequisite to a safe and economical design of structures.

Expansive soils with the potential to shrink or swell are distributed over most of the United States. Much structural damage occurs in areas where expansive soils are known to exist. The problems associated with expansive soils are a result of moisture change in soils due to both environmental effects and human activities. When the moisture condition changes in expansive soils, a differential soil movement occurs (Mitchell 1979). As a result, any geotechnical site investigation for a building or pavement on expansive soils must include the evaluation of shrink-swell properties of the soil and environmental conditions that contribute to soil moisture flow (Nelson and Miller 1992). The damage to structures caused by expansive soils costs house owners and the government billions of dollars each year (Kerrane 2004), so predicting expansive soil behavior and avoiding damage becomes necessary and important. The shrink-swell properties of expansive soils are controlled by soil suction. The theory of soil suction has been used by geotechnical engineers for solving the problems caused by expansive soils for many years. In soil physics, soil suction is defined as the potential energy of water in soil relative to pure water as a reference state. In geotechnical engineering, soil suction is a measurement of soils' need for water. Soil suction increases when soil moisture content decreases, and, conversely, soil suction decreases when soil moisture content increases. At the same time, the expansive soils absorb water molecules and expand when they get wet, and, conversely, the expansive soils shrink and form cracks when they become dry. The zone in which swelling and shrinkage occurs in wet and dry periods or the zone of soil suction variation is referred to as the active zone. The depth of the active zone varies with season and location (Bell 1999). The evaluation of seasonal soil suction variations is critical to the analysis of volume change of expansive soils. An important application of soil suction in engineering practice is predicting the heave of expansive soils. The heave is the vertical swelling of

expansive soils in response to wetting conditions. The heave prediction should be the first step in designing foundations and other ground supported structures (Nelson et al. 2014).

1.2 Problem Statement

Expansion in soils occurs when soil moisture content increases in the unsaturated zone (upper few meters of ground surface) as a result of changes in climatic conditions and environmental factors. The unsaturated zone is the part of the subsurface above the groundwater table. This zone contains soil, rock, air as well as water. The unsaturated zone is the place where water moves from the land surface to the aquifer. In geotechnical engineering, the active zone stays within the unsaturated zone. Figure 1.1 illustrates the active zone and how it relates to seasonal fluctuation of moisture. The shrink-swell usually happens within the active zone. When a lightly-loaded structure is built on expansive soils, the climatic conditions greatly impact on the distress provided by the soils. Increased moisture content in soils will cause soils to expand and increase the lateral pressure applied to the foundation (Bobrowsky 2013). During the dry season, evapotranspiration from the soil surface and vegetation cover will take the moisture out of soils and soil cracks will form. The depth of surface cracks in expansive soils influences the depth of the active zone. During the wet season, precipitation and surface runoff can fill the cracks and even travel through the cracks. The water that travels beneath a pavement will remain there and soak into the soil on each side of the crack, and eventually cause swelling.

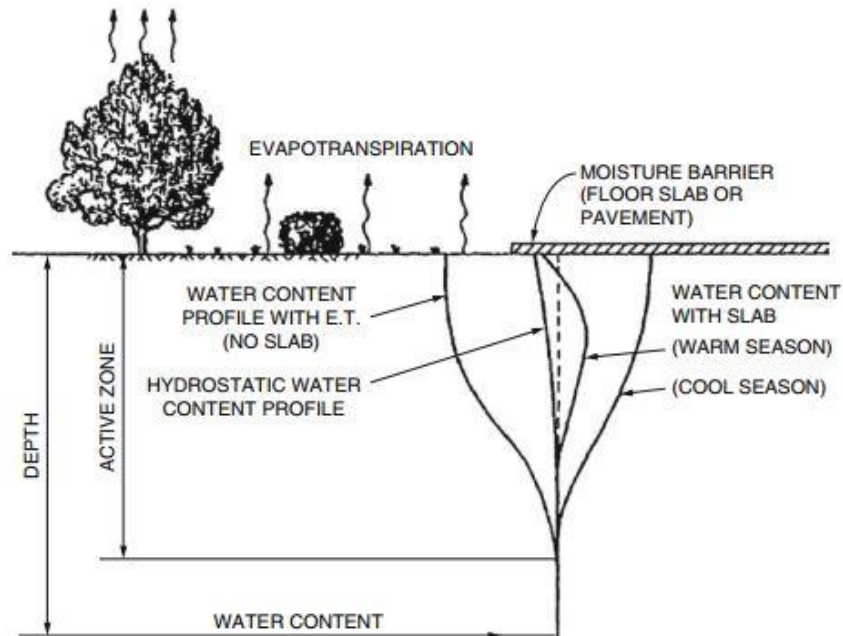


Figure 1.1 Moisture content in active zone with and without moisture barrier
(Nelson and Miller 1992)

Oklahoma is a region with complex climatic conditions and geological features, consisting of mountains, streams, and lakes in different parts of the State (Johnson 2008). The climate of Oklahoma ranges from humid subtropical in the east to semi-arid in the west (The Oklahoma Climatological Survey 2011). The terrain of Oklahoma varies from nearly flat in the west to rolling in the east, and it has a general slope upward from east to west of the State. Based on the soil survey data from the Natural Resources Conservation Service (NRCS), western Oklahoma contains brown to light-brown loamy soils with clay; central Oklahoma has the dark loamy soils with clayey to loamy subsoils; soils in eastern Oklahoma are often brown to light-brown silty soils with clayey subsoils (Carter and Gregory 2008). More than 75% of Oklahoma bedrock units are potential sources for expansive soils with shrink-swell characteristics.

The volume change of expansive soils typically happens in regions with dry periods followed by wet periods. The precipitation in Oklahoma varies by season. Winter is the season with the lowest rainfall and spring is the season with the highest rainfall (Johnson 2008). Due to Oklahoma's soil and climatic characteristics, the problem caused by expansive soils is one of the main geologic hazards in Oklahoma. As a result, it is critical to characterize Oklahoma's soil moisture and suction properties and how they change in response to climatic conditions.

The state of Oklahoma has a world-class network of environmental monitoring stations – the Oklahoma Mesonet, which consists of 120 automated stations collecting a variety of real-time hydrometeorological and soil parameters. Due to the need for soil moisture measurement in Oklahoma, the Oklahoma Mesonet installed sensors at four depths (5 cm, 25 cm, 60 cm, and 75 cm) at some stations to measure soil moisture conditions since 1996 (Illston et al. 2008). Soil matric suction can be derived from soil moisture measurement, thus measured soil moisture data from the Oklahoma Mesonet can be applied in geotechnical engineering practice. In addition to the data from the Oklahoma Mesonet, supplementary data from the Department of Energy's Atmospheric Radiation Measurement (DOE ARM) network were used in this research, since the ARM network has the soil moisture sensors installed up to 1.75 m depth in selected stations in Oklahoma. The investigation of historical soil moisture and matric suction conditions is necessary in geotechnical design procedure. For example, the foundation design for expansive soils involves the evaluation of the active zone depth, which can be determined from climatic and soil suction data.

1.3 Objectives

The active zone depth is a fundamental parameter for foundation design. The capability to predict moisture movement in the soil is critical for engineers to formulate a picture of what

the soil surface and structure interface will be. Soil-structure interaction should always be considered in foundation and pavement design. If environmental conditions and the groundwater table stay constant long enough to reach equilibrium conditions, soil matric suction will decrease linearly from the soil surface with maximum suction to the groundwater table with zero suction. However, in reality, this condition rarely occurs because environmental conditions are changing all the time (Morris et al. 1992). Geotechnical engineers are interested in the soil moisture/matric suction distribution when dealing with expansive soils. Based on the field data and existing theoretical models, geotechnical engineers are capable of predicting expansive soil behaviors. The objectives of this study are:

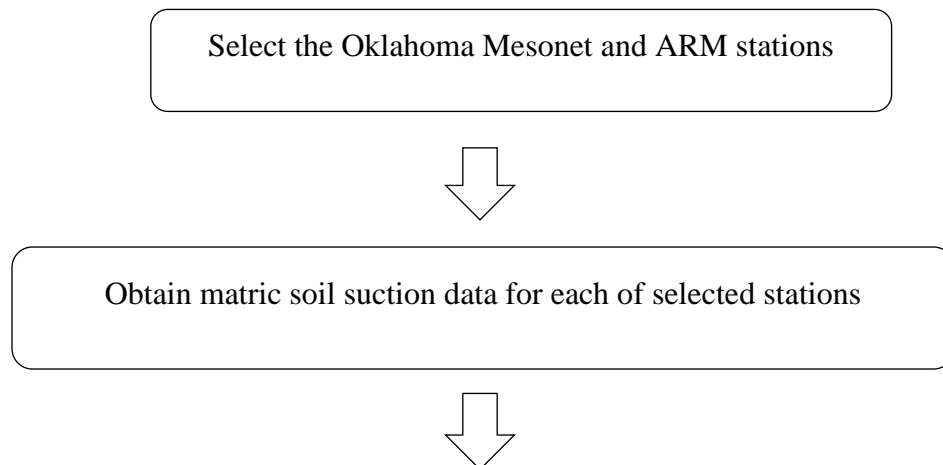
1. Utilize the long-term measured in-situ soil matric suction data from the Oklahoma Mesonet and the ARM network to evaluate matric suction profile and pattern of temporal matric suction variation under different climatic conditions.
2. Investigate active zone depth by using the empirical equation, which requires the evaluation of field measurement of soil matric suction and diffusion coefficient.
3. Evaluate how the climatic conditions can affect the active zone depth.
4. Conduct numerical modeling using SVFlux software to evaluate fluctuations of matric suction within a soil profile.

SVFlux software (part of the SVOOffice5 software package) was developed by SoilVision Systems Ltd. (Saskatoon, SK, Canada). SVFlux makes the use of FlexPDE finite element solver to solve partial differential equations (Thode 2004). The numerical model conducted in this research evaluates the moisture conditions under covered areas. The objectives of numerical modeling are to: (1) analyze the unsaturated flow under different soil properties and

boundary conditions; (2) determine the matric suction profile and active zone depth; and (3) compare the results from numerical models to the results obtained from the empirical equation.

1.4 Methodology

In order to achieve the objectives of this research, two methodologies were applied to evaluate the active zone depth. The first methodology calculates the active zone depth using the empirical equation proposed by McKeen and Johnson (1990). In this methodology, the active zone depth is a function of seasonal soil matric suction variation, climatic frequency, and field diffusion coefficient. The second methodology analyzes the slab-on-grade performance on expansive soils with unsaturated flow by using numerical modeling software SVFlux. This methodology predicts matric suction profile during a seepage process. The suction profile can be further used to determine the active zone depth. To determine the spatial distribution of the active zone depth and other related parameters, ArcGIS software was used to create choropleth maps. The choropleth map offers an easy way to display how a measurement varies across a geographic area or it shows the level of variability within a region. The flow chart below summarizes the methodology used in this research.



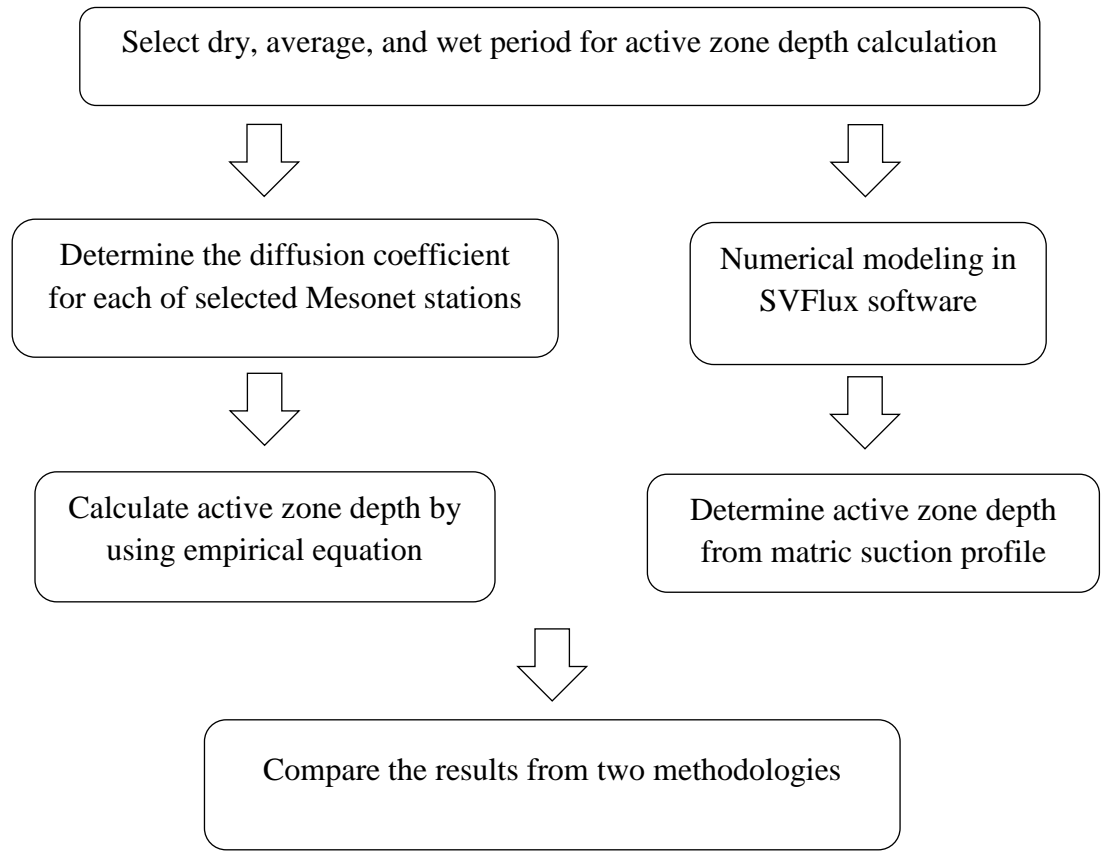


Figure 1.2 Research methodology

1.5 Outline

Chapter 1 introduces the research background, objectives, methodology, and outline of the dissertation.

Chapter 2 reviews the literature on soil suction and active zone depth. The diffusion coefficient is then explained based on laboratory tests and field estimates. The field measurement of matric suction and its application in engineering practice are also discussed.

Chapter 3 introduces the Oklahoma Mesonet and the ARM network. This chapter explains how these networks work and how the parameters, including climatic data, soil properties, and matric suction, are measured in these networks.

Chapter 4 provides the procedures of calculating active zone depth by using an empirical equation. The procedures include determination of evapotranspiration, seasonal matric suction variation, and diffusion coefficient.

Chapter 5 introduces the numerical modeling of the unsaturated flow by using the SVFlux software. Matric suction profile and active zone depth are determined from the models. Comparison is made between the results from empirical equation and numerical modeling.

Chapter 6 presents the results obtained from Chapter 4 and 5. The results are also compared with the field matric suction measurements.

Chapter 7 summarizes the findings of the research and recommendations for future work.

CHAPTER II

LITERATURE REVIEW

2.1 Expansive Soils

Soils that tend to change their volume as a result of change in their moisture content are known as expansive soils. Expansive soils are formed by a mixture of smectite clay minerals, such as montmorillonite and bentonite. Expansive soils are distributed all over the world, in the United States, Egypt, Australia, China, South Africa, etc. (EI-Garhy and Wray 2004). Dry expansive soils will increase in volume by absorbing water. Water molecules consist of two hydrogen atoms and one oxygen atom. Within a single water molecule, the electrical charges are not evenly distributed. The two positively charged hydrogen atoms are grouped together on one side of the negatively charged oxygen atom. The electrical structure of water molecules enables them to become attached to the clay crystals (Foundation Repair Guide 2007). When water is absorbed by expansive soils, the water molecules are drawn into gaps between soil particles, leading to an expansion of soil volume. Conversely, wet expansive soils will decrease in volume when they become dry. The damage of expansive soils causes a range of risks and impacts in the structures, particularly pavements and foundations of light buildings. One-story

buildings are more subjected to the damages of expansive soils than multi-story buildings, which are heavy enough to sustain swelling pressures. However, if multi-story buildings are constructed on wet expansive soils, they may be damaged by the shrinkage of soils due to the moisture loss such as evaporation. The problems of expansive soils are usually overlooked since they take several years to cause damage (Buhler and Cerato 2007). In the United States, the damages of expansive soils to the structures cost \$2.3 billion each year, which is more than twice the damages from other hazards, such as floods, hurricanes, tornadoes, and earthquakes (Kerrane 2004).

The formation of cracks is a key problem to expansive soils. Many geotechnical constructions are affected directly or indirectly by the cracks in drying soils. When the expansive soils lose water and shrink, cracks will form because the tensile stress increases to exceed the tensile strength of the soil particles. Cracks destroy the stability and integrity of soils by decreasing soil bearing capacity. Two main factors can affect crack development. The first factor is the montmorillonite content in expansive soils. The montmorillonite has the stronger hydrophilic ability compared to other clay minerals (Shi et al. 2014). Therefore, the expansive soils that contain a high amount of montmorillonite can shrink or swell up to 1.5 to 2 times their original volume after changing the moisture content. The second factor is the combined effect of environmental conditions, such as temperature, precipitation, wind speed, solar radiation, and evaporation. The exchange of moisture between the soil surface and the environment is one of the main reasons that cause cracks in expansive soils. However, this potential of cracking only occurs in regions that have wet seasons followed by extended dry seasons. In another word, if an area has low

annual precipitation and its climate is relatively dry throughout the year, then there is less chance for a large volume change in expansive soils (Post-Tensioning Institute 1980).

Expansive clay soils are found in many regions in the Great Plains and states in the western United States. More than 75% of Oklahoma's landscape contains possible sources for expansive soils (Luza and Johnson 2005). The climate of Oklahoma ranges from humid subtropical in the east to semi-arid in the west and the amount of precipitation in Oklahoma varies by season, which means periods of drought are followed by periods of precipitation. As a result, the potential of swelling or shrinking of expansive soils is one of the geologic hazards in Oklahoma. Figure 2.1 shows the relative abundance of expansive soils in Oklahoma. Expansive soils are most abundant in areas colored red and decrease in blue areas. Areas which contain a small amount of expansive soils are not colored. Recently, the extremely hot and dry summers of 1998, 2005, 2006, and 2011 in Oklahoma caused soil shrinkage that led numerous foundation failures, pipeline breaks, and pavement cracks (Flanagan & Associates, LLC 2013).

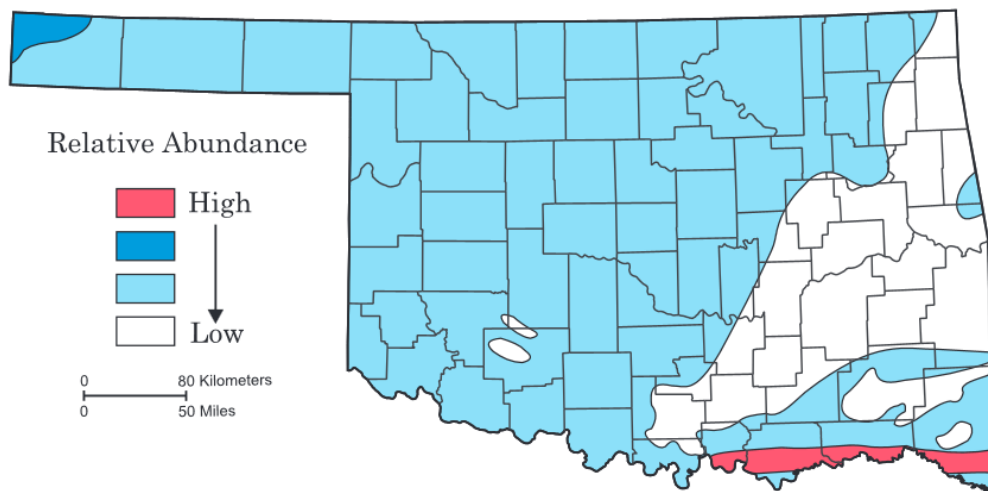


Figure 2.1 Relative abundance of expansive soils in Oklahoma (Luza and Johnson 2005)

Geotechnical engineers have developed a variety of theories and models to predict the volume changes of expansive soils. One of the most common approaches is to define the initial and final soil stress. An important soil parameter – matric suction – is widely used to define the state of stress (Nelson and Miller 1992). The incorporation of soil suction into soil stress can be used to predict the direction and rate of moisture flow as well as the volume change of expansive soils. The analysis of soil suction is highly involved in the studies of cracks in expansive soils (Auvray et al. 2014; Morris et al. 1992). The suction variation cycles in response to the wetting and drying cycles of the environment influence the formation of cracks. Once the variations of soil suction have been predicted, they can be used to analyze soil-structure interaction and moisture flow in soil (Lytton 1977).

2.2 Soil Suction

Soil suction is one of the most important and widely used variables in unsaturated soil mechanics. The theory of soil suction was developed in the discipline of soil physics in the early 1900s, and it was derived from the concept of soil water potential. Soil water potential indicates the potential energy of water per unit volume of soil relative to pure water in reference conditions. The total water potential has four main components: (1) matric potential, caused by the forces between water molecules and the solid particles as well as attractions among water molecules; (2) osmotic potential, a result of the attraction between a water molecules and cations and solutes in the soil solution; (3) gravitational potential, caused by the force of gravity acting on soil water; and (4) pressure potential, due to the water under mechanical pressure. Other potentials may be defined as needed, such as overburden potential, which is similar to pressure potential. It occurs when soil matrix applies pressure on water (Kirkham 2014). In geotechnical engineering, the water potential

is known as suction and it is expressed as a positive value. However, a positive value of soil suction still indicates a negative pore water pressure (Nelson and Miller 1992).

2.2.1 Total Suction, Matric Suction, and Osmotic Suction

The total suction or free energy in soil can be measured in terms of relative humidity in the air adjacent to soil-water. It can be found in soil that lies above the water table, including natural level ground or slopes, compacted soils, and other earth structures (Ridley et al. 2003). The total suction can be calculated from the following equation (Lytton 1994):

$$h = \frac{R T}{m g} \ln \frac{H}{100} \quad (2.1)$$

where h = the total suction measured in cm of water

R = universal gas constant = $8.314 * 10^7$ ergs-K/mol

T = absolute temperature, K

g = gravitational constant = 981

m = mass of 1 mol of water = 18.02 gm/mol

H = relative humidity, %

Total suction is zero when relative humidity is 100%. A relative humidity smaller than 100% indicates suction in soils. The total suction gradients within the soil profile control the diffusion of moisture through unsaturated soil. A decrease in soil suction results in an increases in soil moisture content. Typical units of suction include pF, psi, kgf/cm², kPa, bars, and atmos. Usually suction is measured in pF scale. The conversion between centimeters of water and pF is (Lytton 1994):

$$\text{Suction in } pF = \log_{10} |h| \quad (2.2)$$

where h = the total suction measured in cm of water

The total suction in unsaturated soil has two components: matric suction and osmotic suction. Matric suction is defined as the pressure difference between pore-air and pore-water pressure ($u_a - u_w$) in soil. Osmotic suction results from the forces exerted on water molecules from the dissolved salts in the pore fluid. In most geotechnical practice, osmotic forces in the soil are fairly constant and there is no significant change in osmotic suction. Therefore, changes in total suction are mainly due to changes in matric suction (Nelson and Miller 1992).

Geotechnical engineers are primarily interested in matric suction because matric suction influences many phenomena and processes in unsaturated soil. It has been proved that matric suction is a stress state variable controlling the mechanical behavior of unsaturated soil (Fredlund 1992). Matric suction can be affected by several factors, such as environmental and moisture conditions, ground surface conditions, the depth of the water table, and soil permeability. Matric suction is generally high in dry seasons and low in wet seasons. Hence, the moisture flow through soils is from a state of low suction (high moisture content) to a state of high suction (low moisture content). The matric suction beneath an uncovered surface varies greater between wet and dry seasons than that beneath a covered surface. The depth of the water table can also affect the magnitude of the matric suction. The equilibrium matric suction near the surface is higher when the water table is deeper (Durkee 2000).

2.2.2 Matric Suction Profile and Active Zone

A suction profile is the matric suction measured at intervals of depth down the soil profile, and it indicates the relationship between the state of suction and depth. It is required to estimate or determine the initial soil suction profile when analyzing a geotechnical engineering problem. Figure 2.2 shows the idealized soil suction profile. The suction profile is significantly affected by ground surface conditions, climatic conditions, and vegetation type, and it can vary significantly throughout each year (Fredlund et al. 2012). Dry and wet cycles cause the variations of suction profile, particularly near the ground surface. If the ground surface loses moisture (e.g., evaporation), the suction profile will be drawn to the left. If the ground surface gains moisture (e.g., precipitation and infiltration), the suction profile will be drawn to the right. The suction profile beneath a covered surface (e.g. pavement and foundation) is more stable with respect to time than that of beneath an uncovered surface. A location where expansive soils are abundant and in which the climate has dry/wet seasons followed by wet/dry seasons will have the type of suction profile shown in Figure 2.2.

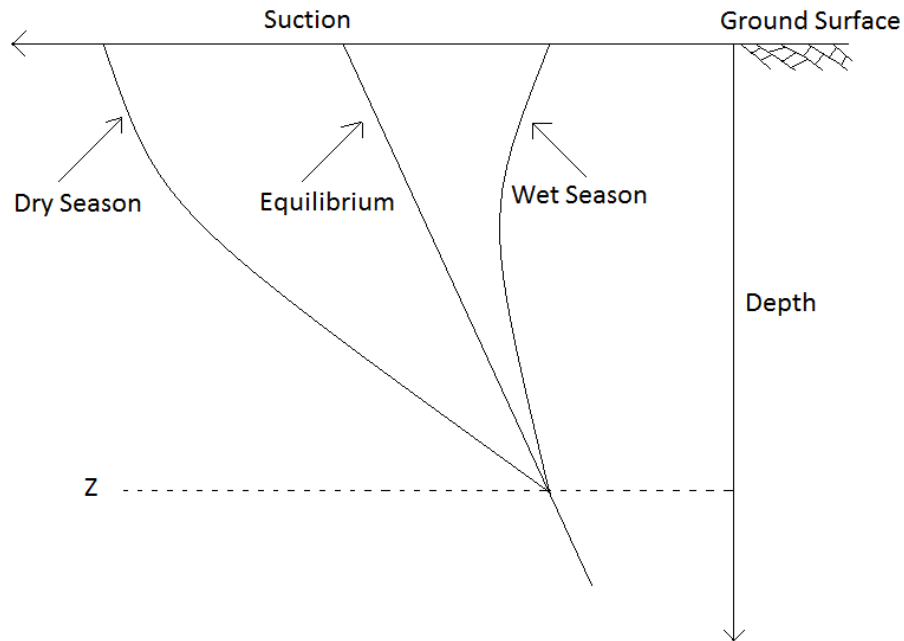


Figure 2.2 Theoretical suction profile for a fairly uniform soil

If environmental conditions and groundwater table stay constant long enough to reach equilibrium conditions, soil suction will decrease linearly from the maximum suction at the soil surface to zero at groundwater table. However, in reality, this condition rarely occurs because environmental conditions are changing all the time (Morris et al. 1992). It is more common to see that maximum suction (occurs in the dry season) and minimum suction profiles (occurs in the wet season) begin at the soil surface, where the water table is deep, and decrease at an exponential rate toward the equilibrium suction. The variation of suction would range between the maximum and minimum values. At a certain depth, the variation of the suction is small enough that it may have little effect on soil moisture fluctuation. In Figure 2.2, the area between ground surface and depth of Z is called active zone. The active zone is the zone of soil that is contributing to its shrinking or swelling. Below the active zone, no significant moisture variation occurs due to climatic conditions (McKeen and Johnson 1990). It has been proved that most of moisture movements occur

near the soil surface or within the active zone. Through the active zone, water vapor is slowly released to the atmosphere. Establishing the depth of active zone is essential in the analysis of volume change of expansive soils. Evaluating the active zone by examining soil suction profile is one of the applications of soil suction theory in engineering practice (Nevels 1995). Similar to suction profile, the active zone changes with time as moisture changes within soil. For different research emphases, the active zone is also called zone of seasonal moisture fluctuation, depth of wetting, and depth of potential heave. The depth of active zone ranges from a few feet (e.g. 5 or 6 feet) to more than 30 feet, depending upon the soil type, climatic conditions, and vegetation type (Nelson et al. 2001).

Below the active zone, suction remains constant and an equilibrium suction exists when the climate is stable. These maximum and minimum suctions will approach the equilibrium suction at the depth of the active zone. The equilibrium suction is the suction when there is a steady flow of moisture in soil. Under the equilibrium condition, neither swelling nor shrinking occurs in soil (Lytton 1977). When soil suction is under the state of equilibrium, all variables affecting soil suction remain constant except the climate-related variables (Wray 1987).

2.3 Models for Soil Moisture Flow

The interest in research on expansive soils in recent years has resulted in numerous methods being proposed for the prediction of matric suction. The prediction of soil suction based on the climatic patterns and numerical models is an important approach for the analysis of heave/shrink of expansive soils. By knowing the seasonal soil moisture movement under soil suction change, the foundation problems in expansive soils could be

overcome. During the last 40 years, a number of models have been developed for predicting the soil moisture flow (Mitchell 1979, Lytton 1994, Fredlund and Vu 2003).

2.3.1 Seasonal Variation of Matric Suction

Mitchell (1979) analyzed seasonal soil suction variation in expansive soils. He pointed out that the climate, drainage, and vegetation type controlled the moisture flow at soil surface. Mitchell's research indicated that the suction change is a periodic function of time. The suction change at the soil surface is given by:

$$u(0, t) = U_e + U_0 \cos(2n\pi t) \quad (2.3)$$

where $u(0, t)$ = suction at the soil surface, pF or kPa

U_e = the equilibrium suction, pF or kPa

U_0 = the amplitude of suction variation, pF or kPa

n = frequency number, which is the number of cycles of wetting and drying in a year

The implication of Equation 2.3 has been confirmed by the measurements of soil suction in Adelaide, Australia. Figure 2.3 shows the soil suction variation with a function of $u = 4.0 + 1.5 \cos(2n\pi t)$. The climate in Adelaide is relatively dry from October to April and wet from May to September. As a result, it is seen from Figure 2.3 that surface suction is high from October to April and low from May to September.

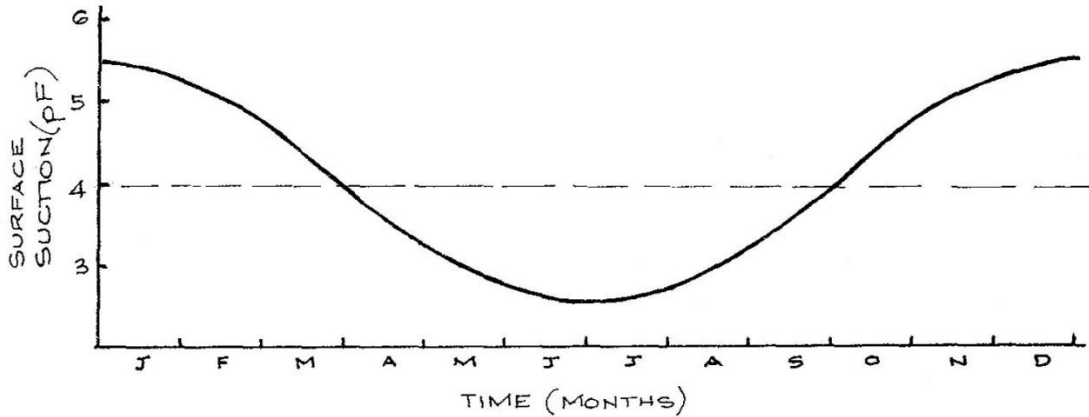


Figure 2.3 Seasonal suction variation at soil surface (Mitchell 1979)

Based on Equation 2.3, Mitchell developed the suction $u(y, t)$ at any depth y :

$$u(y,t) = U_e - U_0 \exp \left\{ -\left[\left(\frac{n\pi}{\alpha} \right)^{0.5} y \right] \right\} \cos \left\{ 2n\pi t - \left[\left(\frac{n\pi}{\alpha} \right)^{0.5} y \right] \right\} \quad (2.4)$$

where $u(y,t)$ = soil suction at depth y (m or ft) and time t (days), pF or kPa

α = diffusion coefficient, cm^2/s

Equation 2.4 indicates that the suction at any depth depends on the diffusion coefficient. The diffusion coefficient is not constant in soil. As a result, the suction profile can be determined by solving the diffusion coefficient. Section 2.4 will explain the diffusion coefficient in detail. Based on the effect of climate on suction variation and soil properties, Mitchell analyzed the suction profile for arid, semi-arid and sub-humid climates, and found a very consistent trend that could be modeled for each climate type. Figure 2.4 shows a theoretical suction profile in a semi-arid climate. The active zone depth is approximately 3 m. The large seasonal movement of the suction is associated with an equal distribution of wet and dry periods in semi-arid climate.

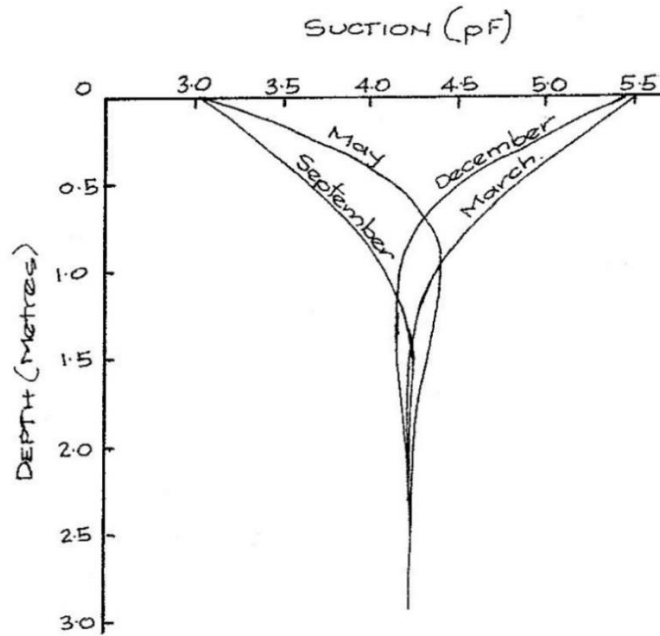


Figure 2.4 Theoretical seasonal suction change in a semi-arid climate (Mitchell 1979)

Mitchell's analysis was developed based on fundamental soil properties, so it is capable of showing the seasonal suction variation due to the seasonal soil moisture variation. Mitchell's method has been widely used in suction research. McKeen and Johnson (1990) modified Mitchell's model (Equation 2.3) and introduced a back calculation procedure. Back calculation means to take the result and see what can be done first, then work backwards to get something similar to the existing result. They compared results between the field suction data measured in Dallas/Ft. Worth area from October 1978 to June 1980 and suction value predicted by:

$$u(0, t) = \sin(2n\pi t - p\pi) U_0 + U_e \quad (2.5)$$

where p = a phase shift to match the starting point of the fitting process.

To build the equation, they first estimated the value of p to match the data at zero time.

Values of U_0 and U_e were estimated based on the evaluation of field data. The value of n

was estimated by computing suction at various time. Once the value of n was established, the values of U_0 and U_e were modified to further increase the correlation coefficient. Figure 2.5 shows the result of result of comparison between the measured data and Equation 2.5. The suction data was measured at a depth of 15 cm. McKeen and Johnson (1990) further applied the suction variation to calculate active zone depth and edge moisture penetration distance. They found that the active zone depth depends on maximum and minimum suction change, climatic conditions, and diffusion coefficient in the field.

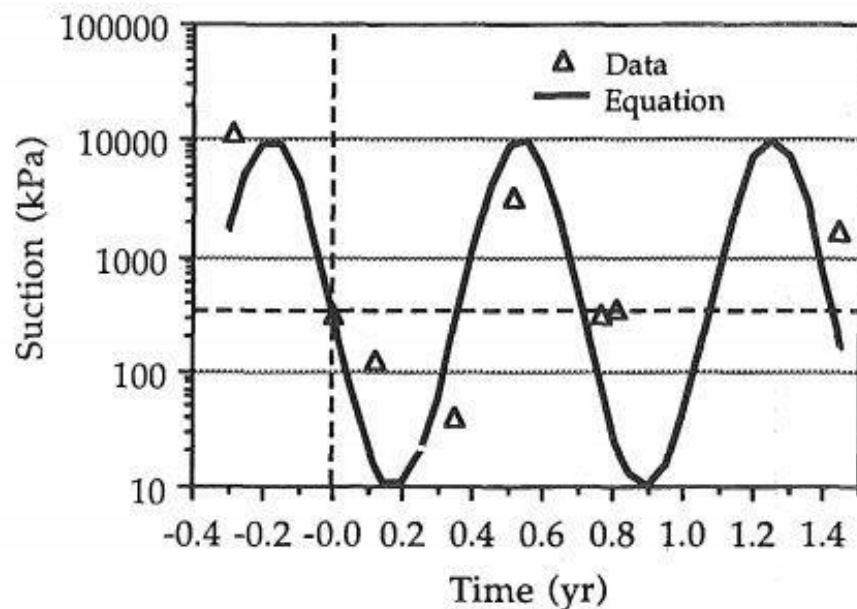


Figure 2.5 Fitting function to field suction data (McKeen and Johnson 1990)

2.3.2 Soil Water Characteristic Curve

Soil water characteristic curve (SWCC), also called water retention curve, indicates the relationship between soil water content and matric suction. In soil science, volumetric water content is commonly used. In geotechnical engineering, gravimetric water content is commonly used (Fredlund and Xing 1994). There are two ways to obtain SWCCs: (1) desorption, by gradually drying the initially saturated sample through applying increasing

suction; and (2) sorption, by gradual wetting the initially dry sample through reducing suction (Hillel 2004). Because of the difficulties in measuring sorption (wetting) curve, the desorption (wetting) portion of the curve is usually measured in the laboratory. The SWCCs are extensively used in agricultural and engineering practice to estimate unsaturated soil properties. However, the estimation of soil suction from SWCCs has been discouraged mainly due to the hysteretic phenomenon of drying and wetting SWCCs (Fredlund et al. 2011). Hysteresis is the phenomenon when the drying and wetting curves of the same soil differ. In another word, at any given water content higher suction exists in drying process than wetting. The hysteresis effect is caused by (1) irregularly shaped voids in the soil; (2) the contact angle effect; (3) entrapped air in the soil; (4) swelling or shrinking in soil structure (Hillel 2004).

Figure 2.6 shows a typical SWCC for a silty soil. The saturated volumetric water content (θ_s), residual volumetric water content (θ_r), and air-entry value (AEV) are three important features in SWCC. The saturated water content is the maximum amount of water stored in the soil. The residual water content is the water content at which a large matric suction change is required to remove additional water from the soil. The air-entry value is the matric suction at which air starts to enter the largest pores of the soil (Fredlund and Xing 1994).

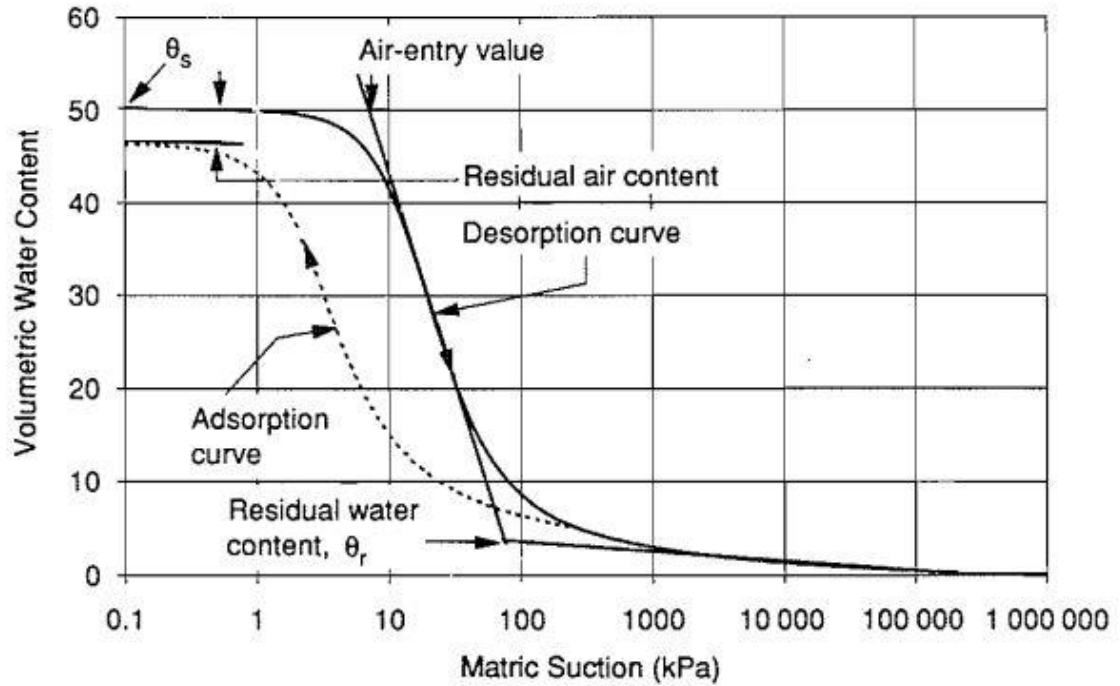


Figure 2.6 Typical SWCC for a silty soil (Fredlund and Xing 1994)

Numerous empirical equations have been developed to simulate the SWCC. Widely used equations include: Gardner fit (1958), van Genuchten fit (1980), and Fredlund and Xing fit (1994). In this research, the van Genuchten fit (1980) is used for all soils, since the Oklahoma Mesonet has the van Genuchten SWCC parameters for all the Mesonet stations. The van Genuchten equation for the relationship between matric suction and water content is expressed as:

$$\Theta = \frac{1}{[1 + (\alpha \cdot \psi)^n]^m} \quad (2.6)$$

where Θ = effective saturation

ψ = matric suction

α , n , m = van Genuchten parameters

2.3.3 Numerical Model

Modeling is a useful tool for engineering design and practice. A model is an approach to simplify real problems. With the development of computational technology, many numerical models and software programs have been developed for various engineering applications. Numerical models are applied in three main categories: interpretation, design, and prediction (Barbour and Krahn 2004). A variety of software, such as SEEP/W, SoilVision, and SEEP2D, have been developed for analyzing groundwater seepage and pore-water pressure dissipation problems within the soil. These software packages can be used in both steady and transient seepage analysis. Seepage analysis is an important part in geotechnical engineering, and it is required in soil volume change prediction, slope stability analysis, and structure design. Solving seepage problems for saturated-unsaturated soil systems involves two non-linear soil property parameters – coefficient of permeability (also known as hydraulic conductivity) and water storage. Several programs have been developed for solving initial and boundary conditions (Thieu et al. 2001).

Zhang et al. (2004) used the software SEEP/W to conduct numerical models to analyze steady state and transient seepage conditions on a slope. They found that under steady state conditions, the matric suction is mostly affected by moisture flux at the ground surface. Under transient conditions, the matric suction depends on rainfall, saturated coefficient of permeability, and soil water storage. Gitirana et al. (2005) used two seepage analysis software packages, SVFux and Vadose/W to verify the validity of runoff and infiltration calculations. SVFlux applied an automatic adaptive mesh technique, which is sensitive to hydraulic conductivity and matric suction. Vadose/W is capable of computing infiltration and runoff based on soil surface conditions. They conducted three problems

with different climatic conditions using these two software packages and the results showed that the runoff is sensitive to the time-stepping methods and upper boundary conditions.

In addition to use existing software to build numerical models, some studies adopt mathematical equations to solve unsaturated soil problems. Farouk et al. (2004) introduced a numerical model to predict the matric suction of unsaturated soils that have low water contents. Their model made use of the surface tension and the capillary action of the water between the soil particles to predict the relationship between the water content and matric suction. The shrinkage of expansive soil is associated with capillarity. As water evaporates from the soil surface, capillary tension is produced through the pore water and developed from a pressure difference across the air-water interface. During the shrinkage process, soil volume change occurs when capillary tension is greater than effective stress within soil particles (Clarke and Nevels 1996). Based on the Laplace equation of capillarity, the matric suction for water in contact with spherical soil particles (shown in Figure 2.7) is

$$u = T_s \left(\frac{1}{r_1} - \frac{1}{r_0} \right) \quad (2.7)$$

where, u = matric suction

T_s = surface tension of water

r_0, r_1 = radii of curvature

The volumetric water content can be derived as

$$\theta_w = \frac{0.375 n_c V_m}{\pi R^3 (1+e)} \quad (2.8)$$

where, n_c = the number of points of contact between particles

$V_m = \text{Vol.A} - \text{Vol.B} - 2\text{Vol.C}$ (Vol.A, Vol.B, and Vol.C are volumes at the points of contact between two particles as shown in Figure 2.7 (a))

e = void ratio

R = radius of sphere

This proposed model gave good results on coarse-grained soils and it can be used to determine the range of matric suction. Moreover, this model can be further used to predict SWCC based on the relationship between matric suction and water content (Farouk et al. 2004).

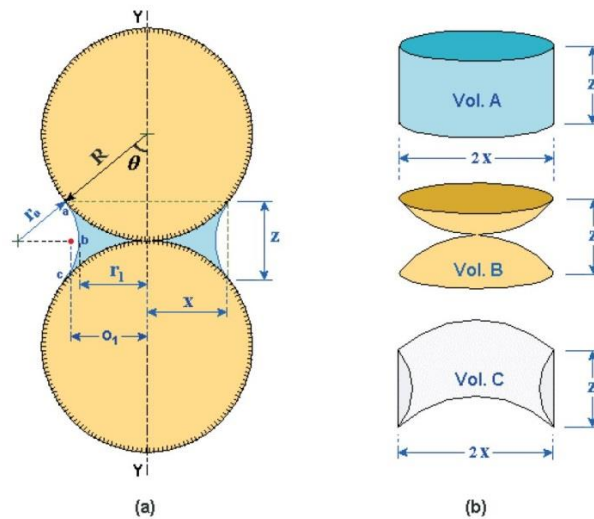


Figure 2.7 Geometry of a spherical particle for unsaturated soil: (a) water menisci between two particles; (b) volumes used to determine water content (Farouk et al. 2004)

2.4 Diffusion Coefficient

Diffusivity is a measure of the rate at which particles, fluids, gas, or heat can spread. In the discipline of unsaturated soil, diffusivity is represented by diffusion coefficient, α , a parameter used to characterize moisture movement in soil. The diffusion coefficient is a

function of SWCC and unsaturated soil permeability, usually expressed in cm^2/sec (Lytton et al. 2006). The diffusion coefficient controls moisture flow conditions within a soil mass in response to suction variations. Accurate estimates of the diffusion coefficient of soil water are important in understanding and predicting the movement of moisture in unsaturated soil.

2.4.1 Diffusion Coefficient from Laboratory Test

Mitchell (1979) developed two laboratory tests, the soaking (wetting) test and evaporation (drying) test, to determine the diffusion coefficient through unsaturated soil using a tube sample of soil. Mitchell (1979)'s tests were based on the theory of one dimensional flow of moisture through unsaturated soil:

$$\frac{\partial^2 u}{\partial x^2} = \frac{1}{\alpha} \frac{\partial u}{\partial t} \quad (2.9)$$

where u = total suction, pF

x = direction of moisture flow

α = diffusion coefficient of the soil, cm^2/sec

t = elapsed time

Equation 2.9 indicates that the distribution of total suction in soil is a function of space, time, as well as diffusion coefficient. As a result, the diffusion coefficient of unsaturated soil can be determined by measuring the rate of suction change with time in soil. However, Equation 2.9 does not consider the effect of gravity. In the drying test, one end of the cylindrical soil sample is exposed to the atmosphere while the remaining soil surfaces are

sealed. A psychrometer is inserted into the soil sample to measure the change in total suction as moisture evaporates from the exposed surface. The procedure of the wetting test is similar to the drying test. Instead of being exposed to the atmosphere, one end of soil sample is exposed to the liquid in the wetting test (Mitchell 1979).

Mitchell (1979)'s laboratory measurements of diffusion coefficients have been widely used in later research. Aubeny and Lytton (2004) built a moisture diffusion model to study slope failures in high plasticity clays. They utilized a drying test developed by Mitchell (1979) to estimate the diffusion coefficient of medium-to-high plasticity clays. Figure 2.8 shows their test design. During the drying test, six psychrometers are inserted into an undisturbed cylindrical soil sample. The suction measured during the test can be used to estimate the diffusion coefficient based on Equation (2.9). Aubeny and Lytton (2004) performed tests on seven samples obtained from Waco, Texas. The test results indicated that the diffusion coefficient ranged from $0.04 \text{ m}^2/\text{year}$ to $0.147 \text{ m}^2/\text{year}$, with an average $0.085 \text{ m}^2/\text{year}$ and a standard deviation of $0.041 \text{ m}^2/\text{year}$. The measurements of the diffusion coefficient in their research appeared to be consistent with the period of the slope failures when soil cracks were taken into consideration.

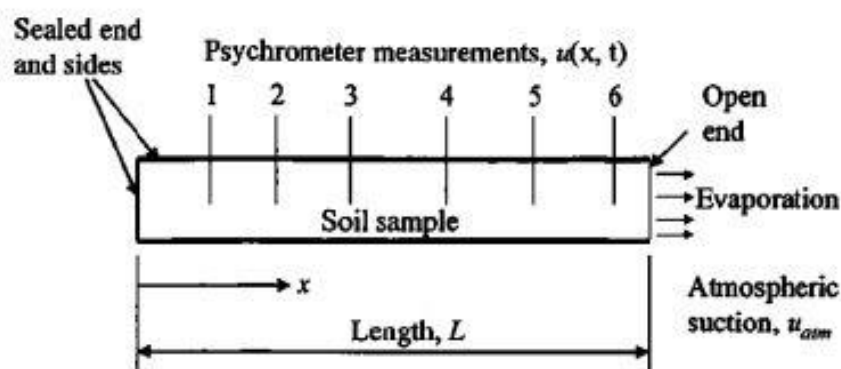


Figure 2.8 Test for measuring diffusion coefficient (Aubeny and Lytton 2004)

Diffusion coefficient can also be estimated from SWCC. Mualem (1976) derived an equation for predicting the relative hydraulic conductivity (K_r) and soil water diffusivity (D) from SWCC:

$$K_r = \frac{\{1 - (\alpha * \psi)^{n-1} * [1 + (\alpha * \psi)^n]^{-m}\}^2}{[1 + (\alpha * \psi)^n]^{\frac{m}{2}}} \quad (2.10)$$

where K_r = relative hydraulic conductivity, expressed in various units

ψ = pressure head or matric suction

α , n , and m = fitting parameters

$$D = \frac{(1-m)K_s}{\alpha m(\theta_s - \theta_r)} \Theta^{\left(\frac{1}{2} - \frac{1}{m}\right)} \left[\left(1 - \Theta^{\frac{1}{m}}\right)^{-m} + \left(1 - \Theta^{\frac{1}{m}}\right)^m - 2 \right] \quad (2.11)$$

where D = diffusivity or diffusion coefficient

K_s = saturated hydraulic conductivity

θ_s = saturated water content (cm^3/cm^3)

θ_r = residual water content (cm^3/cm^3)

Θ , dimensionless water content, = $\frac{\theta - \theta_r}{\theta_s - \theta_r}$

α , n , and m = fitting parameters

Based on the theory of Mualem (1976)'s equations, van Genuchten (1980) proposed an equation to represent SWCC:

$$\frac{\theta - \theta_r}{\theta_s - \theta_r} = \frac{1}{[1 + (\alpha * \psi)^n]^m} \quad (2.12)$$

van Genuchten (1980)'s equation is widely used to describe SWCC, and it is almost appropriate to all the soil textures. θ_s , θ_r , α , and n are known as van Genuchten parameters. The value α (in cm^{-1}) is related to the inverse of matric suction at which the SWCC becomes the steepest, and the value of n is related to the pore-size distribution (van Genuchten 1980). Schaap et al. (2001) set $m = 1 - 1/n$. By knowing the van Genuchten parameters, water content, θ , can be calculated when matric potential is given. In addition, diffusion coefficient can be calculated based on Equation 2.11 when van Genuchten parameters and water content are known.

2.4.2 Diffusion Coefficient from Field Estimates

As described in Section 2.3.1 and Equation 2.4, soil suction varies with time and depth. Suction measurements at different depths provide an effective way to estimate the diffusion coefficient based on the decay of variations of soil suction with depth. Soil suction at depth lags behind soil suction at the surface. Based on Equation 2.4, Mitchell (1979) derived an equation to indicate the relationship between a measured time lag at depth y and the diffusion coefficient:

$$t = \frac{y}{2} \sqrt{\frac{1}{\alpha \pi n}} \quad (2.13)$$

where t = time lag between a peak of suction at surface and at depth

y = depth

n = frequent number, which is the number of cycles of wetting and drying in a year

α = diffusion coefficient

McKeen and Johnson (1990) proposed a back-calculation method to estimate the diffusion coefficient. First, they plotted the suction data versus time for each depth. Then they plotted the suction data versus time again by using Equation 2.4 with various values of diffusion coefficient. By computing correlation coefficients for linear regression between these two methods, the diffusion coefficient can be estimated.

Compared to the laboratory method, estimating the diffusion coefficient from field suction measurements has several uncertainties. The variations of suction waveform shapes can lead to an uncertainty in interpreting diffusion coefficient. In addition, the accuracy of time lag approach can be affected by the suction waveform shapes at different depths (Aubeny and Long 2007).

2.5 Thermal Conductivity Sensor

Soil suction is a fundamental variable in geotechnical engineering. However, this variable is difficult to measure. Making an accurate measurement of soil suction is important for understanding both moisture flow in soil and its impact on geotechnical structures (Basara and Crawford 2000). Soil suction can be measured in both the laboratory and field. Devices used to measure the total suction include psychrometers and filter paper technique. Devices used to measure matric suction include thermal conductivity sensors, pressure plates, and tensiometers. The device used to measure osmotic suction is pore fluid squeezer, which contains a heavy-walled cylinder and position squeezer (Fredlund et al.

2012). All of these methods have both advantages and disadvantages in regard to measurement range, cost, accuracy, and practicality.

2.5.1 Overview of Thermal Conductivity Sensors

Thermal conductivity sensors were initially developed for soil science applications. Recently, they have been applied in geotechnical engineering practice. Thermal conductivity sensors are widely used to measure matric suction, and they have been shown to have a great performance for the measurement either in the laboratory or in the field. Once the sensors are installed in the field, they can be subjected to environmental changes (Shuai et al. 2002). Researchers have developed thermal conductivity sensors that can cover the range of 10 – 1500 kPa (Fredlund 2012). A thermal conductivity sensor is an indirect method of measuring matric suction by measuring the thermal properties of a standard porous medium. Water has better heat capacity than air, which means water can lose or gain a relatively large amount of heat without a large change in its temperature. The thermal properties of soils are an indicator of the soil moisture content. Therefore, the thermal conductivity of soils increases when their moisture content increases. A thermal conductivity sensor is composed of a porous ceramic block with a temperature sensor and a miniature heater. The moisture content in the porous ceramic block depends on the matric suction applied to the block by the surrounding soil. As a result, when the sensor is placed in the soil and comes to equilibrium with soil suction, the measurement at equilibrium is an indication of soil matric suction (Fredlund 1992).

2.5.2 Thermal Conductivity Sensors used by the Oklahoma Mesonet

The soil suction data used in this research were acquired from the Mesonet weather stations dispersed across Oklahoma. The Oklahoma Mesonet was built in 1994, and it is a

statewide mesoscale environmental monitoring network with at least one station in each of Oklahoma's 77 counties (Illston et al. 2008). A number of counties have more than one weather station. The Oklahoma Mesonet has 120 automated weather monitoring stations designed to measure the weather and soil conditions. At each station, climate and soil parameters including air and soil temperature, wind speed, precipitation, relative humidity, solar radiation, atmospheric pressure, and soil moisture are measured by a set of instruments every 5 to 30 minutes each day.

Recognizing the necessity of improving in-situ measurements of soil moisture/suction, the Oklahoma Mesonet designed the soil moisture/suction measuring network in 1996 to meet the needs of different disciplines. The sensor used by the Oklahoma Mesonet for matric potential (matric suction) measurement is the Campbell Scientific 229-L heat dissipation matric potential sensor (Figure 2.9). This type of sensor uses a heat dissipation method to measure the soil matric suction indirectly. The sensor consists of a thermocouple and a resistance heater housed in a hypodermic needle, and the hypodermic needle is embedded in a ceramic matrix. The matrix absorbs water in a similar way to those of silt loam soils, so the ceramic matrix wets and dries on similar time scales to most soils (Illston et al. 2008). When the sensor is placed in soil for measurement, it must come into equilibrium with its surrounding soil. The time required for equilibrium of the water in the ceramic matrix and soil depends on both the magnitude of the suction gradient and the hydraulic conductivity. Typically, this equilibration time is a few minutes or tens of minutes (Campbell Scientific, Inc 2009).

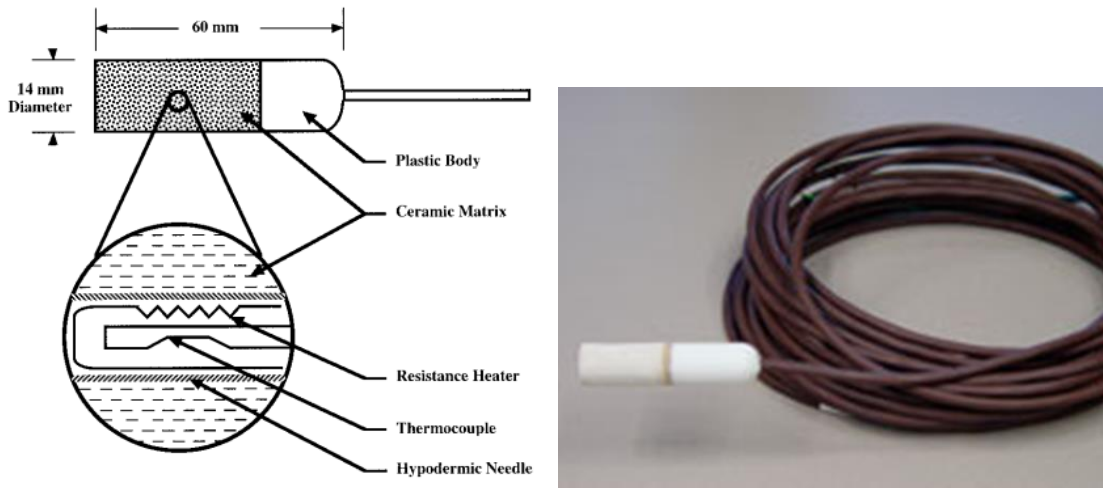


Figure 2.9 The Campbell Scientific 229-L sensor (Basara and Crawford 2000)

Once the equilibrium condition is reached, a 50 mA electric current is sent through the resistance heater for 30 seconds. The thermocouple measures the soil temperature before and after the current. The temperature increase is directly related to the soil matric suction (Basara and Crawford 2000). The temperature increase indicates the heat that is not dissipated. If the water content of the ceramic matrix increases, more heat will be dissipated, then the temperature increase measured by the thermocouple will be reduced. A drier sensor will have a greater temperature rise. When the current passes through the sensor for 30 seconds, the temperature rise ranges from approximately 0.7°C when the sensor and surrounding soil are wet to 3.0°C when dry (Campbell Scientific, Inc 2009). Figure 2.10 shows a typical temperature rise in response to the heating time in a silt loam. It indicates that the higher the matric suction, the greater the temperature increase in the heating process.

A series of laboratory tests have been conducted to determine the relationship between the temperature increase in the 229-L sensor and matric suction. Based on the previous

research, Mesonet scientists determined an empirical relationship between the measured temperature difference and soil matric suction. This will be explained in detail in Chapter 3.

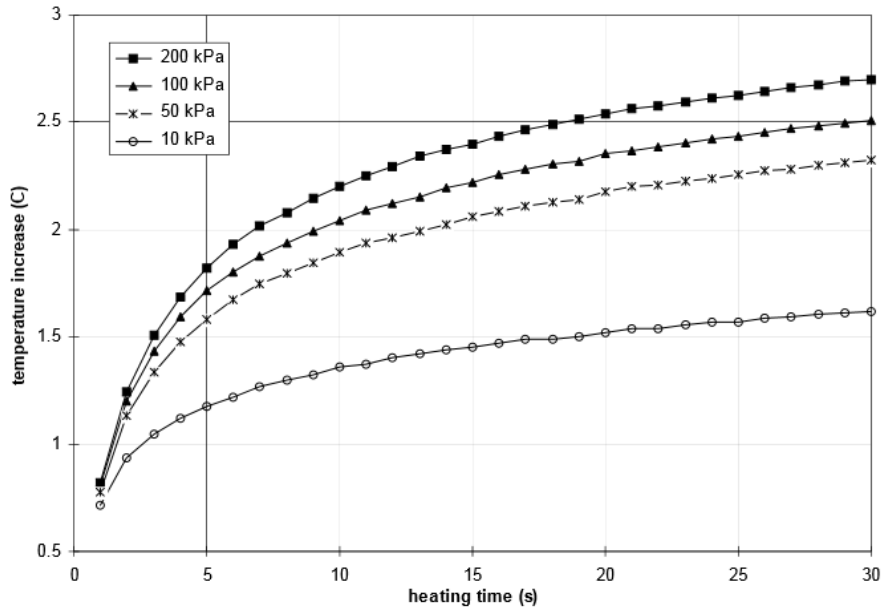


Figure 2.10 Temperature rise vs. heating time of 229-L sensor
(Campbell Scientific, Inc 2009)

2.6 Application of Soil Suction in Engineering Practice

Unsaturated soils, such as expansive clays, have been considered as “problem” soils since they are moisture-sensitive. Geotechnical engineers have been recognized the significance of unsaturated soil in engineering practice. The theory of soil suction is highly involved in the engineering practice of unsaturated soil, such as foundation design, soil movement prediction, soil volume change, etc. The movement of expansive soils is usually associated with suction change near the soil surface (Lytton 1994). As a result, it is necessary to evaluate soil suction in engineering practice.

2.6.1 Crack Analysis

The prediction of movement in expansive soils, such as heave prediction and cracking analysis, is one of the important applications of suction. The vertical swelling of expansive soils is known as heave. Soil heave can cause lifting of structures during periods of wetting. Expansive soils tend to crack when they become dry. Soil cracks can be classified into different types based on its development process. The development of cracks is mainly controlled by both soil suction and soil properties. In geotechnical engineering, desiccation cracks are a common type in practice. Desiccation cracks develop under the condition of water loss in clayey soils, and their formation is a consequence of an excess of tensile stresses induced by shrinkage of the drying soils with constrained kinematics (Hu et al. 2006). Numerous research has been conducted to explore the mechanism of soil cracks, both in the field and in the laboratory. Nevels (1995) applied soil suction data to evaluate the cause of longitudinal cracking under one-year old pavement in Oklahoma. By measuring the in situ suction, this research indicated the significance of soil suction in causing moisture changes and cracks in the pavement. Auvray et al. (2014) performed a laboratory test to examine soil cracks during suction cycles. They applied three suction cycles to soil specimen and the first cycle had the greatest impact on the crack area. In addition, their research also provided an image process method to record the cracks in the laboratory.

2.6.2 Slab-On-Ground Foundation

Slab-on-ground foundations utilize the concrete slab to serve as the foundation for the structures, such as residential and light commercial structures, that are built from a mold set into the ground. This type of construction became quite common in 1950's, and it is

most often seen in warmer areas, where ground freezing and thawing is usually not a concern (Post-Tensioning Institute 1980). Several design parameters must be evaluated for a successful slab-on-ground design. The first parameter is climate. Slab-on-ground cannot be constructed in colder climates, where there is a need for heat ducting underneath the floor. In addition, the semi-arid areas, where the climate has periods of rainfall followed by periods without rainfall, have the potential damage to foundation on expansive soils due to the moisture change in soils. The second parameter is soil parameter, including soil swelling mode, edge moisture variation distance, and differential soil movement. As shown in Figure 2.11, there are two modes of soil swelling – center lift and edge lift. Center lift is a result of long-term condition, either due to the soil under the slab becoming wetter or soil around the slab edge becoming drier, or due to a combination of both. On the other hand, edge lift is a short-term condition. The edge moisture variation distance (e_m) and differential soil movement (y_m) are commonly reported parameters in slab-on-ground foundation design, both of which are related to matric suction change in the soil. Edge moisture variation distance is the distance from the edge of slab to which the soil moisture content varies. Edge moisture penetration is the main reason for foundation becoming unsupported (McKeen and Johnson 1990). The major factor affecting the edge moisture variation distance is the unsaturated diffusion coefficient, which depends on the matric suction, the permeability, and the cracks in the soil. To determine the differential soil movement (y_m), the initial and the final suction profile should be known at the edge of the foundation. The third parameter is structural parameter, including slab length, beam spacing, and loading.

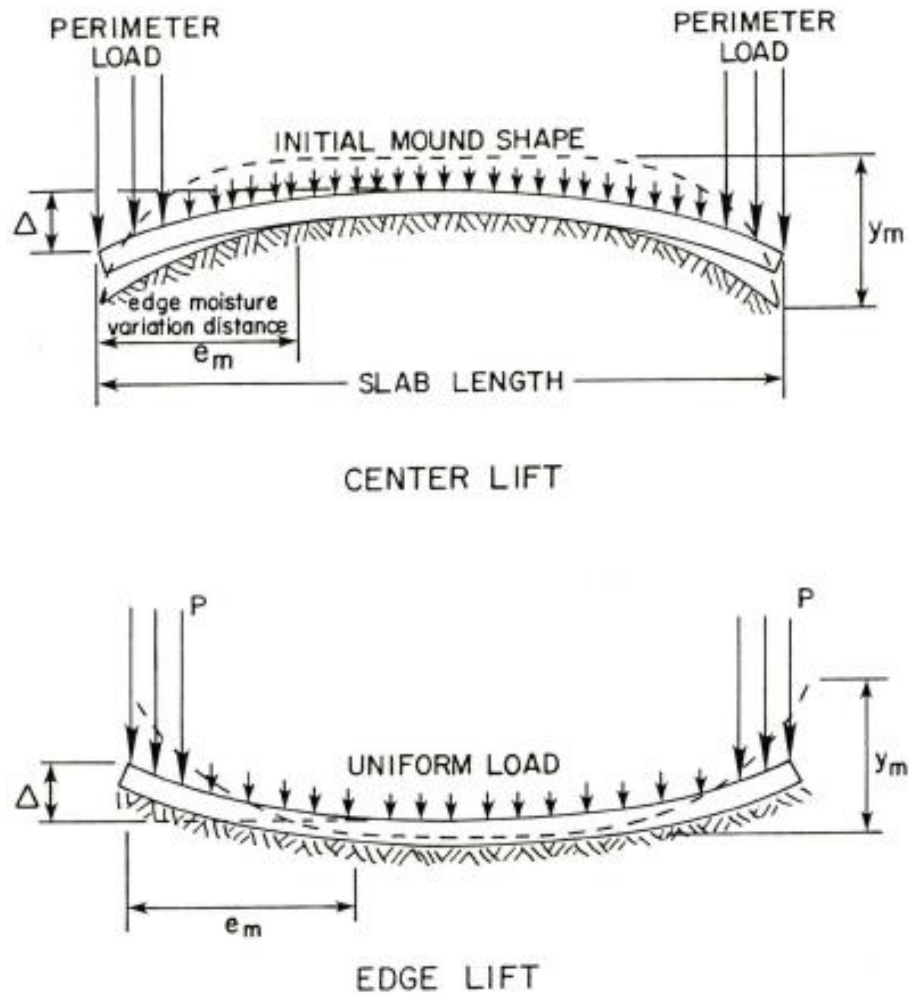


Figure 2.11 Soil-structure interaction mode (Post-Tensioning Institute 1980)

The interaction between slab-on-ground structures and soil volume changes in expansive soil is quite complex. As explained in Section 2.3.3, numerical modeling is widely used in current research to predict the moisture flow in expansive soils beneath a slab-on-ground. Fredlund and Vu (2003) used seepage models to predict matric suction conditions with specified boundary conditions. They performed three scenarios to analyze the center lift and edge lift mode of a slab-on-ground. The results of numerical modeling

indicate the matric suction and stress distribution in soils, and the results are consistent with the observations in the field.

2.7 Summary

The mechanical behavior of unsaturated soils is important to geotechnical engineering concerns. The most important characteristic of expansive soils is the volume change from swelling and shrinkage. The volume change is greatly influenced by soil moisture content, consequently, by matric suction. Changes in matric suction are a result of changes in environmental conditions, groundwater table depth, and vegetation type. Many engineering problems involving unsaturated soils are related to changes in environmental factors, while these changes primarily affect the matric suction. It is clear from the literature reviewed that the understanding of matric suction has been greatly improved during the past few decades. A number of devices have been developed for suction measurement in both laboratory and field. Along with the accurate measurement, soil suction is highly involved in engineering practice and problem solving. However, most of the research focused on the measurement itself and how soil suction affects other soil properties. Due to the lack of long-term suction measurement, little research focused on how the environmental factors affect the seasonal variation of soil suction, and the relationship between the soil suction and the environment is not yet fully understood. With the development of numerical modeling, general unsaturated soil behaviors can be predicted using both environmental and soil parameters. The Oklahoma Mesonet has more than 20 years of environmental and soil parameter observations. It provides a good opportunity to evaluate the influence of the environment on soil suction. By applying the data from the Oklahoma Mesonet, this

research will combine the soil suction and environmental data, and evaluate what environmental parameters affect the variation of soil suction.

CHAPTER III

MATRIC SUCTION FROM FIELD MEASUREMENT

3.1 The Oklahoma Mesonet

The daily weather and soil suction data used in this research was derived from the field measurement by the Oklahoma Mesonet. The Oklahoma Mesonet is a statewide environmental monitoring network with 120 automated stations, at least one station in each of Oklahoma's 77 counties, designed to measure a variety of environmental parameters (Figure 3.1). One of the main objectives in establishing the Mesonet network was to ensure that a station site can be as representative of as large an area as possible. Therefore, site locations for Mesonet stations fulfill a number of general requirements for meteorological and environmental purposes. At each station, the environmental parameters, such as temperature, wind speed, precipitation, relative humidity, solar radiation, atmospheric pressure, and soil parameters, such as soil temperature and soil moisture, are measured by a set of instruments located on or near a 10-meter-tall tower. The environmental parameters are measured every 5 minutes; the soil temperature is measured every 15 minutes; the soil moisture is measured every 30 minutes. A central

collection system at the Oklahoma Climatological Survey receives the data from stations, verifies the quality of the data, and provides them to the public.

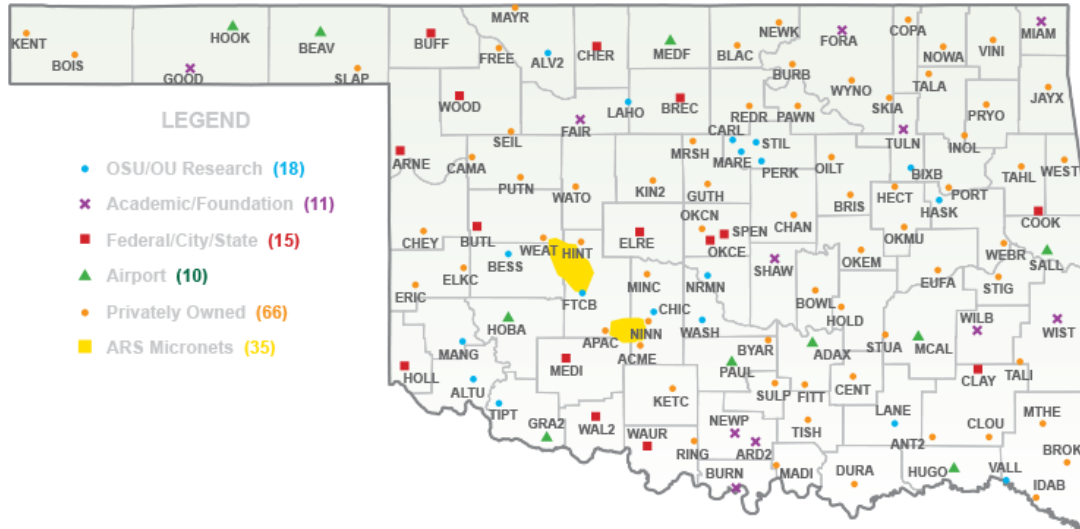


Figure 3.1 Map of the Mesonet stations (The Oklahoma Mesonet 2015)

In 1996, the Oklahoma Mesonet began to deploy soil moisture sensors (Campbell Scientific 229-L sensor, explained in Section 2.5.2) at 60 stations. These stations are evenly distributed to ensure a statewide coverage of monitoring. In 1999, The Oklahoma Mesonet installed sensors at 42 additional stations. As of 2007, the Oklahoma Mesonet had installed the sensors at a depth of 5 cm at 103 stations, at a depth of 25 cm at 101 stations, at a depth of 60 cm at 76 stations, and at a depth of 75 cm at 53 stations.

There were 74 Mesonet stations selected for this research (Figure 3.2). The selection was made to use one station in each of 77 counties. However, three counties do not have the thermal conductivity sensor for suction measurement. As a result, 74 stations were selected in 74 counties. Detailed information of each station and data duration of soil suction is shown in Appendix A. The duration of data mainly depends on when the station installed the soil suction sensor. The information on soil characteristics was obtained from

a soil core sample at each Mesonet station. After collecting a soil sample by field technicians, the particle-size distribution was determined according to the American Society for Testing and Materials (ASTM) D 421–85. In addition, hydrometer and wet sieving analysis were performed according to ASTM D 422–63 and ASTM D 1140–92. Then the percentages of sand, silt, and clay were calculated and soil type was assigned to each site according to the U.S. Department of Agriculture (USDA) classification system (Illston et al. 2008).

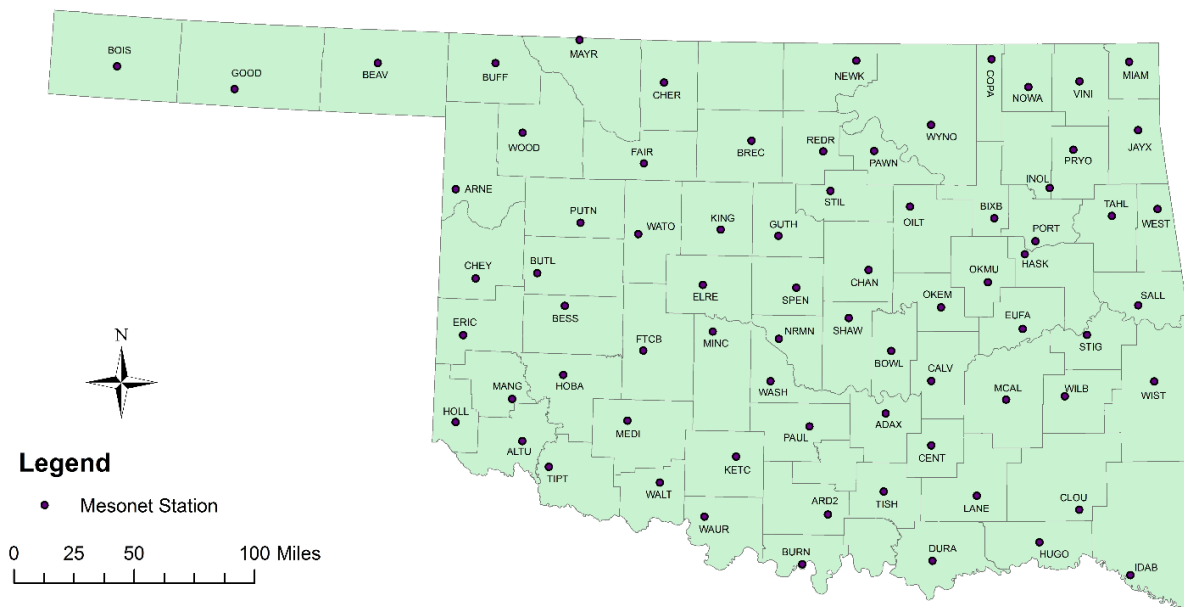


Figure 3.2 Selected Mesonet Stations with Station ID

3.2 The DOE ARM Network

Geotechnical engineers are interested in soil moisture up to 5-m depth (Wray 1987, Nichol et al. 2003, Nguyen et al. 2010). Since significant soil moisture variability occurs below the deepest Mesonet sensor depth of 75 cm, measurements of deeper soil moisture from the Department of Energy’s Southern Great Plains Atmospheric Radiation

Measurement (DOE ARM) network were used to accurately estimate matric suction profiles. The ARM network has 21 automated sites in Oklahoma and Kansas, called Soil Water and Temperature System (SWATS). These systems provide hourly measurements of soil temperature and moisture. The ARM network uses the same soil moisture sensor (Campbell Scientific 229-L sensor) as the Oklahoma Mesonet to provide estimates of matric suction (Swenson et al. 2008). At an ARM site, soil moisture sensors are installed at up to eight different depths in the soil profile: 5 cm, 15 cm, 25 cm, 35 cm, 60 cm, 85 cm, 125 cm, and 175 cm below the soil surface. Two profiles (east and west) of sensors, located 1 m apart from each other, are installed at each site for replication and redundancy of measurements (Bond 2005).

Figure 3.3 and Table 3.1 shows the selected ARM sites with moisture sensors installed deeper than 85 cm and data available period for each site. Although the ARM network has less dense spatial coverage than the Oklahoma Mesonet, the availability of the ARM data allows the exploration of soil moisture below the 75-cm limit of the Oklahoma Mesonet. The ARM data, combined with the Oklahoma Mesonet data, will be used to verify the active zone depth obtained from empirical equation and numerical modeling.

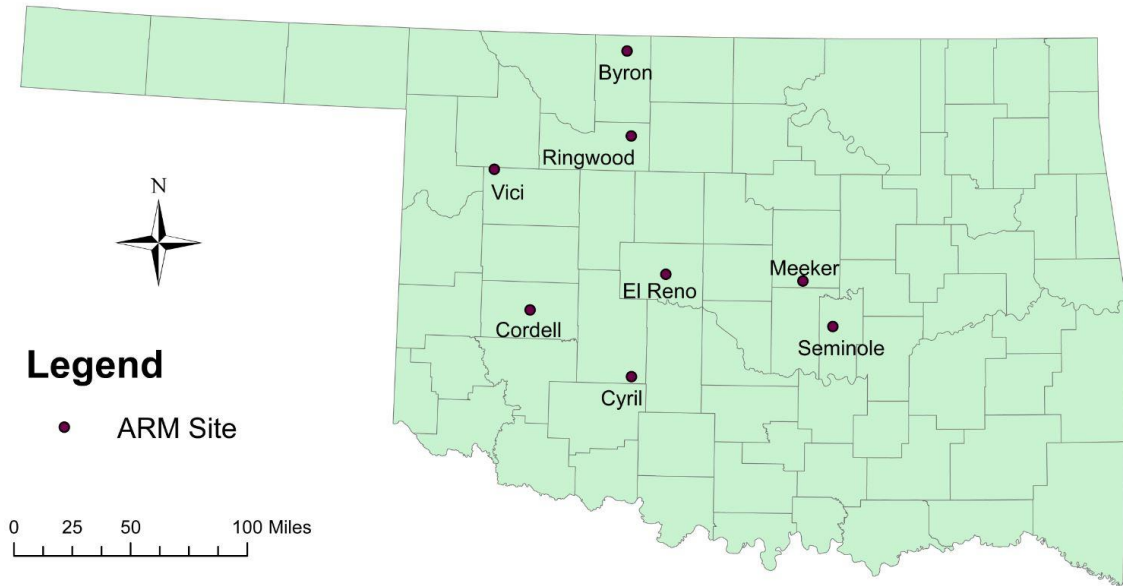


Figure 3.3 Selected ARM sites

Table 3.1 Sensors' depth at ARM sites

Site Location	Depths (cm)	Data Availability Period
Byron	5, 15, 25, 35, 60, 85, 125, 175	1996 - 2016
Ringwood	5, 15, 25, 35, 60, 85, 125, 175	1996 - 2016
Vici	5, 15, 25, 35, 60, 85, 125, 175	1996 - 2011
El Reno	5, 15, 25, 35, 60, 85, 125, 175	1996 - 2002
Cordell	5, 15, 25, 35, 60, 85, 125, 175	1996 - 2011
Seminole	5, 15, 25, 35, 60, 85, 125, 175	1996 - 2009
Cyril	5, 15, 25, 35, 60, 85, 125	1996 - 2009
Meeker	5, 15, 25, 35, 60, 85, 125	1996 - 2002

3.3 Climate in Oklahoma

The 48 contiguous U.S. states have been subdivided into 344 climate divisions based on long-term climatic data maintained by the National Climatic Data Center (NCDC) for a variety of climatic applications (Guttman and Quayle 1996). These divisions are classified mainly for agricultural purpose (Illston et al. 2004). Each of the 48 states was classified up to 10 divisions. The divisions often coincide with county boundaries. One divisional dataset is based on year-monthly averages of temperature and precipitation since 1895. There are nine climate divisions in Oklahoma shown in Figure 3.4. These nine divisions correspond to the nine crop divisions designated by the U.S. Department of Agriculture. Each climate division also has relatively homogeneous weather and climate patterns.

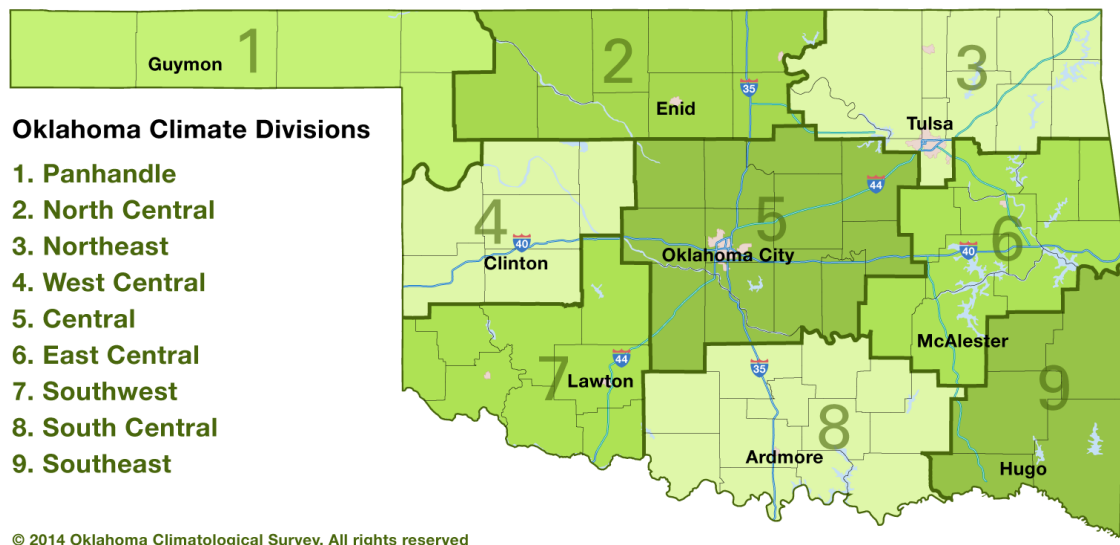
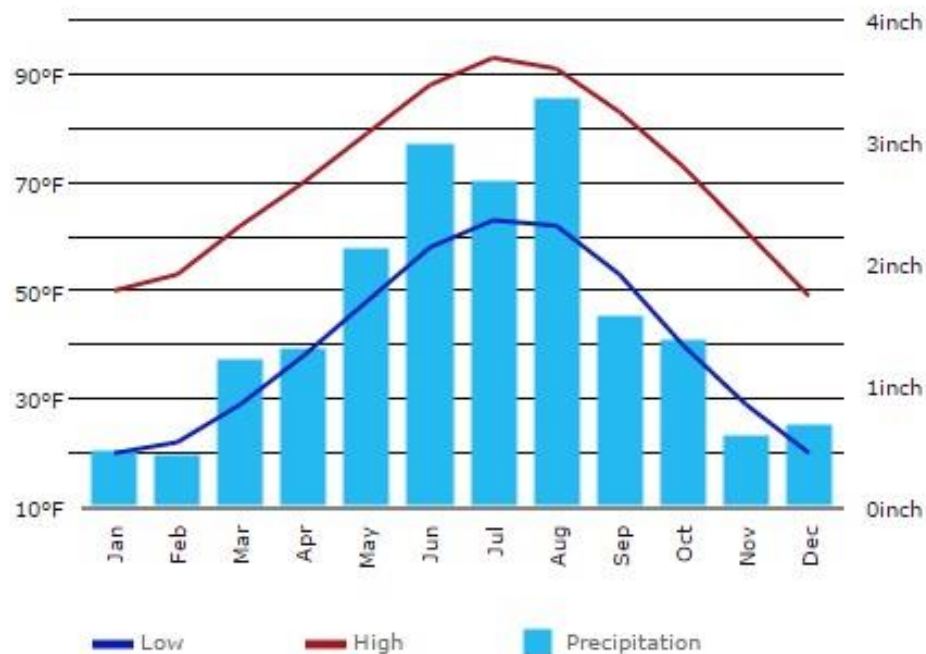


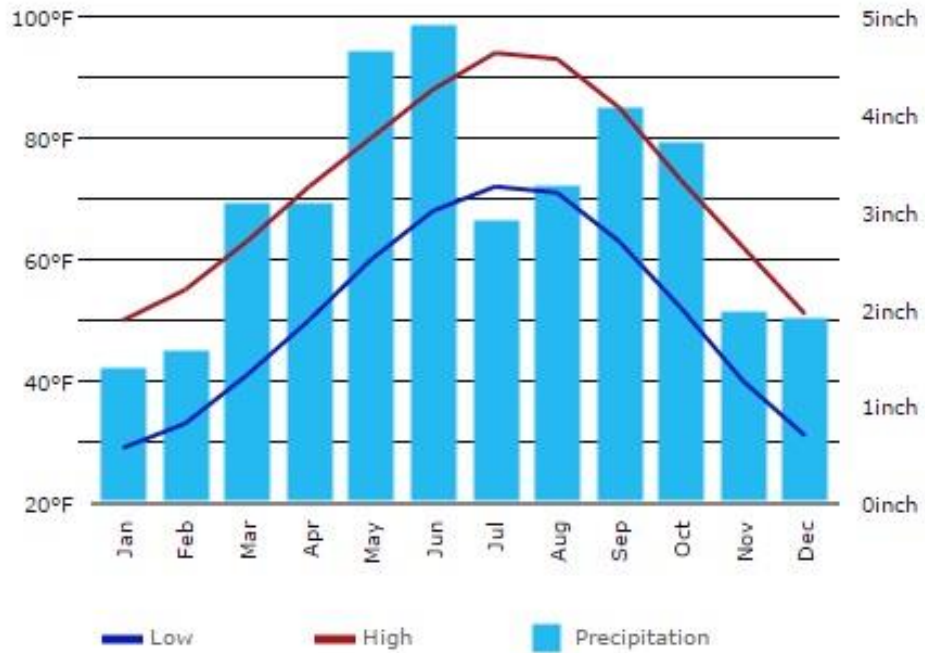
Figure 3.4 Oklahoma climatic divisions (The Oklahoma Climatological Survey 2014)

The climate of Oklahoma ranges from humid subtropical in the east to semi-arid in the west, and it varies significantly across the state. The average annual temperature across the state ranges from 62 °F to 58 °F. The dominant characteristic of the spatial distribution

of precipitation across the state is a sharp decrease from east to west. The average annual precipitation ranges from about 17 inches in the far western panhandle to about 56 inches in the far southeast (The Oklahoma Climatological Survey 2011). Figure 3.5 shows the annual temperature and precipitation from 1981 to 2010 in three cities in Oklahoma (U.S. Climate Data 2010). The precipitation varies by season, particularly in western and central Oklahoma. Spring and autumn offer the largest amounts of precipitation, which is mostly brought by thunderstorms. During winter, rainfall is the dominant type of precipitation for all Oklahoma except panhandle area. Average annual snowfall increases from less than two inches in the southeastern Oklahoma to nearly 30 inches in the western panhandle (The Oklahoma Climatological Survey 2011).



3.5.a Boise City, western Oklahoma



3.5.b Oklahoma City, central Oklahoma



3.5.c Idabel, southeastern Oklahoma

Figure 3.5 Temperature and precipitation in Oklahoma

3.4 Oklahoma Expansive Soils

Expansive soils are often referred to as swelling soils. Geotechnical engineers often use swelling potential to define the expansion level of soil. Several techniques have been used to identify and classify the swelling potential of expansive soils (Snethen et al. 1977). This research used the classification provided by Chen (2012). There is a general relationship between the swelling potential and plasticity index (PI) (Table 3.2). Plasticity index is a measurement of soil plasticity and it is the difference between the liquid limit (LL) and plastic limit (PL). The liquid limit is the moisture content at which the soil behavior changes from plastic to liquid. The plastic limit is the moisture content at which soil behaves as plastic. Liquid limit and plastic limit are also called Atterberg limits. Most of the studies identified soil properties such as Atterberg limits, plasticity index, and hydraulic conductivity are the most influential factors in controlling the moisture conditions under covered areas.

Table 3.2 Expansive soil classification (Chen 2012)

Swelling Potential	Plasticity Index
Low	0 – 15
Medium	10 – 35
High	20 – 55
Very High	35 and above

To determine the swelling potential of soil in Oklahoma, the plasticity index was evaluated for the 74 selected Mesonet stations in this research. The plasticity index was obtained from the USDA Web Soil Survey (WSS). The USDA Web Soil Survey provides

a comprehensive interface of detailed soil survey information. Soil data is depicted within an area of interest, which is defined by the user (Beaudette and O’Geen 2009). The WSS provides soil maps and soil properties, including soil chemical properties, physical properties, erosion factors, soil qualities, and water features for more than 95% of the U.S. counties (USDA Web soil survey 2009). Figure 3.6 shows the soil map and soil property information of one selected Mesonet station from the WSS. To select each Mesonet station, first, latitude and longitude of each station were input in the WSS; second, approximately 0.1-acre square area around the station was extracted; third, plastic index was obtained from the list of soil physical properties.

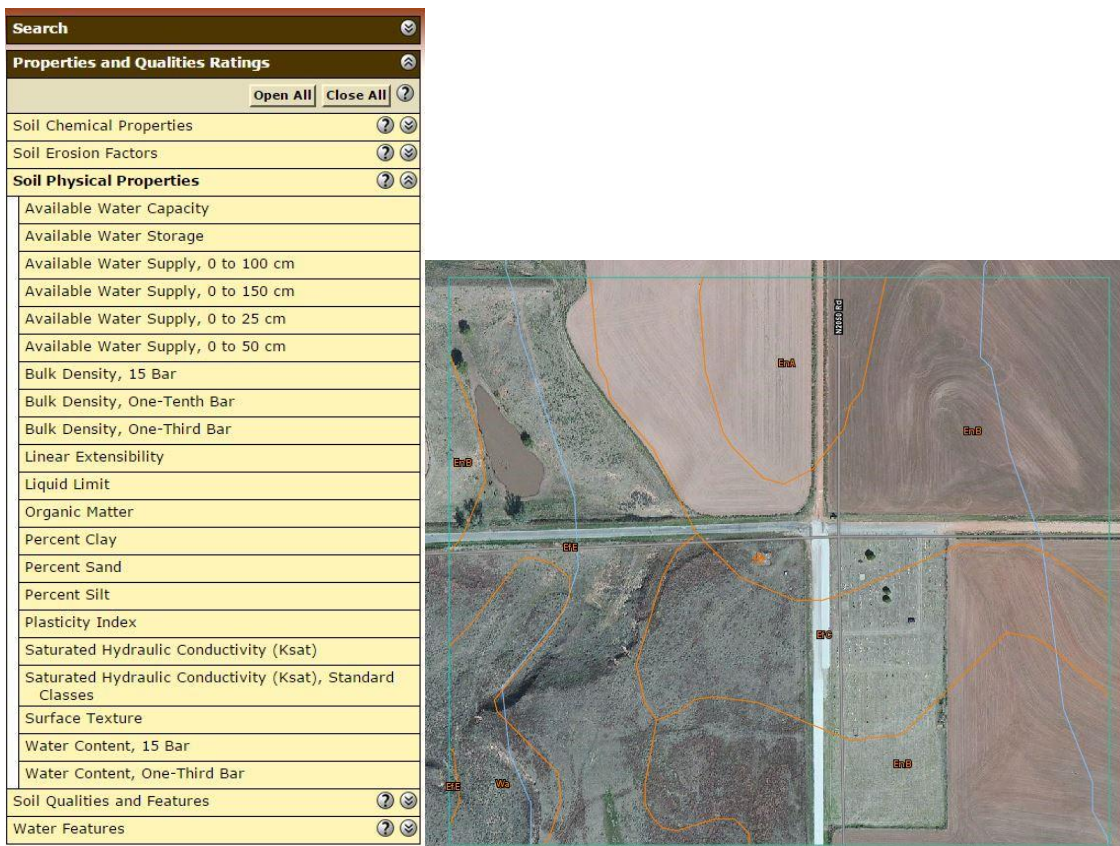


Figure 3.6 Soil information from the USDA web soil survey

After obtaining the plasticity index for each station, to evaluate the expansive soil distribution across the whole state, spatial interpolation was used in ArcGIS software. Spatial interpolation is a technique used to predict the values of locations that lack sampled points. It is based on the measurement of relationship/dependence between near and distance locations (Childs 2004). Geographic information system (GIS) is a system about managing and analyzing the spatial data. ArcGIS software works for conducting spatial analysis and creating maps, and it has been widely used in civil engineering practice. ArcGIS Spatial Analysis extension offers several interpolation methods, including Inverse distance weighting (IDW), kriging, spline, pointInterp, natural neighbor, trend, and topo to raster. Each method uses a different approach for generating the surface from known point data. The selection of the method depends on the type of study and the distribution of sample points. This study used IDW for spatial interpolation. IDW method should be used when the sample points are dense enough. It assumes that locations that are close to each other are more alike than those that are farther apart. The greater the distance, the less influence the sample point has on the output result (Childs 2004). In this research, by knowing the plasticity index at certain stations, IDW can estimate the plasticity index for the places without data. Spatial interpolation and IDW method will be also used to predict the distribution of evapotranspiration and active zone depth in Chapter 4.

Figure 3.7 shows the distribution of expansive soils across the state. Almost the whole state has a medium or high swelling potential of expansive soils. Southern Oklahoma and part of northeastern and panhandle area have high swelling potential of expansive soils.

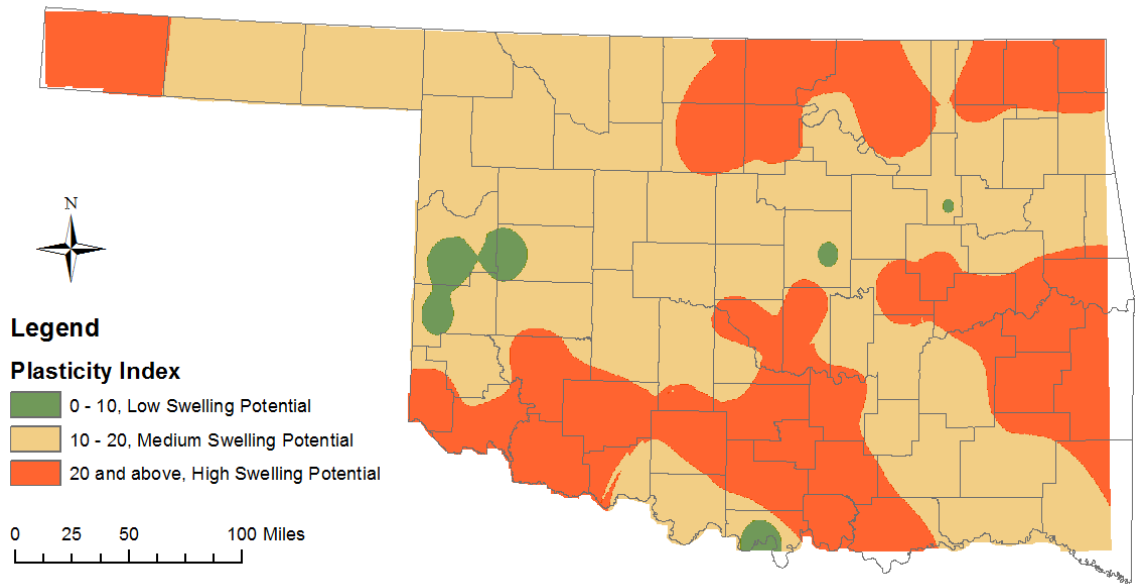


Figure 3.7 Oklahoma expansive soils

3.5 Thermal Conductivity Sensor Installation at Oklahoma Mesonet

One approach to investigate the soil matric suction in the field is using in situ measurement. The sensors installed at different depths are effective to monitor matric suction distribution and variation. Thermal conductivity type sensors have been used by geotechnical engineers for different investigations, and the sensors are performed well both in the laboratory and in the field. As discussed in Section 2.5, the soil moisture sensor installed at Oklahoma Mesonet is called the Campbell Scientific 229-L sensor (shown in Figure 2.9), a type of thermal conductivity sensor. This sensor records the temperature change after a heat pulse. Soil water content and soil matric potential/suction can be calculated using the measured temperature difference. This sensor was chosen because of its small size, easy incorporation into the whole network, and absence of harmful radiation (Illston et al. 2004). Before the installation, the sensors are calibrated in laboratory to remove the sensor-to-sensor variability. Calibration is the very first and fundamental step

towards the use of the sensor to identify and remove the sensor-to-sensor variability. The Mesonet personnel first connected each sensor to a data logger and measured the resistance of the thermocouple circuit and the heating element circuit. Next, they placed the sensor into a bag alone for 3–4 days to remove the majority of residual moisture within the sensor and recorded the largest temperature difference from the period. Then they placed the sensor into distilled water to remove as many air bubbles as possible from its porous ceramic matrix and recorded the smallest temperature difference for 3–4 days (Illston et al. 2008). After the calibration, the sensors are installed at multiple independent depths (5 cm, 25 cm, 60 cm, and 75 cm). Figure 3.8 shows the vertical profile of sensor installation. The sensors at the 5-cm and 25-cm depths were placed horizontally, while the sensors at the 60-cm and 75-cm depths were placed at a 45° angle (Basara and Crawford 2000).

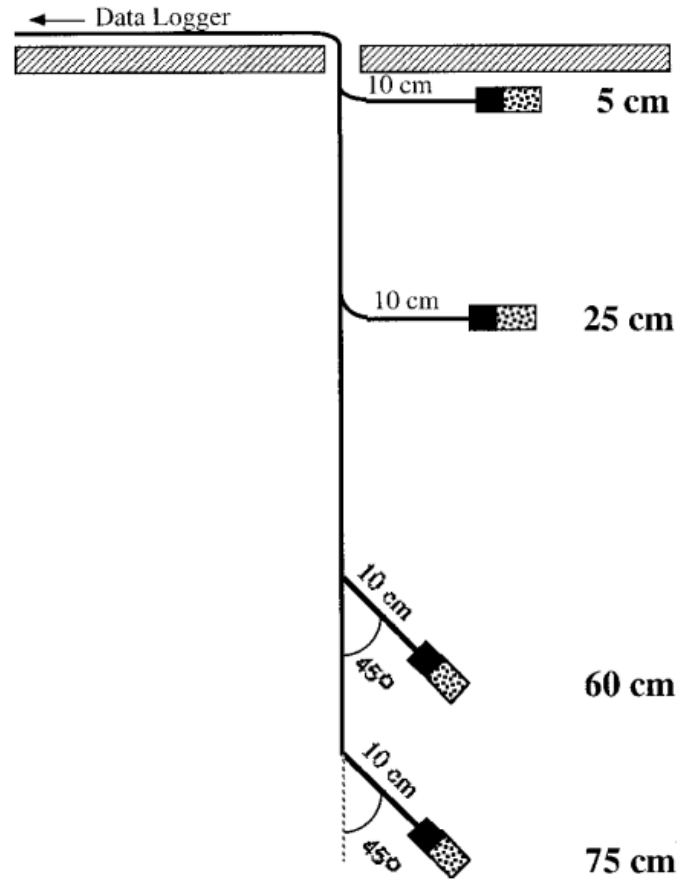


Figure 3.8 Vertical profile of soil moisture sensors (Basara and Crawford 2000)

The Oklahoma Mesonet provides daily averaged normalized temperature difference, ΔT_{ref} , which can be used to calculate soil matric suction. ΔT_{ref} is derived from the temperature difference measured after a heat pulse is introduced. An example of ΔT_{ref} time-series data is presented in Figure 3.9. The daily ΔT_{ref} at different depths and monthly total precipitation were measured in Stillwater, Oklahoma, from March to September 2011. Since January 2011, the Oklahoma Mesonet decommissioned the sensors at 75 cm depth, so the figure only shows three depths of data. The decreasing ΔT_{ref} values indicate a wetting trend and the increasing ΔT_{ref} values indicate a drying trend. The shallower depths (5 and

25 cm) are more sensitive to the precipitation. The deeper depths (60 cm) respond more gradually to wetting and drying.

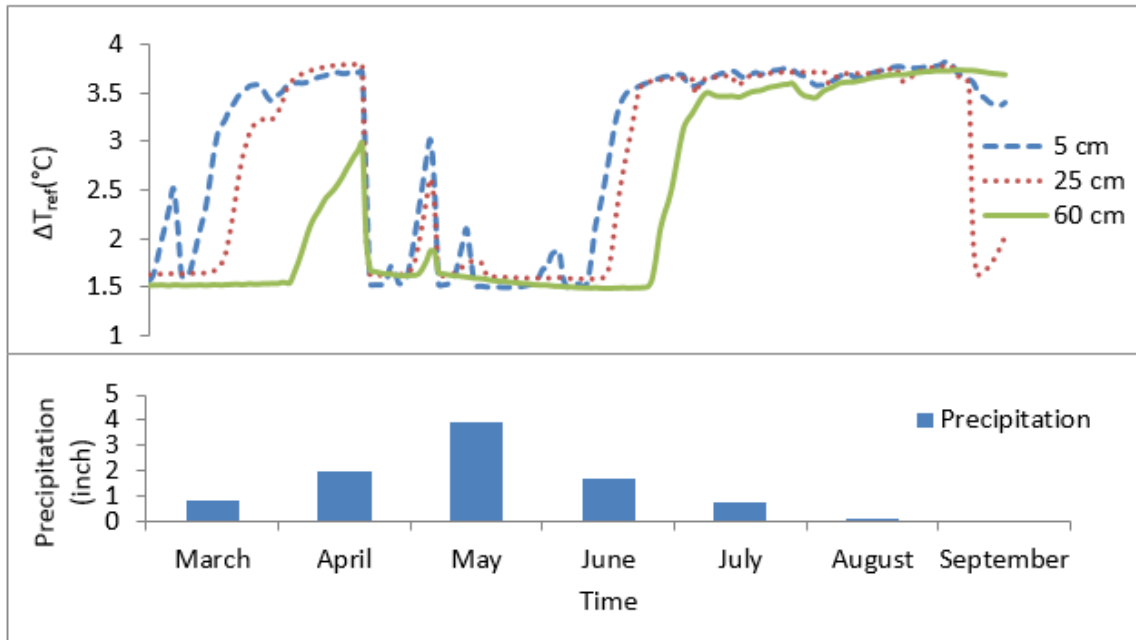


Figure 3.9 Daily ΔT_{ref} and monthly precipitation in Stillwater from March to September 2011

3.6 Soil Matric Suction derived from ΔT_{ref}

The values of ΔT_{ref} support the calculation of a variety of soil variables such as soil moisture content and soil matric suction. To establish the relationship between the sensor measurement and matric suction, laboratory tests are needed to determine the relationship between the sensors and matric suction. Based on the previous research, Illston et al. (2008) derived an empirical equation to calculate soil matric suction:

$$MP = -c \exp(a \Delta T_{ref}) \quad (3.1)$$

where, MP = soil matric potential, kPa

$a = \text{calibration constant} = 1.788 \text{ } ^\circ\text{C}^{-1}$

$c = \text{calibration constant} = 0.717 \text{ kPa}$

$\Delta T_{\text{ref}} = \text{measured temperature difference, } ^\circ\text{C}$

The value of soil matric potential is negative because it indicates a negative pore water pressure. In geotechnical engineering, soil matric potential is known as soil matric suction and soil matric suction is expressed as a positive value. As a result, soil matric suction is the positive value of the matric potential in Equation 3.1. Because of the range of the sensor, values of soil suction greater than 850 kPa and smaller than 8.5 kPa are not accurate (Illston et al. 2008).

Figure 3.10 shows matric suction profiles and precipitation from April 15 to July 15 in three different years in Stillwater, Oklahoma. Based on the annual precipitation data, 2001 is a year with the average amount of precipitation, while 2007 is a relatively wet year and 2011 is a relatively dry year (see Figure 4.4 in Chapter 4). These figures indicate: (1) matric suction at the soil surface and shallower depth is more sensitive to climatic conditions than that in deeper depth. Especially in the wet year of 2007, matric suctions between 60 cm and 75 cm remained almost constant from April to July; (2) matric suction has a gradual decrease during the wet season and an increase during the dry season; (3) matric suction at the soil surface is much larger than that at 60 cm and 75 cm, especially during dry periods.

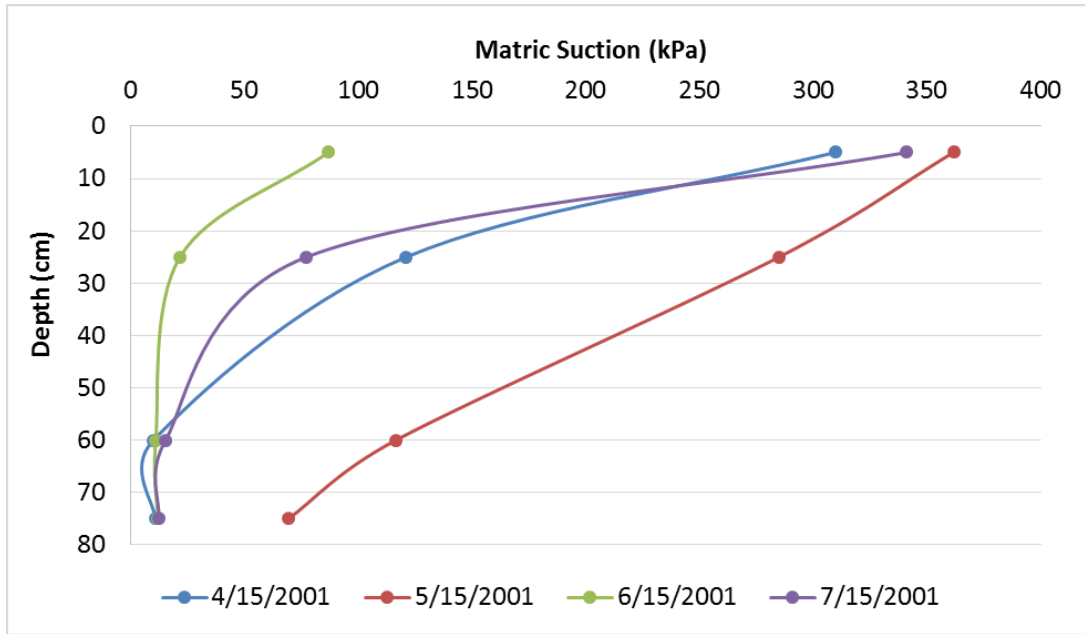


Figure 3.10.a Matric suction profile in 2001

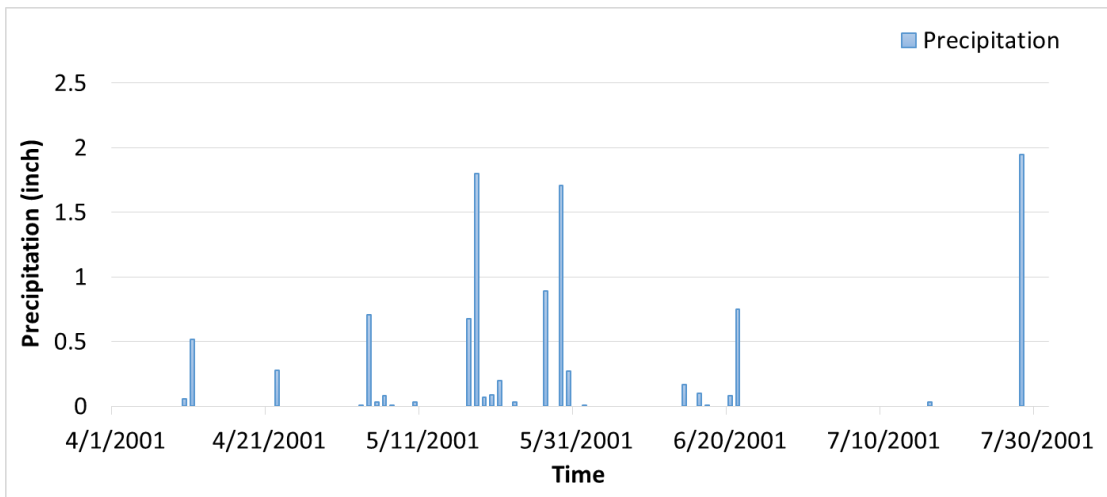


Figure 3.10.b Precipitation in 2001

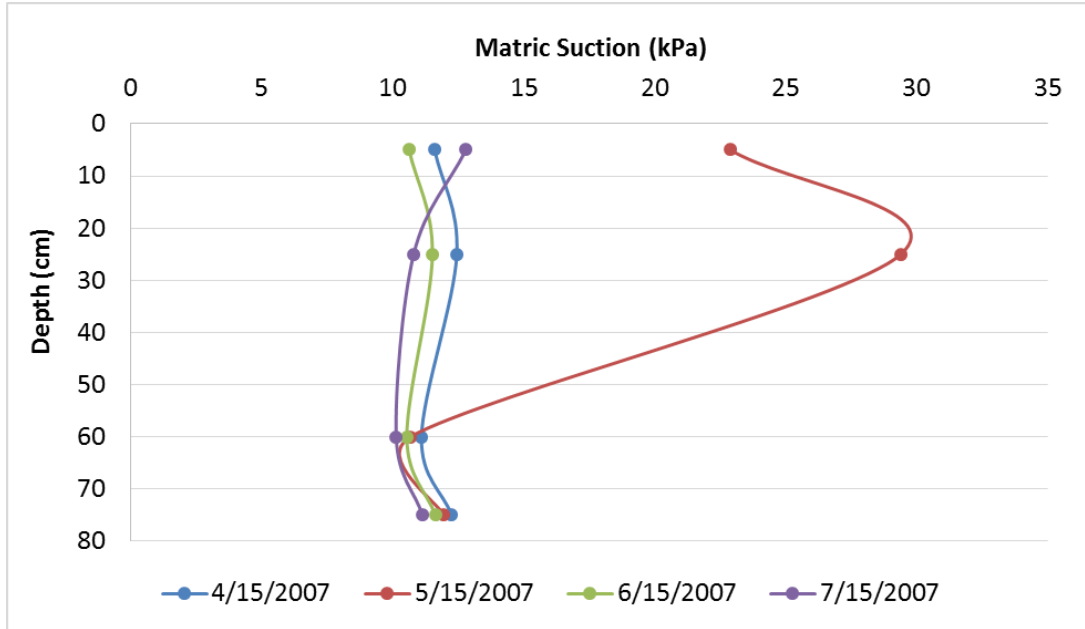


Figure 3.10.c Matric suction profile in 2007

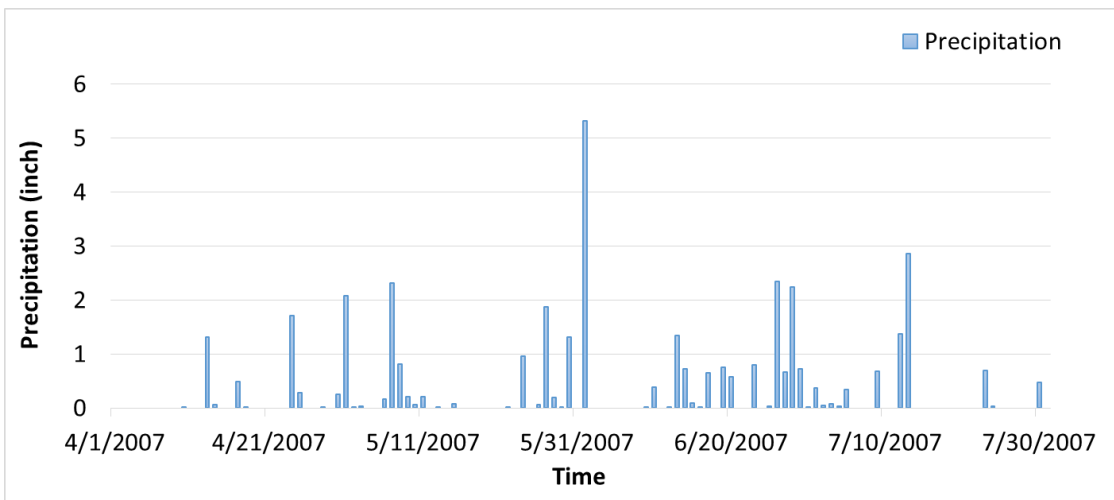


Figure 3.10.d Precipitation in 2007

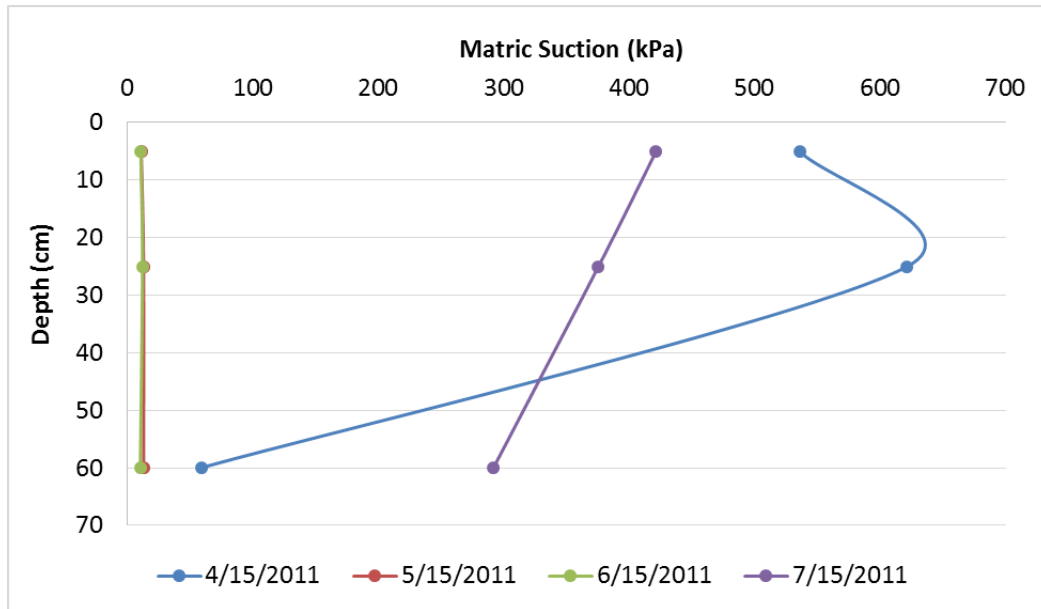


Figure 3.10.e Matric suction profile in 2011

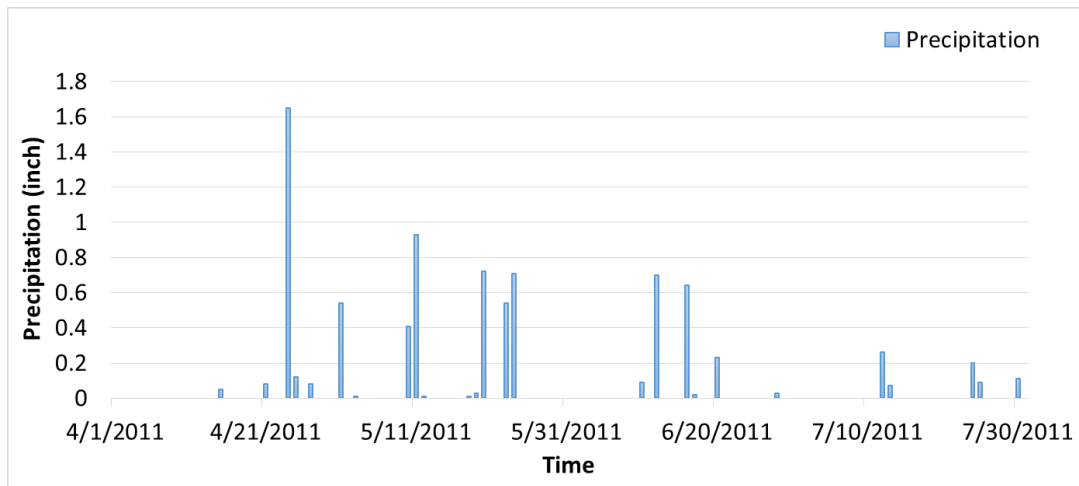
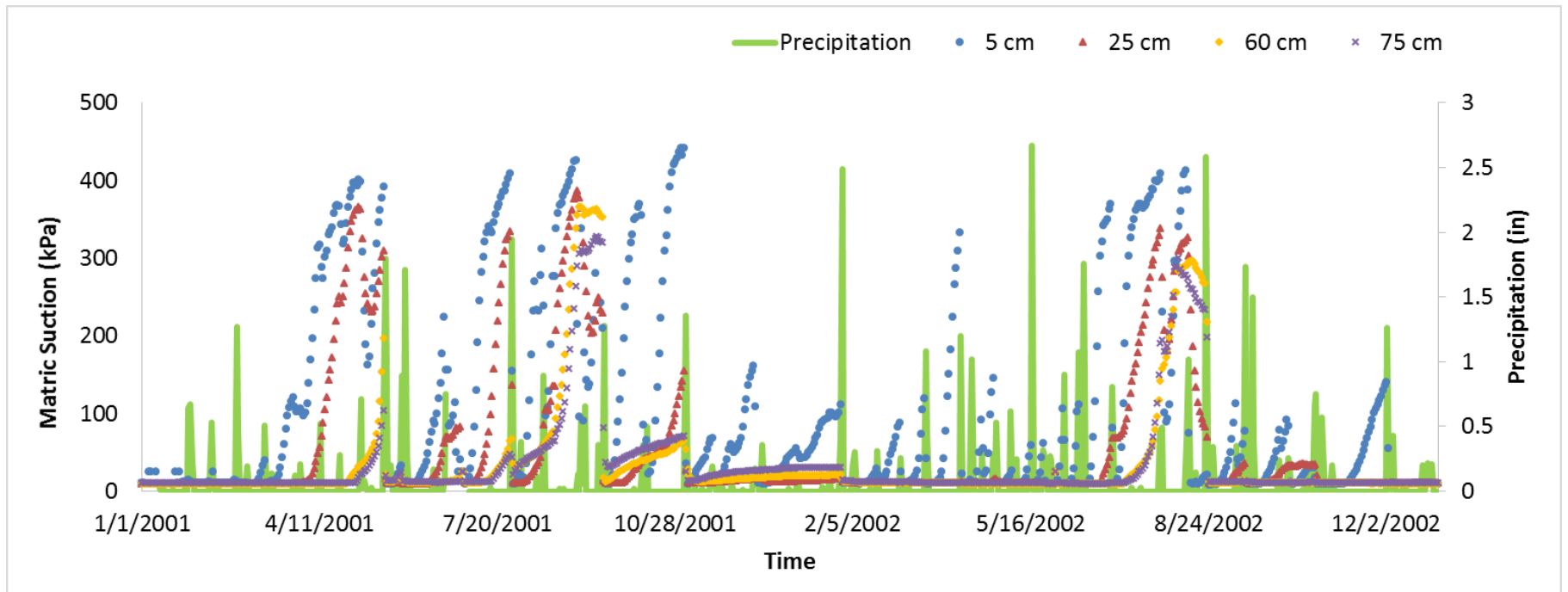


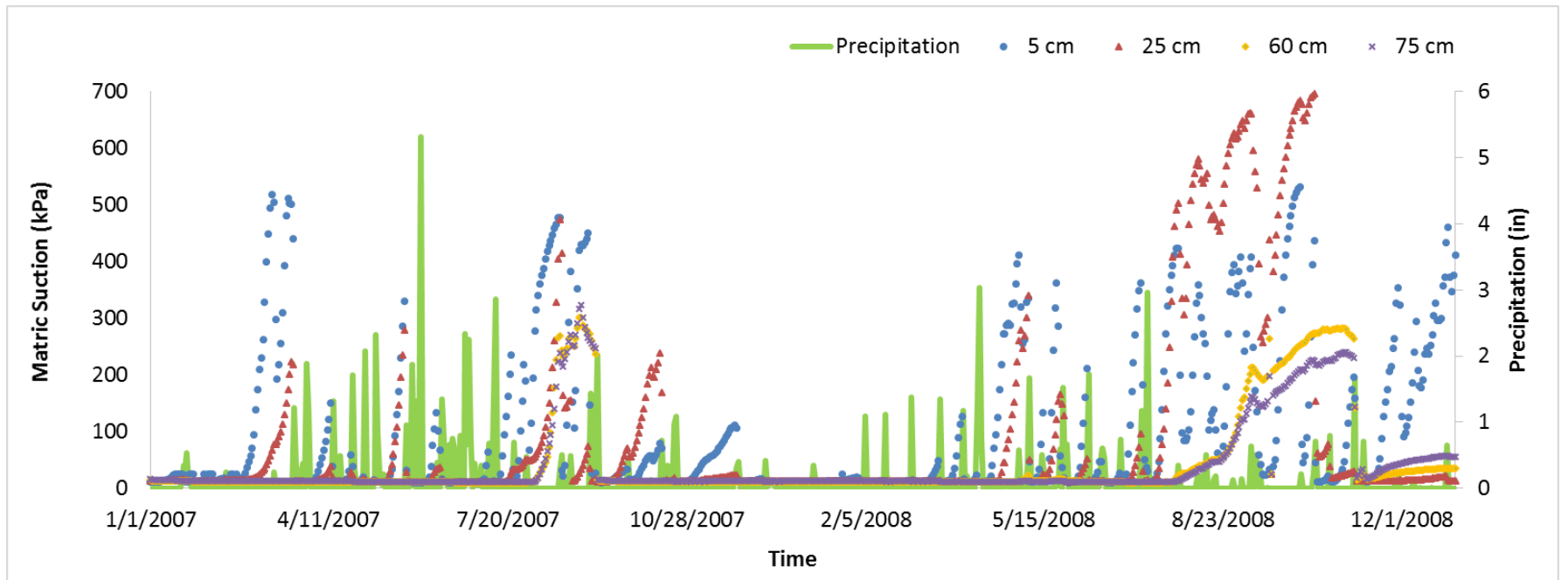
Figure 3.10.f Precipitation in 2011

Figure 3.10 Matric suction profile vs precipitation in Stillwater

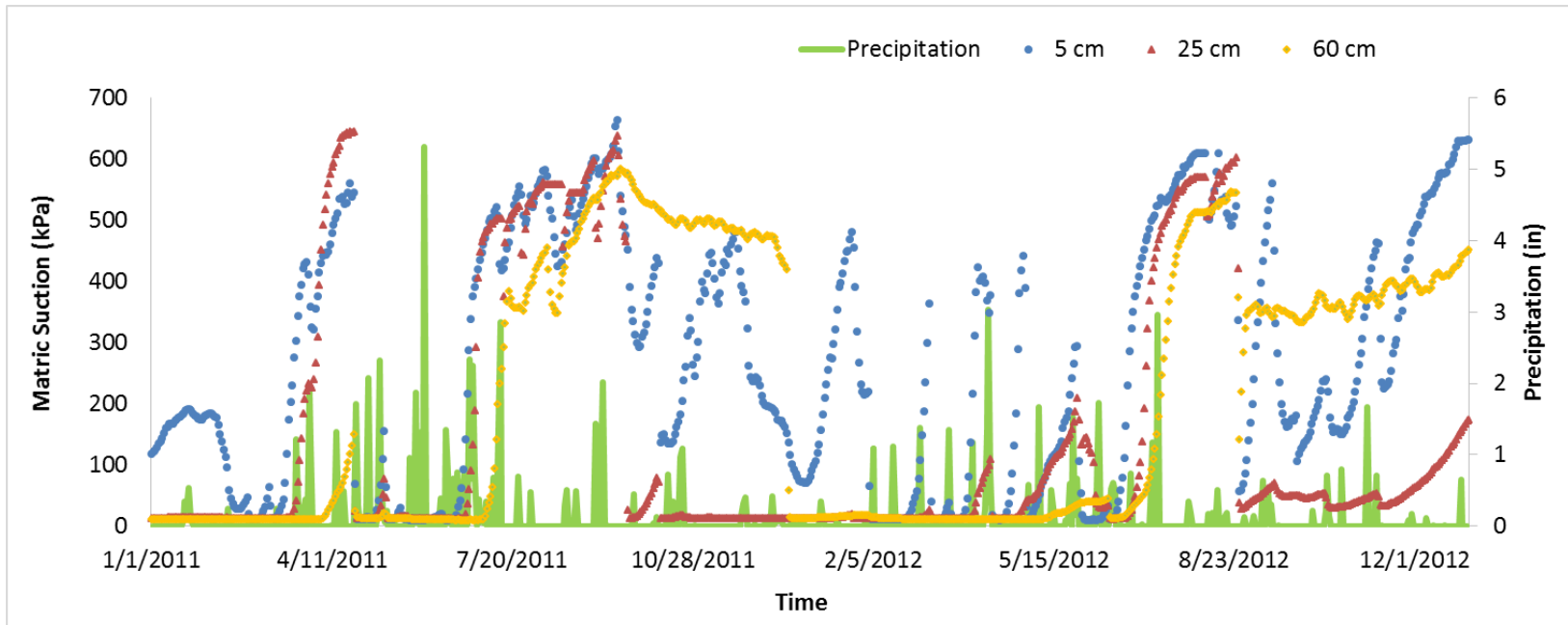
Figure 3.11 shows the temporal matric suction variation during different moisture periods. One dominant feature is that matric suctions measured at 5 cm and 25 cm are more dynamic than those at 60 cm and 75 cm, especially in spring. Matric suctions measured at 60 cm and 75 cm have very similar variation trend throughout the year. There is a time lag of the matric suction variation pattern with depth. The deeper the depth, the greater the time lag. This delay could be the time required for water to travel within soils (Nguyen et al. 2010). The annual average of matric suction is higher in dry years than that of in wet and average years. By analyzing the matric suction variation patterns in different years, it is proved that thermal conductivity sensors installed at the Oklahoma Mesonet provide durable and reliable measurements under harsh weather conditions.



3.11.a 2001-2002



3.11.b 2007-2008



3.11.c 2011-2012

Figure 3.11 Temporal matric suction variation vs precipitation in Stillwater

CHAPTER IV

DEPTH OF ACTIVE ZONE FROM FIELD DATA

This chapter discusses how to determine the evapotranspiration from climatic data and active zone depth from matric suction measured in the field. As discussed in the previous chapter, the active zone depth is a time and spatially dependent parameter and is a function of a wide range of variables such as climate, soil properties, and ground surface conditions. Of all the variables, evapotranspiration and infiltration are two of the most important variables (Durkee 2000). The purpose of this chapter is to analyze the pattern of evapotranspiration in Oklahoma and investigate how the evapotranspiration and matric suction can affect the active zone depth across Oklahoma. The calculation of evapotranspiration followed Penman-Monteith's equation. The calculation of the active zone depth was carried out in the following steps for each Mesonet station:

1. Estimate equilibrium suction and amplitude of suction variation from curve fitting by the Origin software;
2. Determine the diffusion coefficient using van Genuchten parameters and equilibrium suction;
3. Estimate maximum suction change;

4. Calculate active zone depth using the McKeen and Johnson (1990)'s equation based on parameters obtained in step 1-3;
5. Estimate active zone depth for places without Mesonet stations using the IDW interpolation method in the ArcGIS software.

The following sections will explain the procedures of calculating evapotranspiration and active zone depth in detail.

4.1 Evapotranspiration of Oklahoma

Evapotranspiration is an important factor in water resources and cycle. Evaluating the evaporative fluxes and water balances at the soil surface is a critical component in engineering practice. One significant effect of evapotranspiration on geotechnical engineering is soil-crack formation. During the process of evapotranspiration, especially in drying seasons, soil cracks can develop at the soil surface due to the change of soil-water content and other soil properties (Novak 1999). Evapotranspiration is the combination of evaporation from soil surface as well as transpiration from plants (Thorthwaite 1948). Changes in soil suction are mainly caused by moisture movement in soil, which is due to evaporation from the soil surface and transpiration from plants. In semi-arid regions, transpiration is a major cause of water loss from the soil surface. The spread of root systems is a major factor in soil swelling and shrinkage problems (Bell 1999). Evaporation and transpiration usually occur at the same time and there is no easy way to separate these two processes. Geotechnical engineers started to use the "potential evapotranspiration" back to the 1940s, when Thorthwaite (1948) first introduced this term. Potential evapotranspiration is the maximum possible amount of water that would come from soil and plant surfaces under prevailing weather conditions (Jensen et al. 1990). Actual evapotranspiration is the

actual amount of water, which has been evaporated. Actual evapotranspiration depends on (1) climatic factors; (2) soil types; (3) soil moisture contents; (4) vegetation types; and (5) land use; while potential evapotranspiration depends almost completely on the energy from the sun (Mather 1974). Actual evapotranspiration can be less than potential evapotranspiration (Fredlund et al. 2011).

The necessary conditions for evapotranspiration include a supply of heat, water, and a vapor pressure gradient (Hillel 2004). The existing methods of calculating evapotranspiration are based on climatic variables, such as air temperature, wind speed, solar radiation, and relative humidity. These climatic variables are also important in geotechnical engineering. For example, all these four variables are included in the mechanistic-empirical pavement design guide (MEPDG), a software that involves analysis of water and heat flow through pavement layers in response to climatic, soil, and boundary conditions above and below the ground surface in the pavement structure. As a result, improving the understanding of environmental interactions with pavement systems can predict the changes in pavement material properties over time. Soil parameters also play a significant role in evapotranspiration. Soil temperature, which governs physical, chemical, and biological processes in soil, is closely related to water in the atmosphere - soil cycle (Hillel 2004). Previous studies indicated that evapotranspiration will increase when soil surface temperature increases if other parameters are held constant (Tabari et al. 2012). Wetter soils tend to have a lower temperature than drier soils due to the process of evaporation (Qiu and Ben-Asher 2010). In addition to soil temperature, soil suction is also closely related to evaporation. Evaporation at unsaturated soil surfaces at a high suction is smaller than it is from saturated soil surfaces (Wilson et al. 1997). Wilson et al. (1997)

showed that the ratio between actual and potential soil evaporation decreased when the total suction of soil exceeded 3,000 kPa. In addition, Fredlund et al. (2011) demonstrated a number of different solutions that can be applied to calculate actual evaporation using soil suction. The consideration of the relationship between evaporation and soil surface suction is important in geotechnical engineering designs.

4.1.1 Data and ASCE-PM Method

Although direct measurement of evapotranspiration is possible, evapotranspiration is usually calculated by existing models. There are a variety of methods of estimating evapotranspiration. This research applies to the American Society of Civil Engineers Penman-Monteith (ASCE-PM) equation (Jensen et al. 1990) for calculating the standardized reference crop evapotranspiration. This equation has been recommended by Food and Agriculture Organization of the United Nations (FAO), and it has been well applied in research all over the world. Reference crop evapotranspiration, which was introduced by irrigation engineers, is “the rate at which water, if available, would be removed from the soil and plant surface of a specified crop, arbitrarily called a reference crop” (Jensen et al. 1990: 56-57). The equation is expressed as:

$$ET_{SZ} = \frac{0.408 \Delta (R_n - G) + \gamma c_n u_2 (e_s - e_a) / (T + 273)}{\Delta + \gamma (1 + C_d u_2)} \quad (4.1)$$

where ET_{SZ} = standardized reference crop evapotranspiration (mm/day);

R_n = net radiation at the crop surface (MJ/m²/day);

G = soil heat flux density at the soil surface (MJ/m²/day);

T = mean daily air temperature at 1.5 to 2.5-m height ($^{\circ}\text{C}$);

u_2 = mean daily wind speed at 2-m height (m/s);

e_s = mean saturation vapor pressure at 1.5 to 2.5-m height (kPa);

e_a = mean actual vapor pressure at 1.5 to 2.5-m height (kPa);

Δ = slope of the vapor pressure-temperature curve (kPa/ $^{\circ}\text{C}$);

γ = psychrometric constant (kPa/ $^{\circ}\text{C}$);

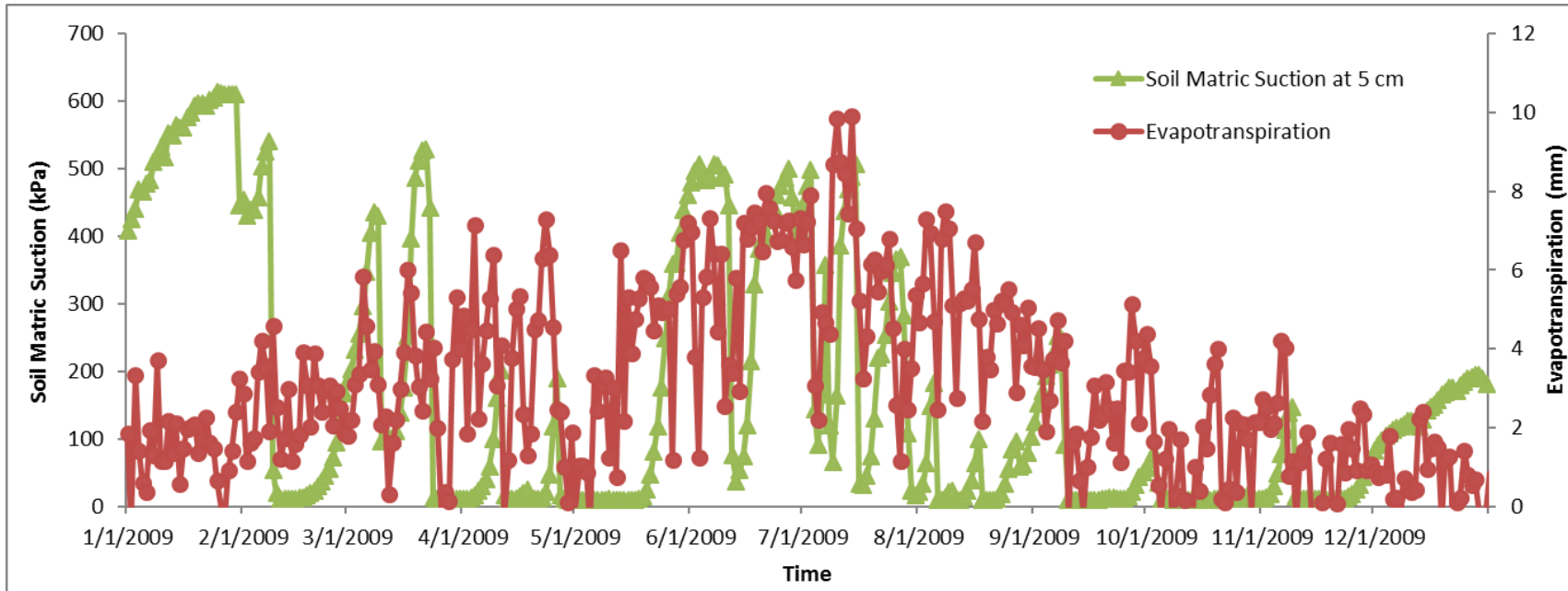
C_n = numerator constant for reference type (900 for short reference crop),

C_d = denominator constant for reference type (0.34 for short reference crop).

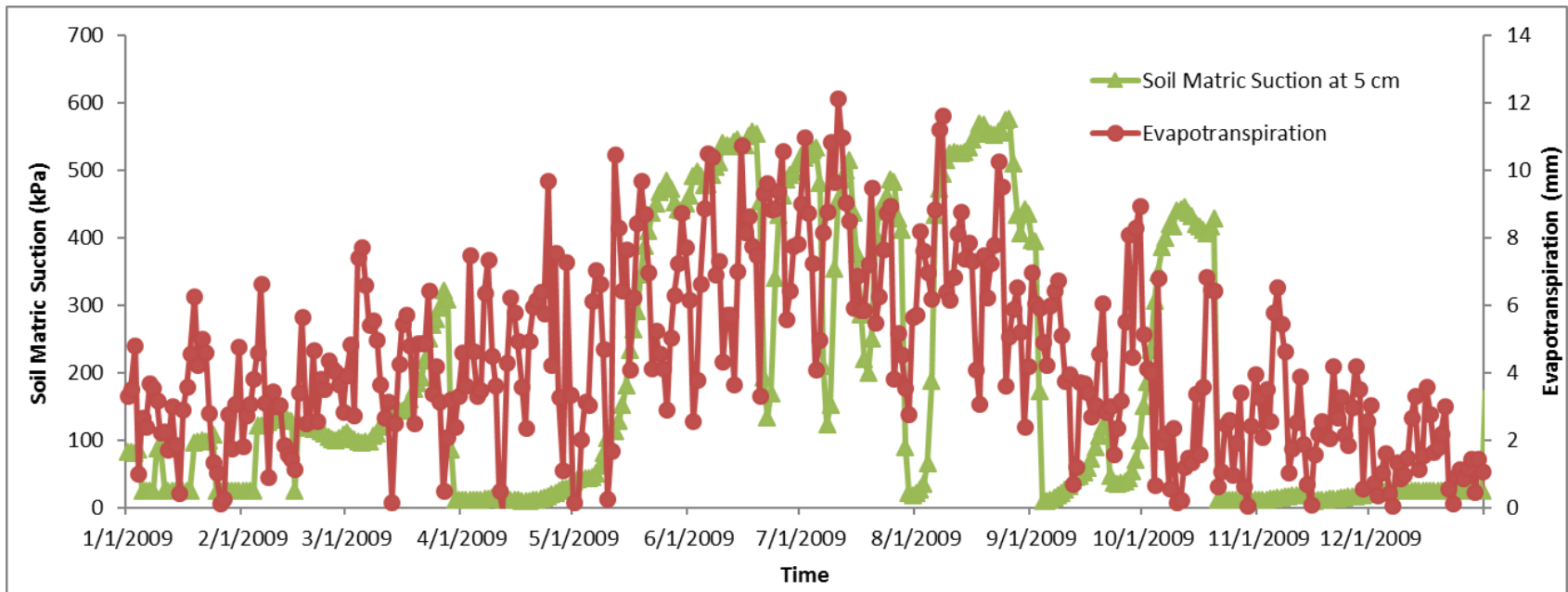
Detailed procedures of evapotranspiration calculated using Equation 4.1 are listed in Appendix B.

To use Equation 4.1 for the calculation of evapotranspiration, the following daily meteorological data from 1998 to 2013 were collected from the 74 Oklahoma Mesonet stations selected in this research: temperature (including minimum, maximum, and dew point temperature), wind speed, and solar radiation. In addition, weather station sea level and latitude were also required. Figure 4.1 shows the temporal variation of evapotranspiration versus matric suction measured at 5-cm depth in three Mesonet stations in 2009. The three stations are located in central, eastern, and western Oklahoma, respectively, representing different moisture conditions in Oklahoma. The reason why matric suction measured at 5-cm depth was used for comparison is that the shallower depths respond at a faster rate to the near-surface conditions (Illston et al. 2008). All of the

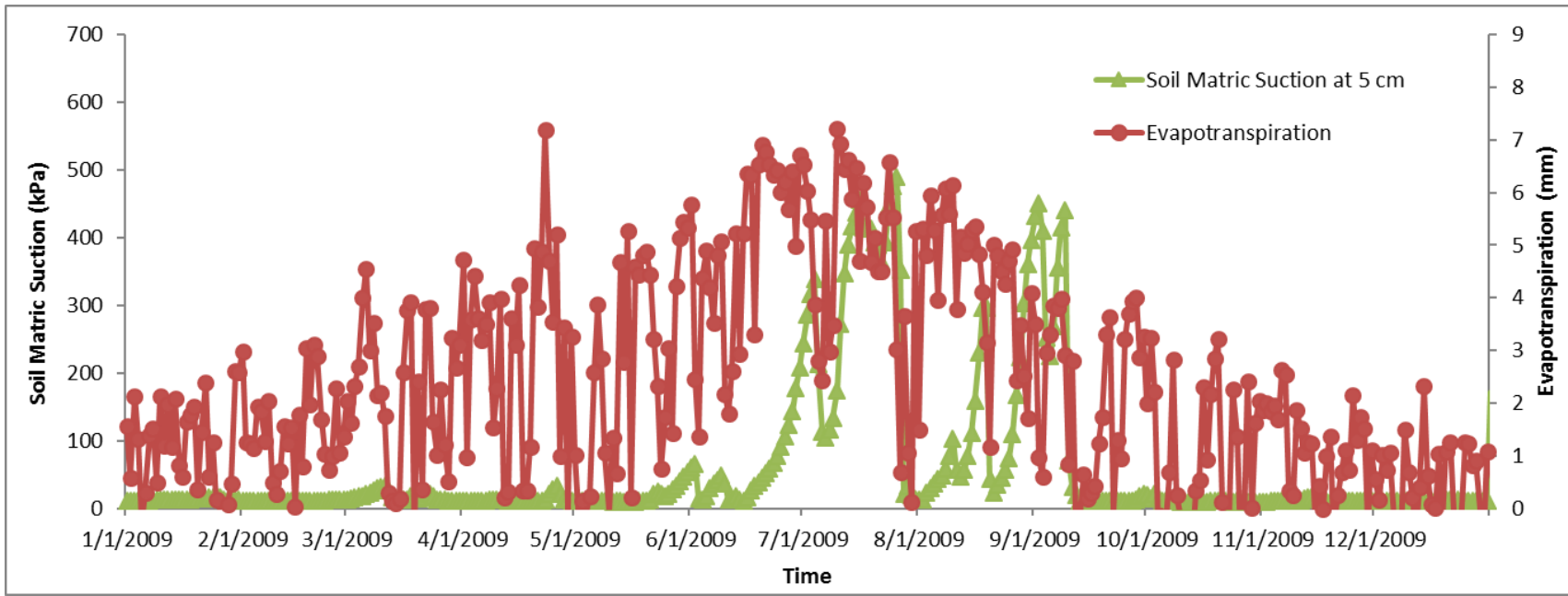
three stations indicate a higher evapotranspiration and a higher matric suction during the growing season.



4.1.a Stillwater, central Oklahoma



4.1.b Boise City, western Oklahoma



4.1.c Wister, eastern Oklahoma

Figure 4.1 Evapotranspiration vs. matric suction in 2009

4.1.2 Spatial Distribution of Evapotranspiration

The distribution of average annual evapotranspiration (mm/year) is presented in Figure 4.2. The distribution pattern is opposite to precipitation distribution across Oklahoma. The annual precipitation decreases from the east to the west, while the annual evapotranspiration increases. The average annual evapotranspiration varies from 943 mm at the Cloudy station in the southeast of Oklahoma to 1722 mm at Goodwell station in the panhandle area of Oklahoma. The distribution of evapotranspiration is an indicator of the combined effect of the climatic parameters in Equation 4.1. Based on the analysis of climatic data from 1998 to 2013, the higher values of evapotranspiration in the west of Oklahoma are primarily due to the higher solar radiation, higher wind speed, and lower relative humidity.

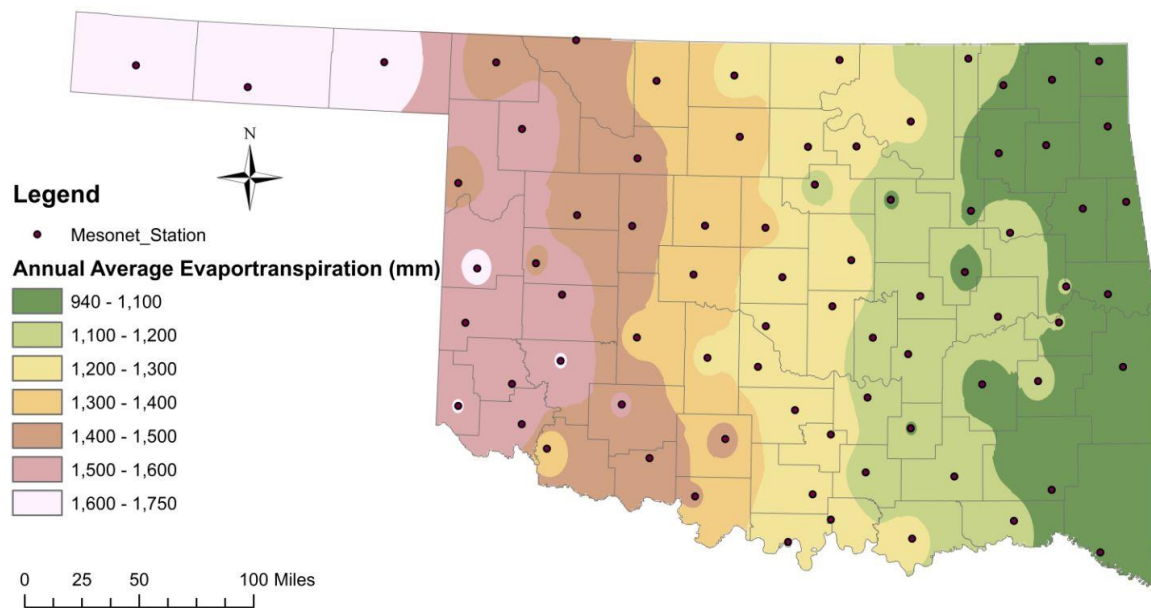


Figure 4.2 Spatial distribution of average annual evapotranspiration in Oklahoma

The Oklahoma Mesonet provides daily-standardized reference evapotranspiration for short and tall canopies. Figure 4.3 shows the spatial distribution of daily evapotranspiration on July 5, 2016. The annual and daily evapotranspiration in Oklahoma have similar spatial distribution pattern, which is low in eastern area and high in western and panhandle area.

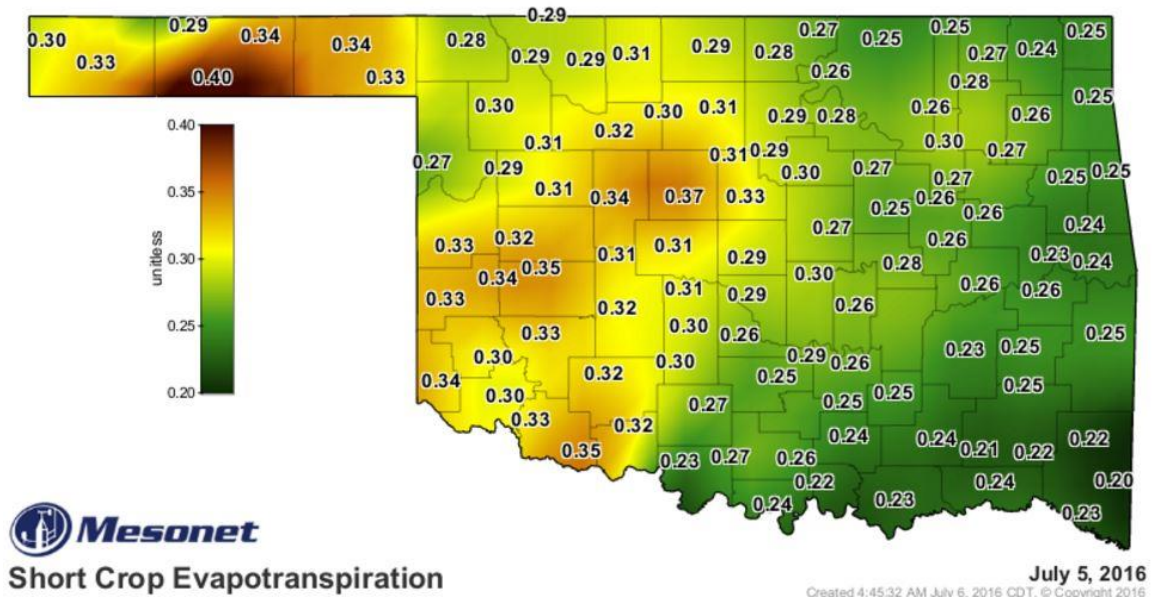


Figure 4.3 Spatial distribution of daily evapotranspiration in Oklahoma
(The Oklahoma Mesonet 2016)

4.2 Seasonal Variation of Matric Suction

The curve fitting method is used to analyze the sinusoidal pattern of matric suction variations. Curve fitting constructs a curve and/or mathematical function to best fit a series of data points. Origin software (OriginLab Corporation, Northampton, MA) was used to complete curve fitting process. Origin is a scientific graphing and data analysis software. It has a nonlinear curve fitting tool that includes more than 200 built-in fitting functions. The function for sinusoid fitting is

$$y = y_0 + A \cdot \sin\left(\pi \frac{x - x_c}{\omega}\right) \quad (4.2)$$

where y_0 = offset

A = amplitude

x_c = phase shift

ω = period

By comparing Equation 2.3 and Equation 4.2, y_0 is the equilibrium suction (U_e); A is the amplitude of suction variation (U_0); $\frac{365}{2\omega}$ is the frequency number, which is the number of wetting and drying cycles per year (n); the determination of diffusion coefficient will be explained in Section 4.3. Figure 4.4 shows the sample curve created by a sine function fitting. By inputting a series of matric suction data, the software offers the fitting equation in the form of Equation 4.2 for each station. In addition to the fitting equation, the Origin software also provides the statistical summary of the model including the R-square. The R-square is a measurement of how closely the data are fitted to the regression line.

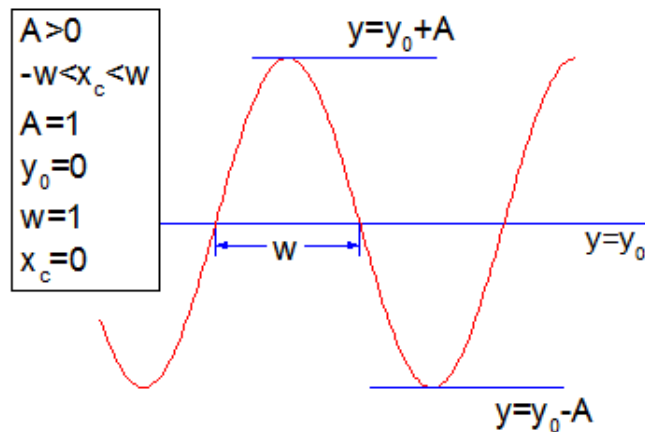


Figure 4.4 Sample curve fitting in Origin software

The frequency number, n , cycles/year, is an important site-dependent variable when determining the active zone depth. Based on the value of n , McKeen and Johnson (1990) suggested a relationship between the frequent number and potential active zone depth shown in Table 4.1. When the value of n becomes smaller, a moisture change occurs over a longer time interval, and the active zone depth becomes larger.

Table 4.1 Relationship between frequent number and potential active zone depth (McKeen and Johnson 1990)

Frequency, n (cycles/year)	Years/cycle	Potential Active Zone depth
≤ 0.5	≥ 4	Design case
0.5	2	Deep
0.75	1.33	Moderate
1	1	Shallow
≥ 1.25	≤ 0.8	Unstable climate

It is difficult to use one single sinusoidal equation to represent long-term variations of suction. Some research simplified the dataset by separating the long-term data into short-term data and paying attention to specific short-term data. Visser et al. (2006) used 20 years (1980 – 2000) of daily phreatic surface depth and daily meteorological data to forecast water table depth and soil moisture profiles. In their research, in order to test model performance, they selected three sets of 5-year periods, which can be considered as representing relative dry, average, and relative wet climate conditions. Similar to Visser et al.'s (2006) method, based on the duration of data, this study will select three 2-year periods to represent relatively dry, average, and relatively wet conditions. Figure 4.5 shows the statewide annual total precipitation from 2000 to 2014. According to the Oklahoma Climatological Survey, the statewide average annual precipitation from 1895 to 2009 was

33.6 in. Three sets 2-year periods are 2001-2002 (average), 2007-2008 (relatively wet), and 2011-2012 (relatively dry).

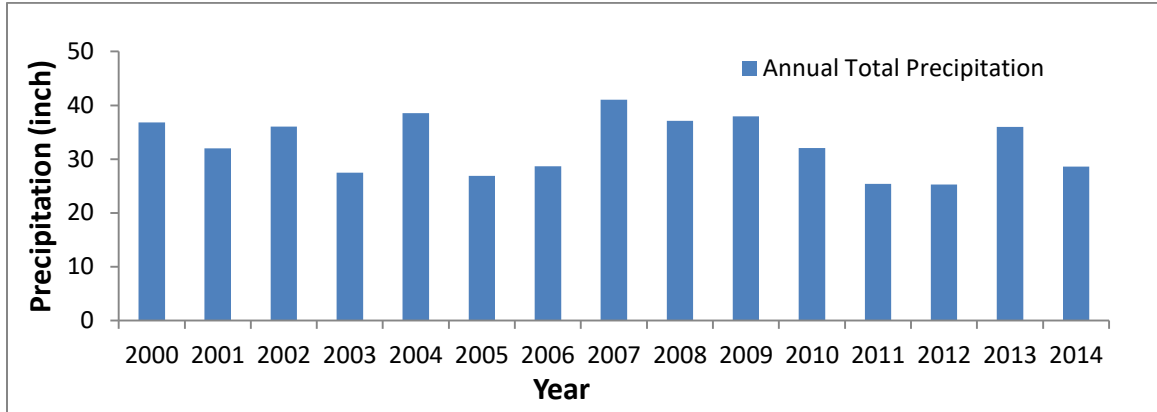


Figure 4.5 Statewide annual total precipitation

4.2.1 Dry Period

The Oklahoma Mesonet decommissioned sensors at 75 cm depth in January 2011, however, archived data at 75 cm depth before 2011 is still available (Scott et al. 2013). As a result, for the analysis of dry period (2011-2012), matric suction measured at 60 cm depth is the deepest data available and they were used for curve fitting. To keep the consistency of analysis, matric suction data for average (2001-2001) and wet (2007-2008) periods were also measured at 60-cm depth. However, it should be noted that geotechnical engineers are more interested in suction at a deeper depth than at or near the soil surface, usually from a few tens of centimeters down to 5 meters, since the deeper depths are less affected by the surface conditions and the more stable performance of suction.

Of all the 74 stations selected in this research, 54 stations have sensors installed at 60 cm depth. The matric suction data from 2011 to 2012 of 54 stations were input individually into Origin software for curve fitting. After the fitting process, by comparing the fitting

curve and actual measured points for each station, stations with an R-square larger than 0.5 were selected for further calculation of the active zone depth. There is no general rule of what values of R-square are high, adequate or low. In some pipeline constructions in geotechnical engineering, an R-square of pipeline repair rate and ground velocity larger than 0.7 was considered as acceptable (O'Rourke and Bonneau 2007). Figure 4.6 shows 38 stations that have an R-square larger than 0.5 from the fitting models. Figure 4.7 shows measured matric suction data and fitting curves for four stations (ARD2 and COPA are located in the eastern Oklahoma; HOBA and ARNE are located in the western Oklahoma). When doing the curve fitting, the unit of matric suction was converted from kPa to pF, since the matric suction in pF is the logarithmic form. A logarithmic form is more useful when the rate of change in the data increases or decreases quickly.

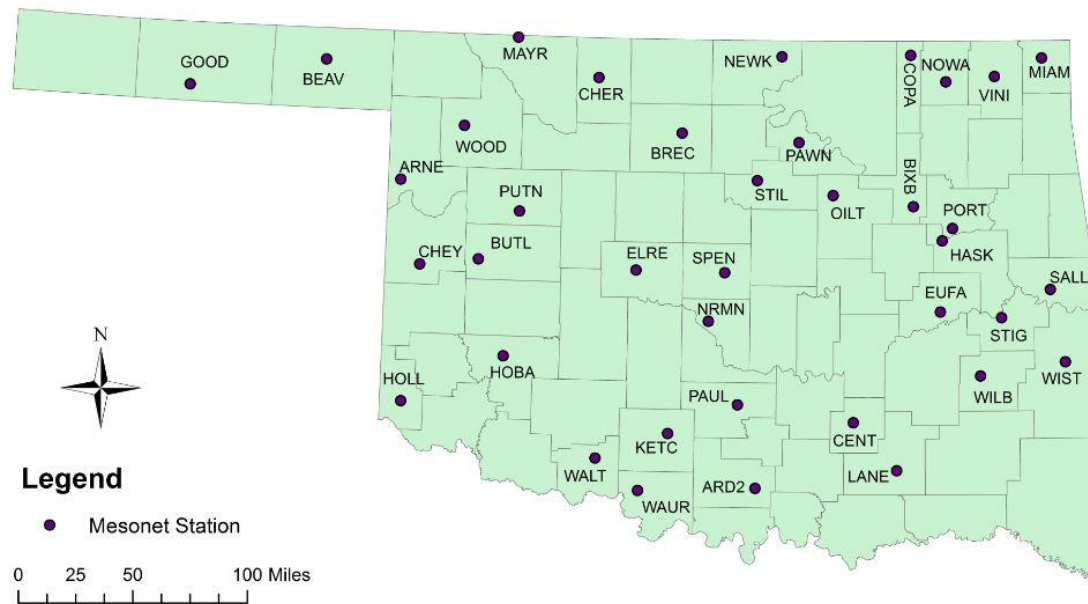
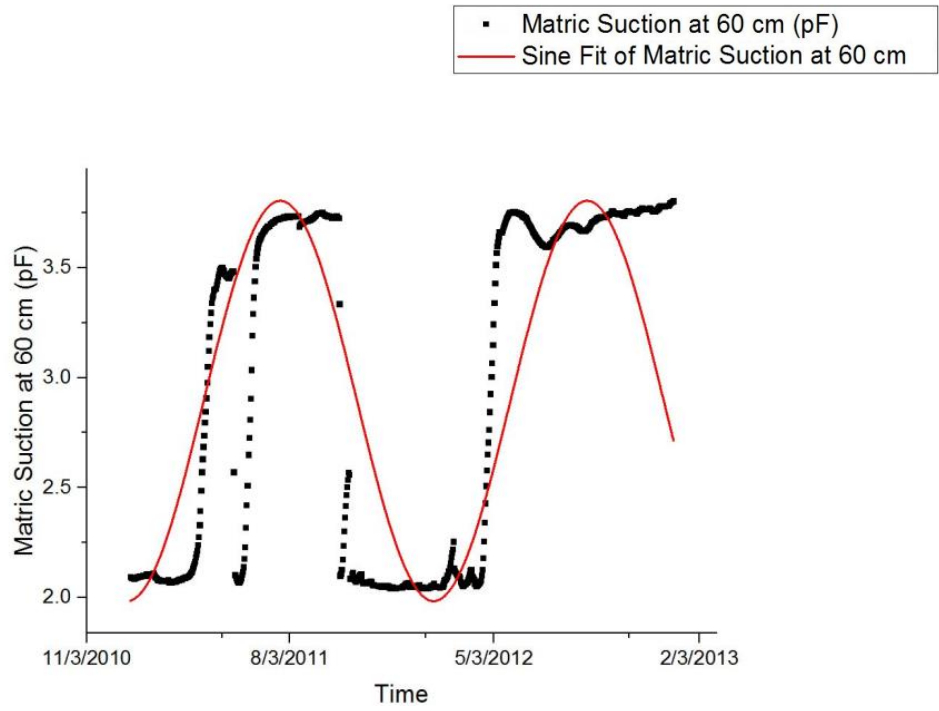


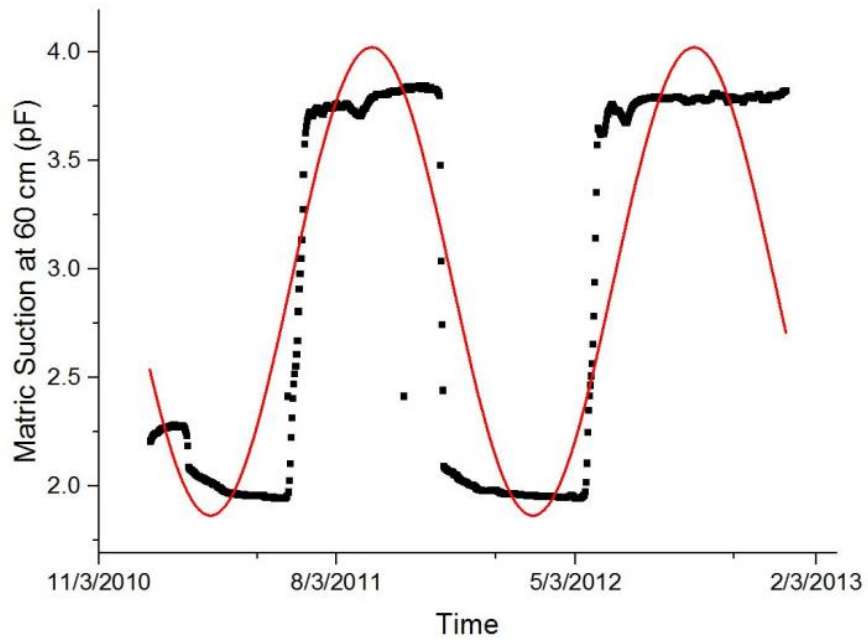
Figure 4.6 Stations selected to calculate the active zone depth for the dry period

In the curves shown in Figure 4.7, approximately one cycle per year ($n=1$) is represented, which means there is one dry and one wet season in one year. However, the

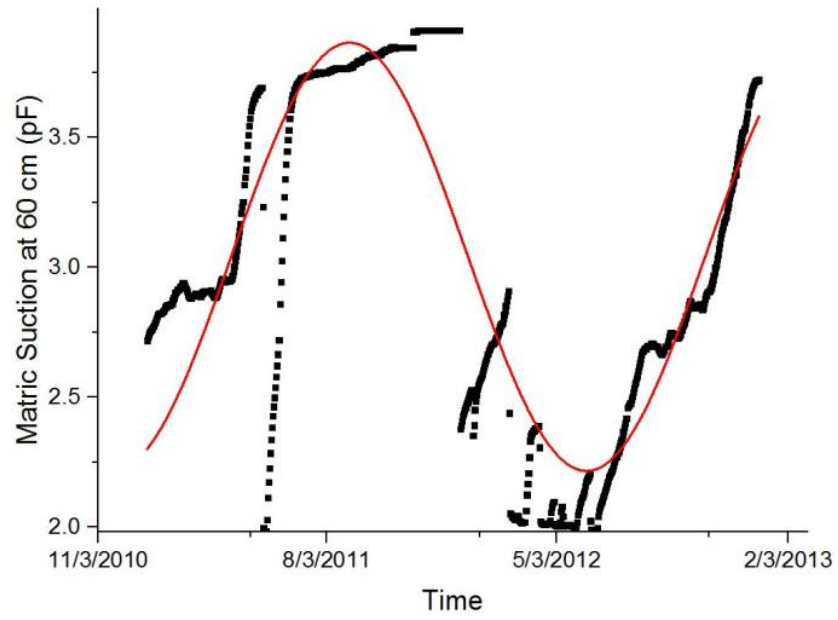
number of cycles can change from year to year. Detailed values of parameters for each station are listed in Appendix C. The State of Oklahoma experienced an extreme to exceptional drought during 2011-2012. In February 2011, the eastern part of the state received a high amount of precipitation in the form of severe snowstorms. Figure 4.7 listed the fitting curves for four stations located in different parts of Oklahoma. As shown in Figure 4.7, ARD2 and COPA, which are located in the eastern half of the state, had lower matric suction during February and March in 2011. The tremendous early summer heat in 2011 accelerated the drought. According to data from the Oklahoma Mesonet, the May 24-June 22, 2011 statewide average precipitation total was 1.24 inches, 3.23 inches smaller than the average and the driest such period in Oklahoma since 1921. The extreme heat continued in July and August. Fortunately, the drought was relieved from the precipitation in winter and early spring. The October 2011-March 2012 period was the 13th wettest since 1895. March 2012 was the sixth wettest on record. However, the drought-relief precipitation disappeared in April, when the state's primary rainy season begins. Drought hit the state once again in the summer of 2012, and wasn't relieved until February 2013. All of four stations in Figure 4.7 show high matric suction in the winter of 2012.



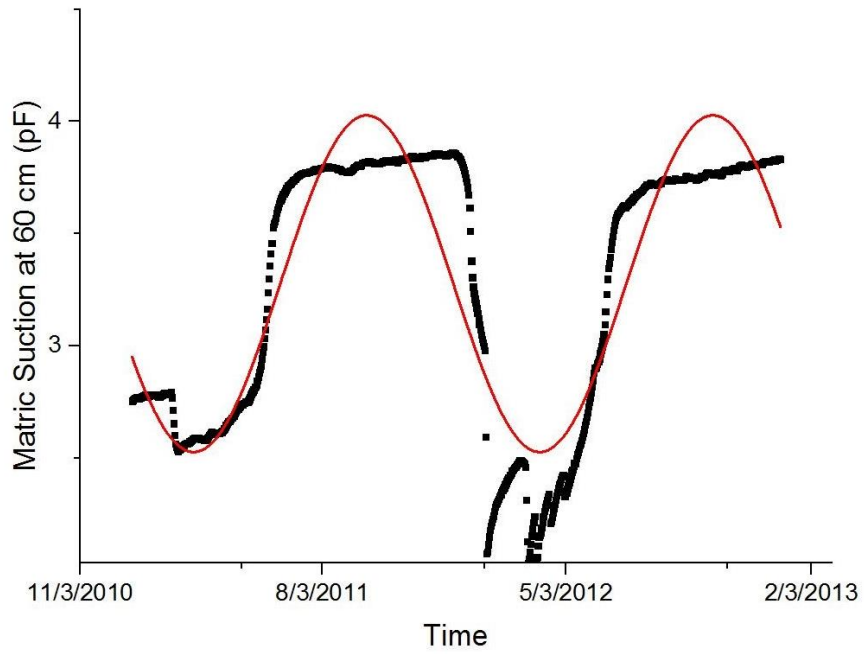
4.7.a ARD2 Station, $R^2 = 0.66$, $n = 0.89$ cycles/year



4.7.b COPA Station, $R^2 = 0.79$, $n = 0.99$ cycles/year



4.7.c HOBA Station, $R^2 = 0.74$, $n = 0.65$ cycles/year



4.7.d ARNE Station, $R^2 = 0.83$, $n = 0.94$ cycles/year

Figure 4.7 Curve fitting for dry period

Figure 4.8 shows the spatial distribution of equilibrium matric suction determined by the curve fitting during the dry periods. Equilibrium suction represents the suction a soil has when it reaches equilibrium with its environment. If the soil suction does not change with time at a given combination of water vapor pressure and air temperature, the soil has reached the equilibrium suction at that water vapor pressure and air temperature. At equilibrium suction, the soil neither gains nor loses moisture. The experimental determination of equilibrium suction is difficult due to hysteresis, initial soil moisture content, and test techniques (Kumaran et al. 2007).

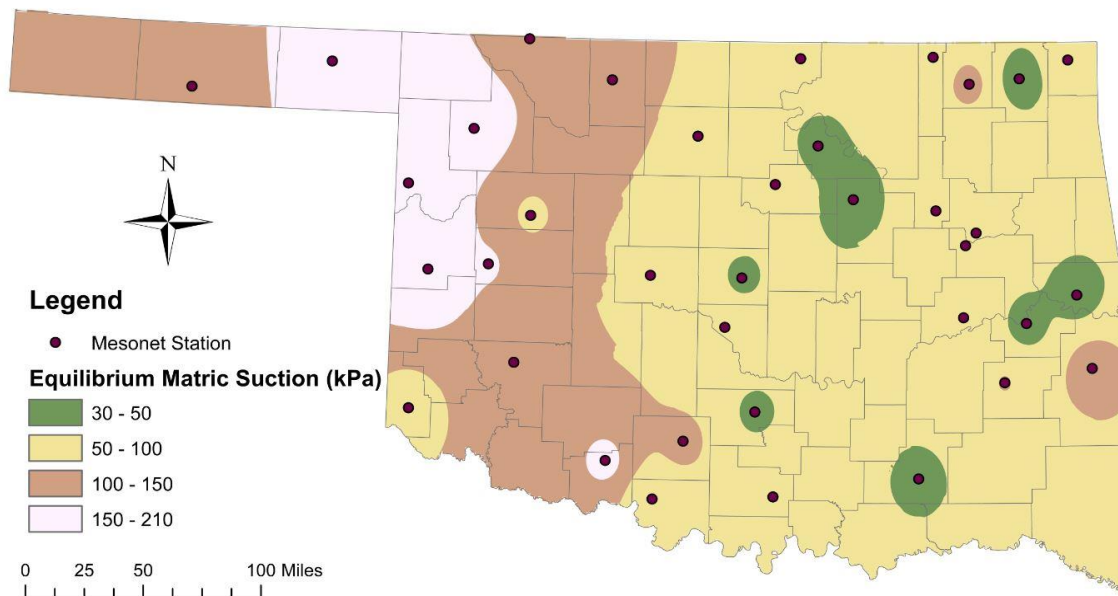


Figure 4.8 Spatial distribution of equilibrium matric suction during dry period

4.2.2 Wet Period

Figure 4.9 displays 18 stations with an R-square larger than 0.5 in the curve fitting process for the active zone depth calculation. Figure 4.10 shows measured matric suction data and fitting curves for four stations, located in northern and southern Oklahoma. Compared to those in the dry period, the frequent number of stations in wet period is a little

higher, which is consistent with the guidance provided by McKeen and Johnson (1990). Similar to the dry period, during the wet period, May has the lowest matric suction, and September to October has the highest matric suction. Spatial distribution of equilibrium matric suction is also similar to the dry period as shown in Figure 4.11. However, equilibrium matric suction is lower during wet periods than that during dry periods.

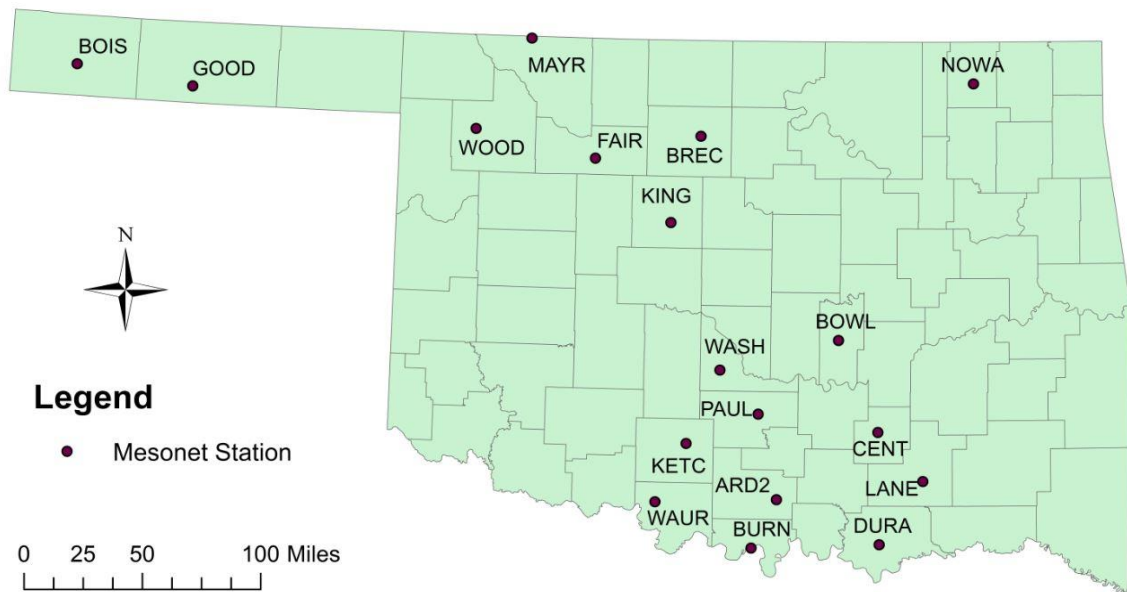
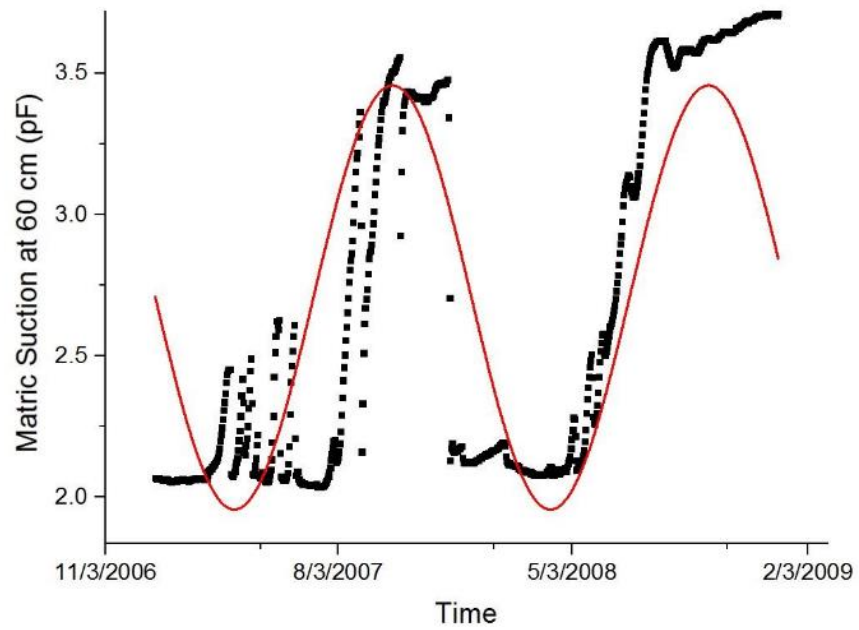
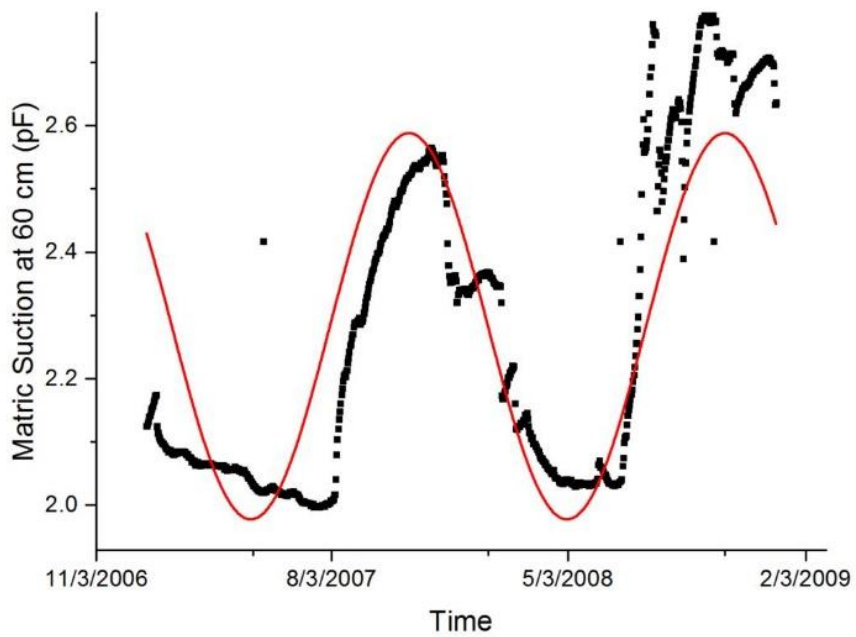


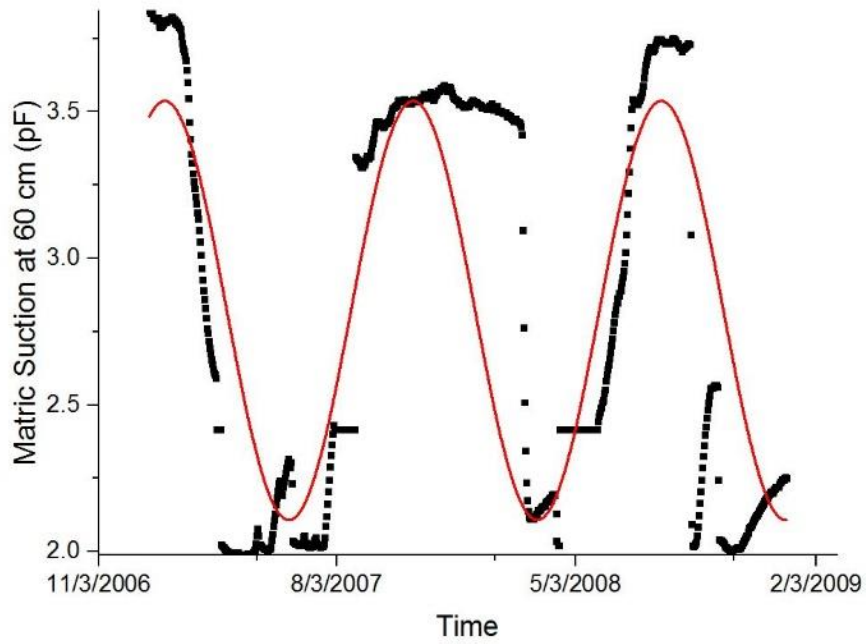
Figure 4.9 Stations selected to calculate the active zone depth for wet period



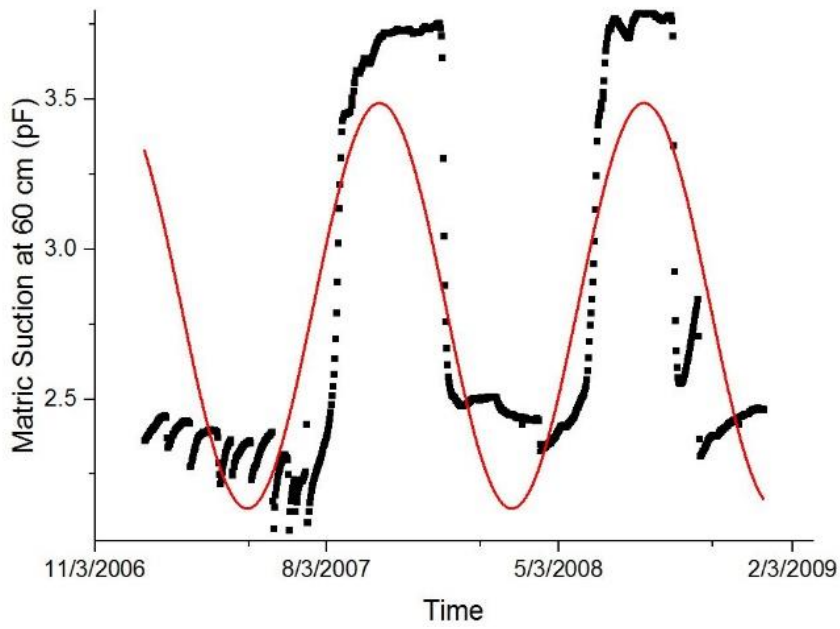
4.10.a ARD2 Station, $R^2 = 0.66$, $n = 0.99$ cycles/year



4.10.b CENT Station, $R^2 = 0.72$, $n = 1.00$ cycles/year



4.10.c MAYR Station, $R^2 = 0.56$, $n = 1.28$ cycles/year



4.10.d WOOD Station, $R^2 = 0.62$, $n = 1.17$ cycles/year

Figure 4.10 Curve fitting for wet period

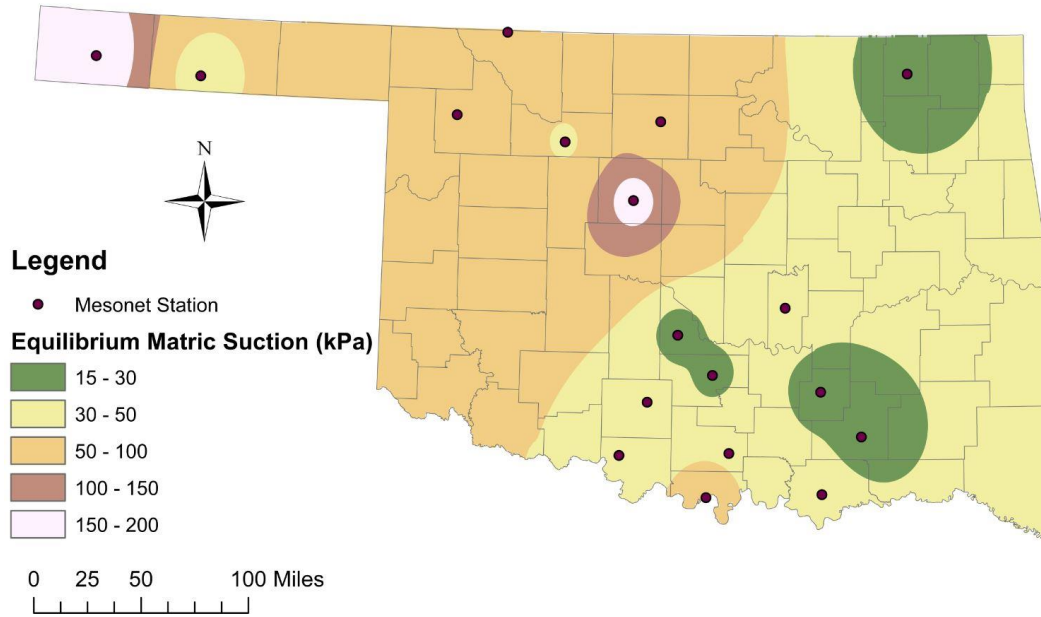


Figure 4.11 Spatial distribution of equilibrium matric suction during wet period

4.2.3 Average Period

27 stations with an R-square larger than 0.5 in the curve fitting process were selected for the active zone depth calculation for the average period as shown in Figure 4.12. Of all the 27 stations, there are six stations with an n value smaller than 0.6: BUTL, MAYR, ERIC, ARNE, CHER, BEAV, all of which are located in the western Oklahoma. The smaller n value is a result of drought in western Oklahoma in 2001-2002. However, southeastern Oklahoma was above the annual average precipitation in 2001. The drought in western Oklahoma began in early summer of 2001, and continued through mid-summer of 2002 (The Oklahoma Climatological Survey 2002). Due to the severe drought, the matric suction stayed high from approximately July 2001 to July 2002 as shown in Figure 4.13.c. Figure 4.14 shows the spatial distribution of equilibrium matric suction during the average period, which is similar to the dry and wet periods.

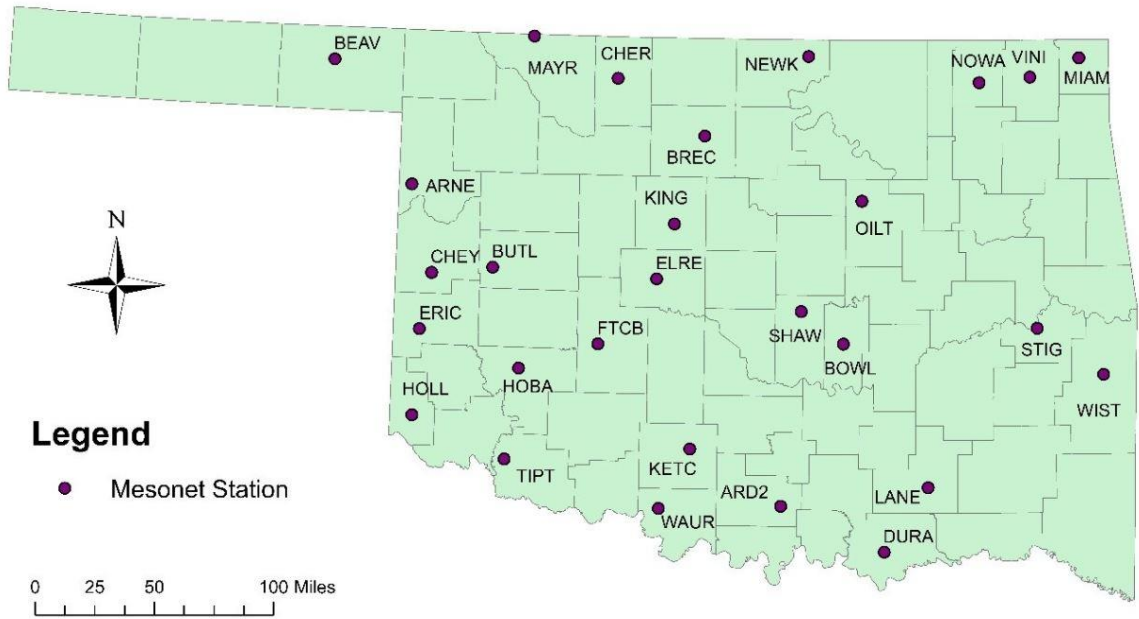
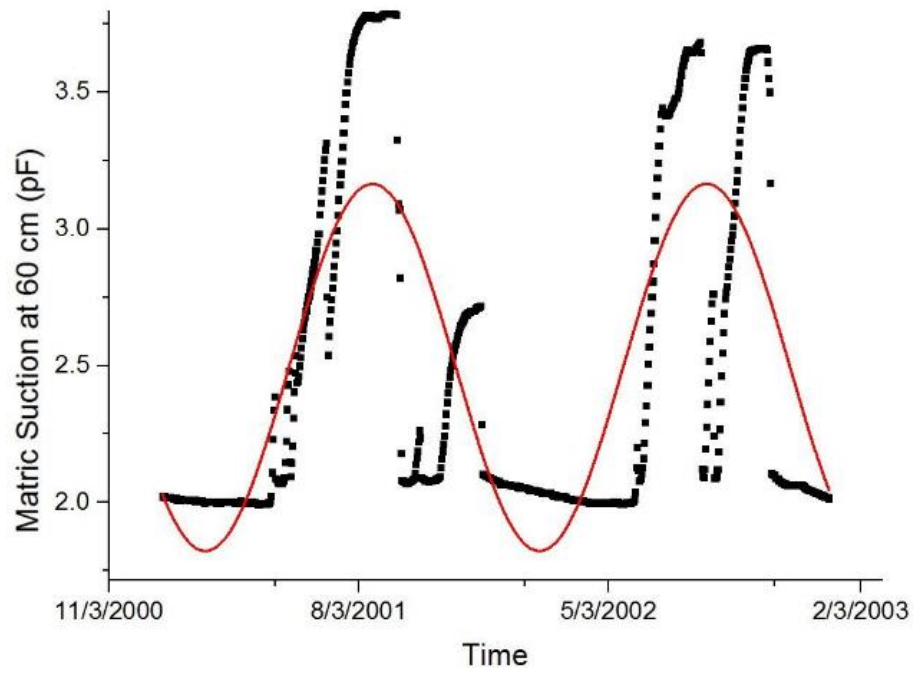
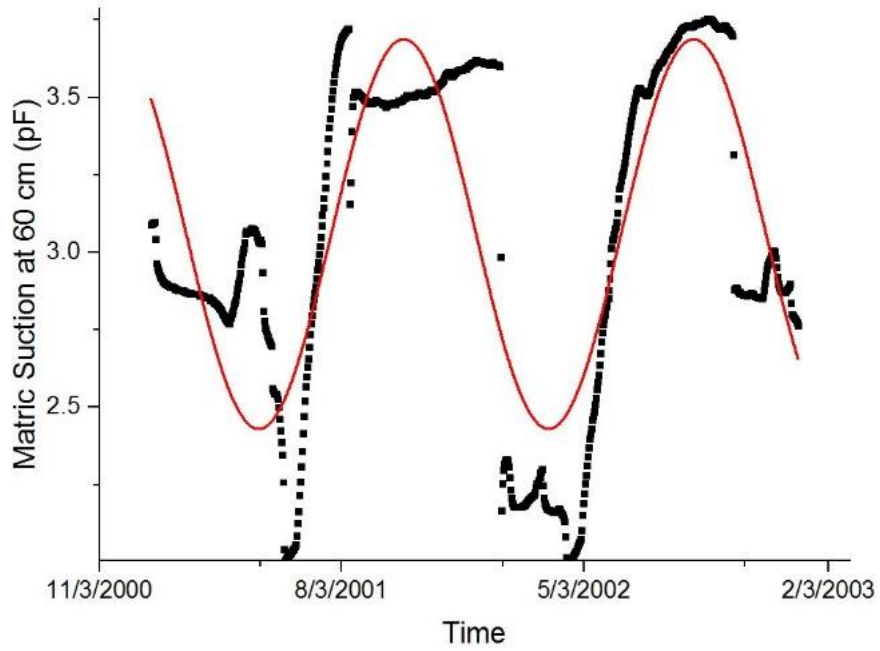


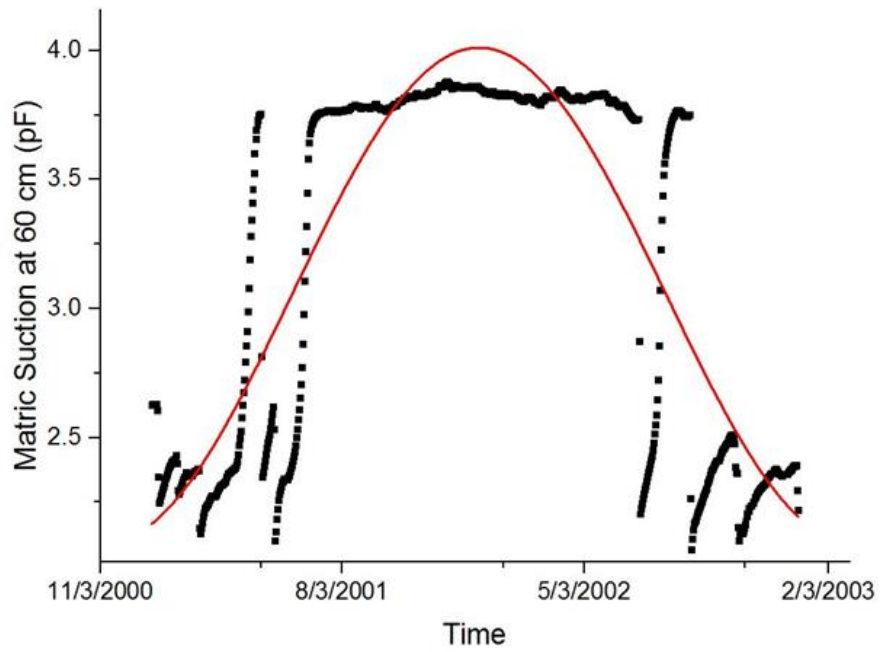
Figure 4.12 Stations selected to calculate the active zone depth for average period



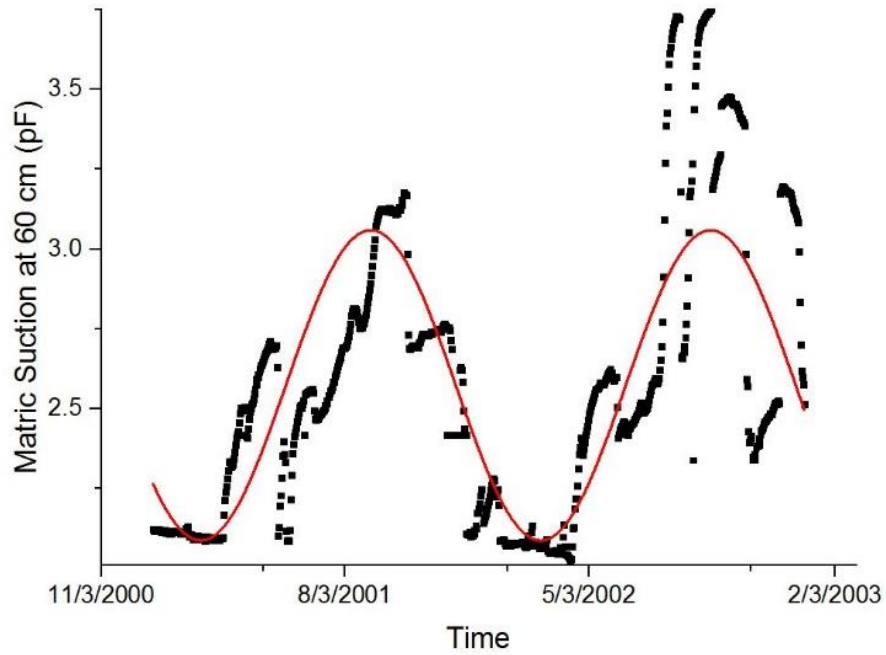
4.13.a ARD2 Station, $R^2 = 0.56$, $n = 1.00$ cycles/year



4.13.b HOBA Station, $R^2 = 0.65$, $n = 1.12$ cycles/year



4.13.c ERIC Station, $R^2 = 0.75$, $n = 0.43$ cycles/year



4.13.d STIG Station, $R^2 = 0.61$, $n = 0.96$ cycles/year

Figure 4.13 Curve fitting for average period

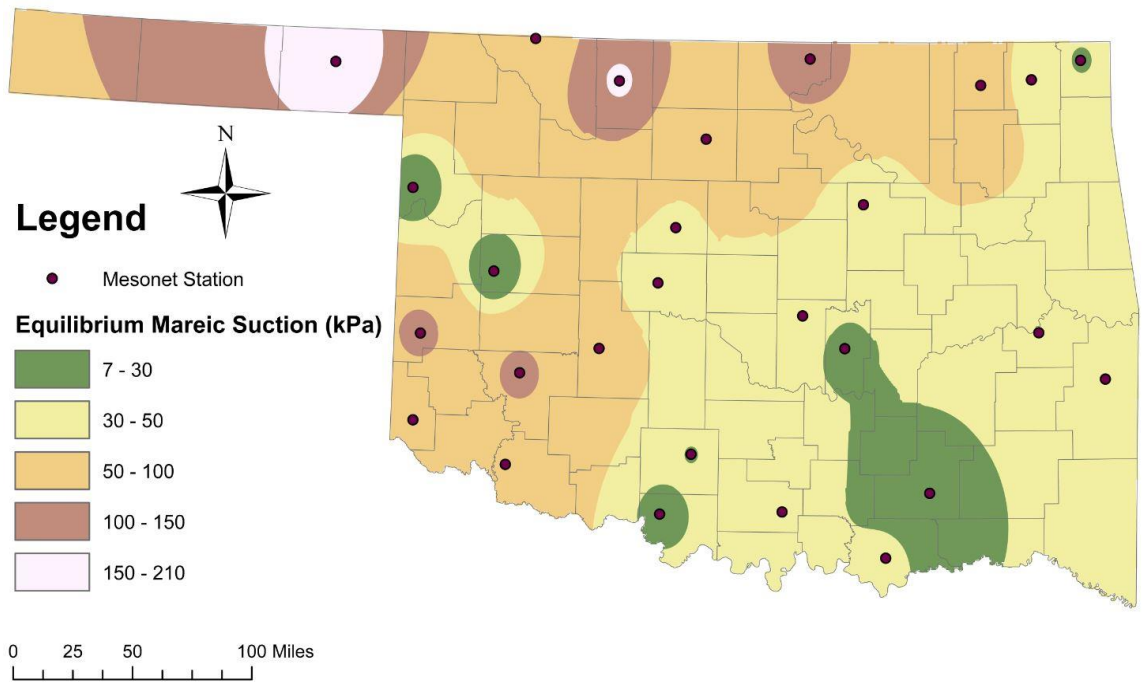


Figure 4.14 Spatial distribution of equilibrium matric suction during average period

4.2.4 Summary

By comparing the number of stations with an R-square larger than 0.5 in the curve fitting process, it indicates that Mitchell's sinusoidal periodic suction variation works better in dry periods than in wet periods, since during wet period the moisture fluctuation is more frequent. The equilibrium suction is controlled by the climatic conditions, and it tends to be higher during dry periods.

The plots of matric suction values of most of Mesonet stations indicate seasonal trends during a given period. These time series plots provide comparisons of wetting and drying trends. Illston et al. (2004) evaluated the annual cycle of soil moisture conditions by using time series plots of fractional water index (FWI), a measure of soil moisture index derived from Campbell Scientific 229-L sensor. The statewide-averaged time series of FWI values indicate four distinct phases of soil moisture conditions: (1) the moist plateau phase: this phase occurs between November to mid-March, when soil has the highest amount of moisture throughout a year; (2) the transitional drying phase: this phase occurs between mid-March to mid-June, when Oklahoma is under wet season and evapotranspiration becomes higher; (3) the enhanced drying phase: this phase occurs in July and August, due to the end of precipitation season and increased evapotranspiration, soil moisture has a steep decline in this phase; and (4) the recharge phase: this phase occurs between late August to November due to the moisture obtained from the autumn precipitation (Illston et al. 2004).

By examining the time series plots of matric suction, most of Mesonet stations reveal the similar pattern of the distinct moisture phases defined by Illston et al. (2004). Since this research evaluated the matric suction at 60 cm depth, there is a time lag between the

precipitation and matric suction at a deeper depth. The response time between the 5-cm depth and 60-cm depth is approximately three weeks (Illston et al. 2004). Matric suction is low between November to March and starts to increase between April to July. Matric suction reaches the maximum in August and September and starts to decline in October.

4.3 Determination of Diffusion Coefficient

To calculate the active zone depth, diffusion coefficient must be determined first. The soil diffusion approach is relatively new in geotechnical practice, so only a little research on soil diffusivity has been conducted in geotechnical engineering. Since the diffusion coefficient is one of the factors that influence the matric suction variation, a good engineering judgement on the diffusion coefficient is necessary. This research applied Mitchell's (1979) seasonal soil suction variation approach to determine the diffusion coefficient. Equations 2.3 and 2.4 indicate that matric suction at any depth decreases as a function of the diffusion coefficient. The matric suction at the depth y lags behind that at the soil surface ($y=0$) by a time equal to

$$t = \frac{y}{2} \sqrt{\frac{1}{\alpha \pi n}} \quad (4.3)$$

where t = time lag in matric suction between two depths

y = depth measured from the soil surface

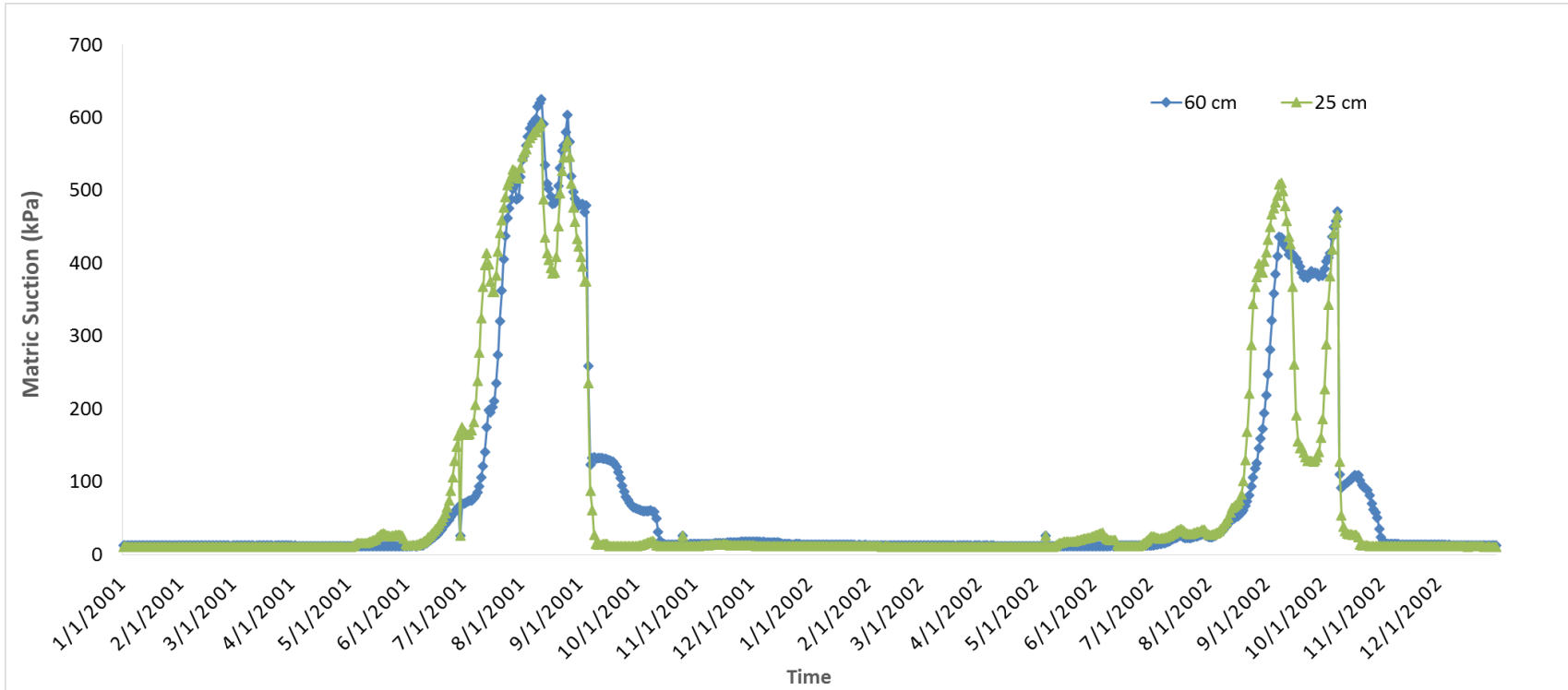
α = diffusion coefficient

n = frequency number, wetting and drying cycles/year

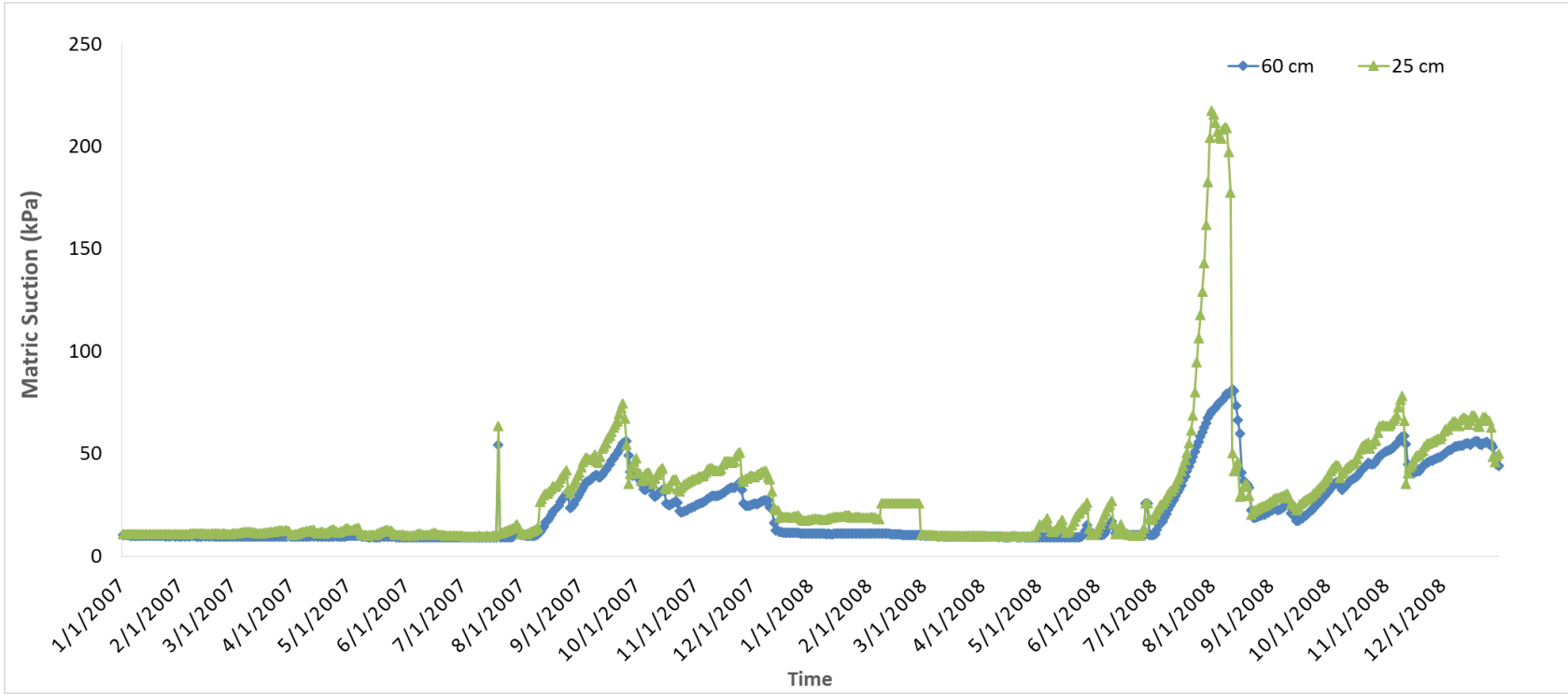
This relationship had been confirmed by the field measurements of the matric suction profile (Mitchell 1979). If matric suction at the soil surface and certain depths is measured, and if the time lag in matric suction between two depths is measured, the diffusion coefficient can be determined from Equation 4.3:

$$\alpha = \frac{y^2}{t^2 4\pi n} \quad (4.4)$$

This research used Equation 4.4 to determine the diffusion coefficient. Time lags were estimated by the field measurements of matric suction at 25 cm- and 60 cm-depth, since matric suction at 25-cm depth had a better sinusoidal pattern than that at the soil surface due to the less effect of near-surface climatic conditions. The time lag is the time of maximum matric suction at 60 cm-depth minus the time of maximum matric suction at 25 cm-depth. Figure 4.15 shows a set of matric suction measured at 25 cm- and 60 cm-depth at two stations. It can be seen that the time lag with movement mainly occurred between July to September for both stations. Since a two-year period of suction was evaluated, the time lag was the average of time difference at the maximum suction during two years. From Figure 4.15, it can be seen that there was a one-day time lag at the maximum suction between the two depths for BOWL station for both 2001 and 2002. As a result, the time lag for BOWL station was one day during 2001-2002. For LANE station, there was a three-day time lag in 2007 and nine-day time lag in 2008, so the time lag for LANE station was six days during 2007-2008. Based on the analysis of all selected Mesonet stations, the time lag between 25 cm- and 60 cm-depth ranged from one day to more than 60 days. The values of the diffusion coefficient for each Mesonet station were listed in Appendix C.



4.15.a BOWL Station

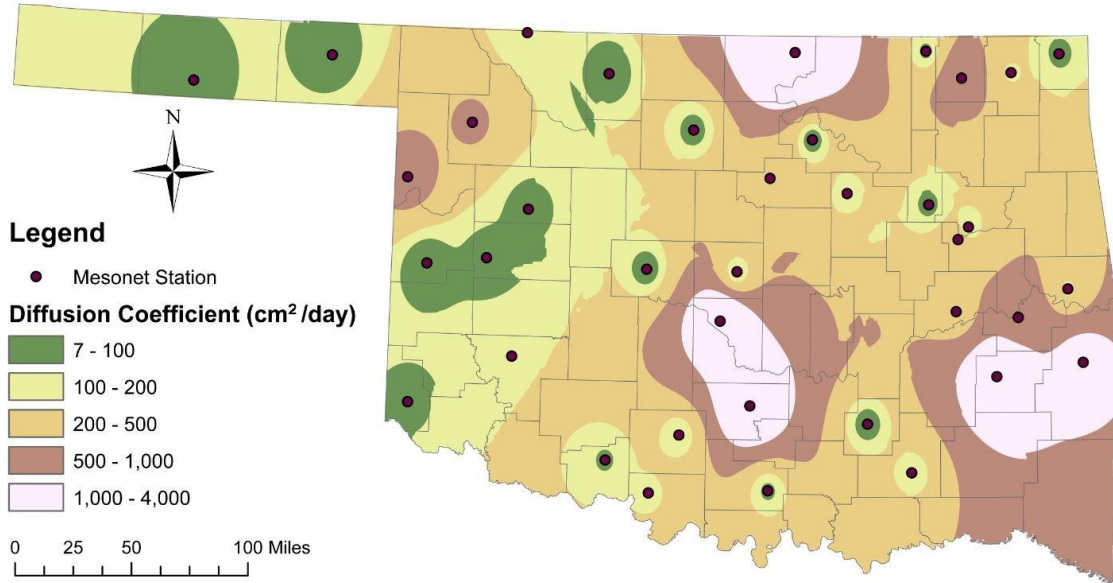


4.15.b LANE Station

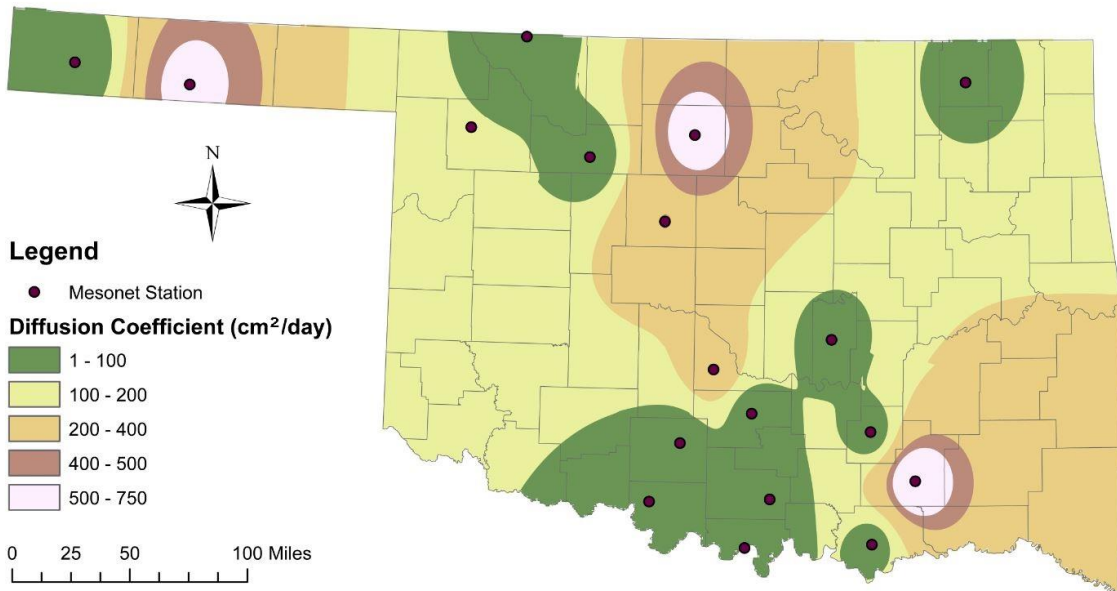
Figure 4.15 Field measurement of matric suction

Since the diffusion coefficient is a function of water content, it will vary when water content varies. Figures 4.16.a – 4.16.c provide the spatial distribution of diffusion coefficient under different moisture conditions in Oklahoma. Generally, no matter under dry, average, or wet conditions, eastern Oklahoma has higher diffusion coefficient than western Oklahoma, which means the higher the water content, the higher the diffusion coefficient. However, the lack of stations made the spatial distribution of diffusion coefficient under wet condition a little different from those under dry and average conditions. The diffusion coefficient ranged between 100 cm²/day to 500 cm²/day for most parts of Oklahoma during dry and wet period. However, the diffusion coefficient was smaller than 150 cm²/day for the whole State of Oklahoma during average period.

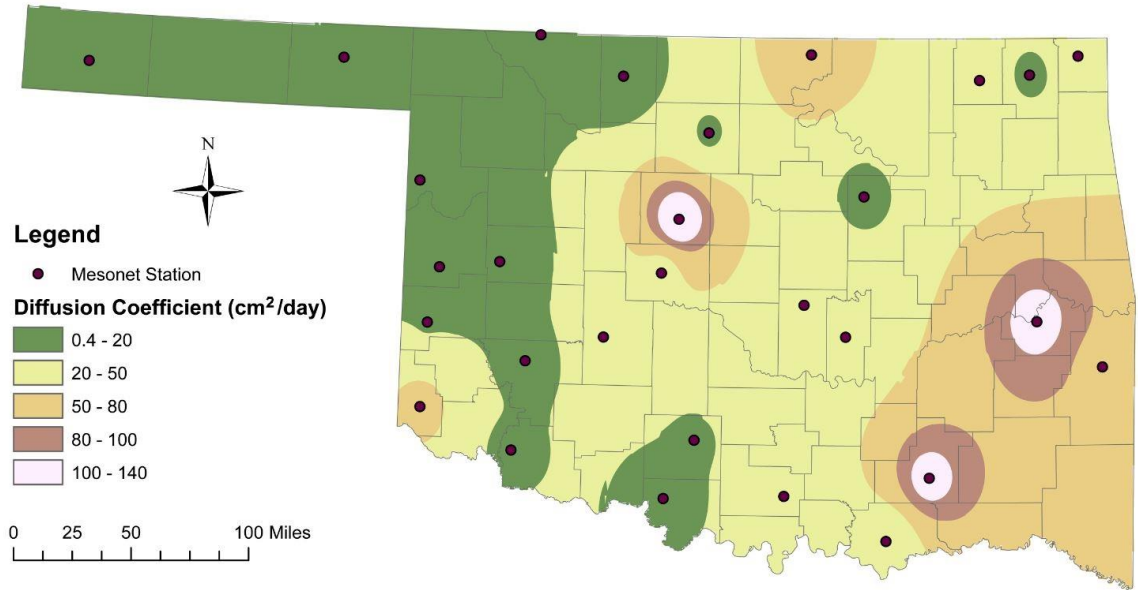
A wide range of diffusion coefficient was observed from the maps. Aubeny and Long (2007) tested diffusion coefficient of soil samples obtained in several Texas sites (Fort Worth, Austin, and Waco) in the laboratory. The tests yielded a range of diffusion coefficients from 2.7 cm²/day to 8.2 cm²/day. However, by estimating diffusion coefficient using Equation 2.4, McKeen and Johnson (1990) reported the diffusion coefficient for Dallas/Fort Worth as 151 cm²/day, which indicated that the field values of diffusion coefficient can be much greater than the laboratory values to nearly two orders of magnitude. The diffusion coefficient estimated by Equation 4.4 highly depends on the matric suction waveform and the surface suction variation, which can affect the diffusion coefficient by a factor of two or more (Aubeny and Long 2007).



4.16.a Dry period



4.16.b Wet period



4.16.c Average period

Figure 4.16 Spatial distribution of diffusion coefficient

Although there are some uncertainties in the magnitude of the diffusion coefficient, the relationship between the diffusion coefficient and moisture content obtained in this research is consistent with previous research. Bai et al. (2007) tested the water diffusion coefficients of horizontal soil columns obtained in a wetland in China. Their tests revealed that the water diffusion coefficients of wetland soils had a significant positive correlation with the soil water volumetric contents, and they increased exponentially with increases in the soil water volumetric contents. In addition, the positive correlation between the diffusion coefficient and moisture content was also found in concrete. Sakata (1983) clarified the behavior of moisture in concrete during the drying process. The test results suggested that the diffusion coefficient in concrete is dependent on the concrete's moisture content. The diffusion coefficient increased with the moisture content while at high moisture content (above 80%) or in the early period of drying.

4.4 Determination of Active Zone Depth

Based on Mitchell's (1979) approach, McKeen and Johnson (1990) proposed an equation to calculate active zone depth using diffusion coefficient and matric suction data:

$$Z = \frac{\ln\left(\frac{2U_0}{\Delta U_{\max}}\right)}{\sqrt{\frac{n\pi}{\alpha}}} \quad (4.5)$$

where Z = active zone depth

U_0 = the amplitude of suction variation

ΔU_{\max} = maximum suction change, which is the difference between the maximum and minimum extremes or envelopes of the suction profile for a given depth

n = frequency number, which is the number of cycles of wetting and drying in a year, cycles/year

α = diffusion coefficient

U_0 was obtained from the curve fitting process, which is the value of A in Equation 4.2. U_0 is equal to the difference between the equilibrium matric suction and the minimum suction during wet period, or the difference between the equilibrium matric suction and the maximum suction during dry periods. U_{\max} is the maximum suction change below which the soil volume change is considered insignificant. U_{\max} is usually assumed based on long-term moisture conditions. Richards and Chan (1971) analyzed moisture changes that occurred in pavements and subgrades of sealed roads. They recommended that there are no seasonal moisture variations below 0.1 pF. As a result, the maximum suction change was

0.1 pF. McKeen and Johnson (1990) predicted the active zone depth using the U_{\max} at 0.1 pF, 0.2 pF, and 0.4 pF. As shown in Table 4.2, when other parameters stay constant, the smaller the U_{\max} , the deeper the active zone depth.

Table 4.2 Active zone depth predicted by McKeen and Johnson (1990)

Surface Suction Change		Active Zone [m (ft)] ΔU_{\max} @ $\alpha = 0.00175$			Active Zone [m (ft)] ΔU_{\max} @ $\alpha = 0.0035$		
$2U_o$ [kPa (pF)] (1)	n (cycle/yr) (2)	0.25 kPa (0.4 pF) (3)	0.16 kPa (0.2 pF) (4)	0.12 kPa (0.1 pF) (5)	0.25 kPa (0.4 pF) (6)	0.16 kPa (0.2 pF) (7)	0.12 kPa (0.1 pF) (8)
9,864 (5.0) (extreme)	0.25	6.7 (22.0)	8.5 (28.0)	10.4 (34.0)	9.5 (31.0)	12.1 (39.6)	14.7 (48.1)
	0.50	4.7 (15.5)	6.0 (19.8)	7.3 (24.0)	6.7 (22.0)	8.5 (28.0)	10.4 (34.0)
	1.00	3.4 (11.0)	4.3 (14.0)	5.8 (17.0)	4.7 (15.5)	6.0 (19.8)	7.3 (24.0)
986 (4.0) (normal design)	0.25	6.1 (20.0)	7.9 (26.0)	9.8 (32.0)	8.6 (28.3)	11.2 (36.8)	13.8 (45.3)
	0.50	4.3 (14.2)	5.6 (18.4)	6.9 (22.7)	6.1 (20.0)	7.9 (26.0)	9.8 (32.1)
	1.00	3.1 (10.0)	4.0 (13.0)	4.9 (16.0)	4.3 (14.2)	5.6 (18.4)	6.9 (22.7)
98.6 (3.0) (moderate design)	0.25	5.3 (17.5)	7.2 (23.5)	9.0 (29.6)	7.6 (24.8)	10.1 (33.3)	12.7 (41.8)
	0.50	3.8 (12.4)	5.1 (16.6)	6.4 (20.9)	5.3 (17.5)	7.2 (23.5)	9.0 (29.6)
	1.00	2.7 (8.8)	3.6 (11.8)	4.5 (14.8)	3.8 (12.4)	5.1 (16.6)	6.4 (20.9)
9.9 (2.0) (mild)	0.25	4.3 (14.0)	6.1 (20.0)	7.9 (26.0)	6.0 (19.8)	8.6 (28.3)	11.2 (36.8)
	0.50	3.0 (9.9)	4.3 (14.2)	5.6 (18.4)	4.3 (14.0)	6.1 (20.0)	7.9 (26.0)
	1.00	2.1 (7.0)	3.1 (10.0)	4.0 (13.0)	3.0 (9.9)	4.3 (14.2)	5.6 (18.4)
1 (1.0) (stable climate)	0.25	2.4 (8.0)	4.3 (14.0)	6.1 (20.0)	3.4 (11.3)	6.0 (19.8)	8.6 (28.3)
	0.50	1.7 (5.6)	3.0 (9.9)	4.3 (14.2)	2.4 (8.0)	4.3 (14.0)	6.1 (20.0)
	1.00	1.2 (4.0)	2.1 (7.0)	3.1 (10.0)	1.7 (5.6)	3.0 (9.9)	4.3 (14.2)

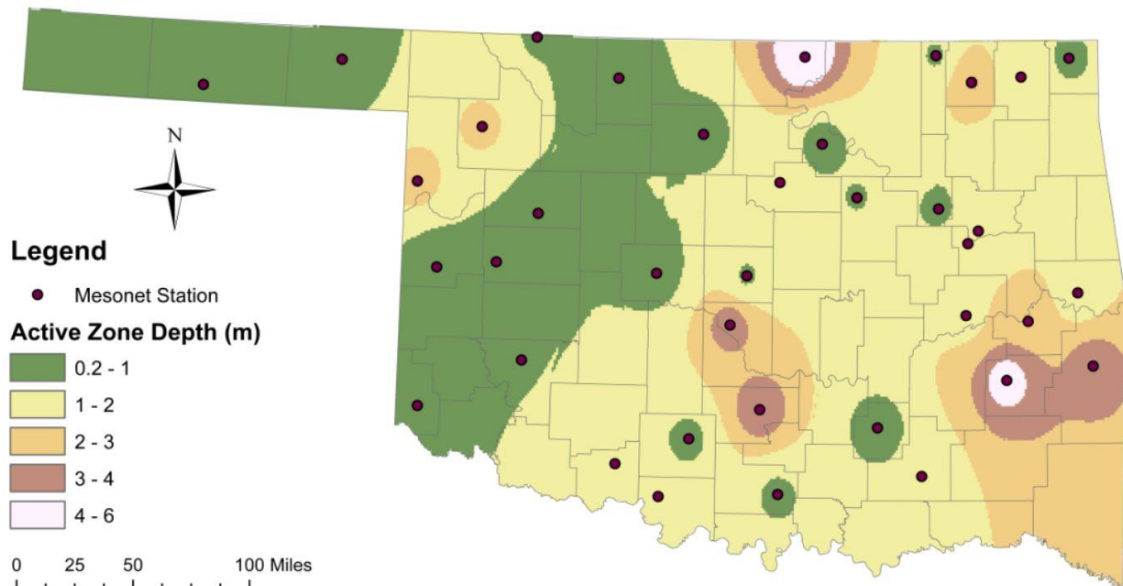
El-Garhy and Wray (2004) used a computer program called SUCH (SUCTION-Heave) to determine a relationship among the edge moisture variation distance, the amplitude of suction change, the diffusion coefficient of the soil, and the active zone depth. They set U_{\max} as 0.1 pF according to Richards and Chan (1971)'s research. Their research (Table 4.3) indicated that the active zone depth varies dramatically under different values of diffusion coefficients. The larger the diffusion coefficient, the deeper the active zone depth. Based on the previous research, this research used 0.1 pF for U_{\max} .

Table 4.3 Active zone depth predicted by El-Garhy and Wray (2004)

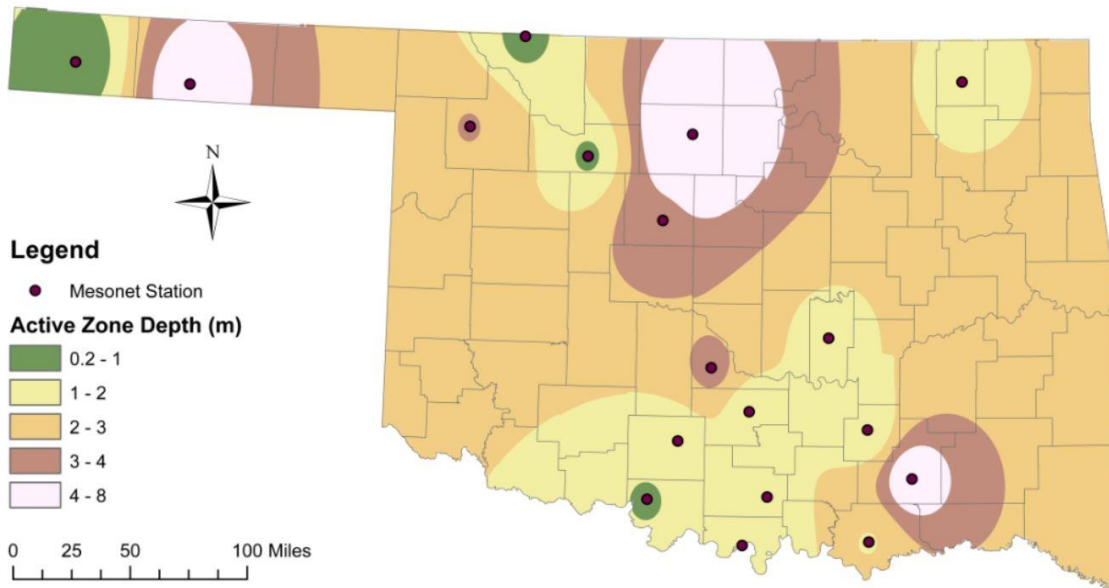
TMI (in./year)	U_e		U_0		Frequency number (n) cycle/year	ΔU_{max}		Active zone depth (m) ^a at each value of α (cm ² /s)			
	kPa	(pF)	kPa	(pF)		kPa	(pF)	5.8×10^{-3}	1.9×10^{-3}	5.65×10^{-4}	1.97×10^{-4}
-55	50,119	(5.70)	0.20	(0.30)	0.5	0.12	(0.1)	6.0	3.6	1.8	0.6
-50	31,623	(5.50)	0.32	(0.50)	0.5	0.12	(0.1)	7.8	4.5	2.4	0.9
-40	10,000	(5.00)	0.98	(1.00)	0.5	0.12	(0.1)	10.2	5.7	3.3	1.8
-30	3,311	(4.52)	3.00	(1.48)	0.5	0.12	(0.1)	11.7	6.6	3.6	2.1
-20	1,148	(4.06)	8.30	(1.94)	0.5	0.12	(0.1)	12.3	7.2	3.9	2.4
-10	437	(3.64)	4.40	(1.64)	0.5	0.12	(0.1)	11.7	6.9	3.6	2.1
0.0	209	(3.32)	2.10	(1.32)	0.5	0.12	(0.1)	11.1	6.3	3.6	2.1
10	132	(3.12)	1.32	(1.12)	0.5	0.12	(0.1)	10.5	6.0	3.3	1.8
20	100	(3.00)	0.98	(1.00)	0.5	0.12	(0.1)	10.2	5.7	3.3	1.8
30	69	(2.84)	0.70	(0.84)	0.5	0.12	(0.1)	9.6	5.4	3.0	1.8
40	53	(2.72)	0.53	(0.72)	0.5	0.12	(0.1)	9.0	5.1	2.7	1.5

^aActive zone depth $Z_a = -\ln(\Delta U_{max}/2U_0) / \sqrt{n\pi/\alpha}$.

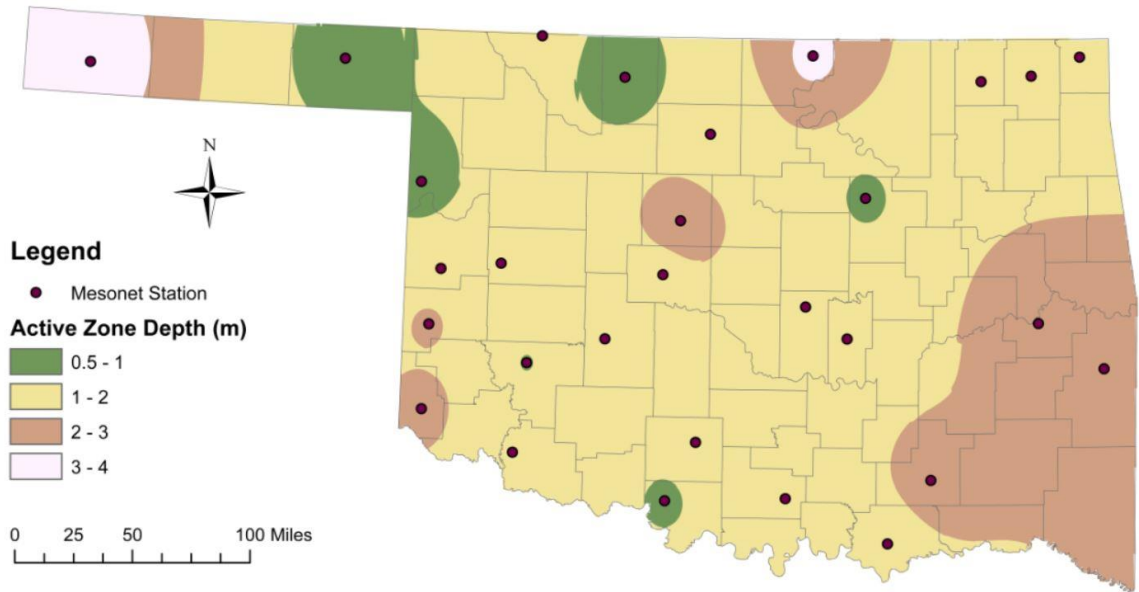
As presented in Figures 4.17.a – 4.17.c, the spatial distribution of active zone depth is similar to the spatial distribution of diffusion coefficient. As a result, by using Equation 4.5 to determine the active zone depth, the most significant factor is the diffusion coefficient. Since the diffusion coefficient was determined by the sinusoidal pattern of matric suction, the most significant factor affecting the active zone depth is matric suction. The active zone depth is deeper in eastern Oklahoma and shallower in western Oklahoma under all three moisture conditions, and most parts of Oklahoma had an active zone depth ranging from 1 to 3 m.



4.17.a Dry period



4.17.b Wet period



4.17.c Average period

Figure 4.17 Spatial distribution of active zone depth

CHAPTER V

NUMERICAL MODELING

Moisture flow beneath foundations and pavements is critical to construction because moisture flow directly affects the soil strength and stiffness. Almost all the engineering structures are built near the ground covered by unsaturated soils that would probably stay unsaturated during the lifetime of the structures (Perera et al. 2004). When a slab barrier is built on expansive soils, moisture differentials occur between the uncovered soil and the soil beneath the slab mainly due to evapotranspiration and precipitation. The ability to predict differential soil movement and the active zone depth is an important application in foundation design. This research performed two-dimensional numerical modeling to analyze slab-on-ground placed on expansive soils. The goal of the numerical modeling is to (1) evaluate moisture redistribution between the uncovered soil and the soil beneath the slab; (2) evaluate the active zone depth and compare it to the results from Chapter 4.

5.1 Model Description

The commercial software SVFlux, part of SVOoffice software package, developed by SoilVision Systems Ltd. was used for the analysis of matric suction distribution within unsaturated soil. SVFlux is capable of solving two-dimensional and three-dimensional

seepage problems under either steady state or transient conditions. The interface of SVFlux is simply CAD-based, which can create models effectively. SVFlux uses the general purpose partial differential equation (PDE) solver FlexPDE, which is capable of solving nonlinear PDE problems, such as water flow in unsaturated soils. The steps of numerical modeling in SVFlux are as follows:

1. Create a model – This step includes defining the model dimension, type (steady- or transient-state), duration, and unit.
2. Define model geometry – Model geometry includes a set of regions, and it can be either drawn by the user or input a set of coordinates.
3. Define initial condition – proper initial condition is important for a stable solution. SVFlux provides two types of variables that can be used to set up initial condition – initial head and initial pore-water pressure.
4. Define boundary conditions – All the boundary conditions in engineering practice can be expressed as a value or a gradient. The top boundary of the model is set as a flux boundary where climatic conditions such as evapotranspiration can be input in order to determine the flux through the soil surface.
5. Define material/soil properties – soil properties include specific gravity, residual and saturated volumetric water content, hydraulic conductivity, and SWCC parameters must be defined.
6. Specify model output - Before starting to analyze the problem, the required outputs should be defined properly. The output features include color contour plots, vector plots, mesh plots, etc.

7. Analyze the result: Once the model has been run successfully, the output files will be created by SVFlux and used by the FlexPDE solver to analyze and solve the problem.

5.1.1 Unsaturated Transient-State Seepage Theory

A transient-state model with volumetric water content and hydraulic conductivity is widely used in geotechnical engineering research. As water flows through unsaturated soils, the matric suction and moisture content vary as a function of time and space (Nelson et al. 2014). In the study of unsaturated flow in soils, the Richards' equation, introduced by Richards (1931) is the most often used theory. The Richards' equation written in the one-dimensional horizontal soil is:

$$\frac{\partial \theta}{\partial t} = \frac{\partial}{\partial x} \left(k(\psi) \frac{\partial h}{\partial x} \right) \quad (5.1)$$

where θ = volumetric water content

t = time

x = the distance from one of the ends of the soil column

$k(\psi)$ = hydraulic conductivity of the soil

h = metric head induced by capillary action

The Richards' equation indicates that the rate of change of moisture content is equal to the rate of change of flow in soils. This equation has been widely used in multidisciplinary fields and it can be derived in several forms. The most commonly used form, which is also

adopted in SVFlux, is pressure head- based (h-based) form (Thode 2004). The h-based equation for two-dimensional transient seepage is

$$\frac{\partial}{\partial x} \left(k_x(\psi) \frac{\partial h}{\partial x} \right) + \frac{\partial}{\partial y} \left(k_y(\psi) \frac{\partial h}{\partial y} \right) = m_w^2 \gamma_w \frac{\partial h}{\partial t} \quad (5.2)$$

where h = total head

$k_x(\psi)$ = hydraulic conductivity of the soil in x direction

$k_y(\psi)$ = hydraulic conductivity of the soil in y direction

ψ = water content

m_w^2 = Slope of the SWCC

γ_w = Unit weight of water = 9.81 kN/m³

Equation 5.2 states that the difference between the water flow entering and leaving a unit volume is equal to the volumetric water content change.

5.1.2 Model Geometry and Boundary Conditions

A two-dimensional model of slab-on-grade foundation was simulated within the SVFlux software. Figure 5.1 illustrates the geometry and boundary conditions of the model. Based on the active zone depth obtained from Chapter 4 and previous literature (Fredlund and Vu 2003), the model geometry for this study was set as a 6-m depth of expansive soil below a 12-m wide concrete cover. The soil is allowed to move in the vertical direction and to be fixed in horizontal direction. Due to the geometrical symmetry, only half of the concrete cover and its surrounding soil were considered in the analysis. The initial boundary condition should always be known before setting up the model. The boundary

conditions include a constant head/equilibrium matric suction at the bottom boundary and zero/no flux on both lateral boundaries. Below 6-m depth, there is no seasonal moisture variation. The 6-m depth was assumed based the results of active zone depth obtained in Chapter 4. At the top boundary, there is no flux applied on the slab-on-ground cover, and an annual average of evapotranspiration is applied to the soil cover.

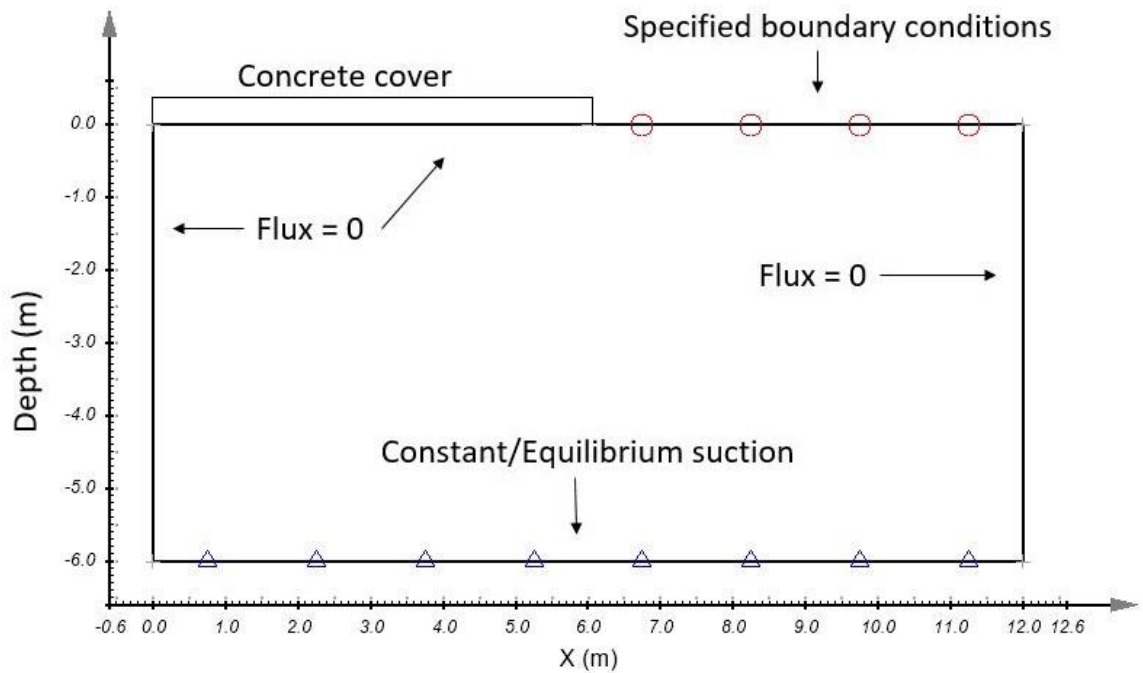


Figure 5.1 Model geometry

5.1.3 Model Parameters

One of the key elements to conduct a successful numerical modeling of unsaturated flow is to properly describe the model parameters. There are two types of parameters required in SVFlux – soil/material properties and boundary conditions, as listed in Table 5.1. Soil proper data includes specific gravity, saturated hydraulic conductivity, saturated

volumetric water content, and SWCC parameters. Both two types of data can affect the numerical modeling accuracy.

Table 5.1 Model parameters

Type	Parameter	Parameter obtained from
Seepage	Specific gravity, G_s	Set as 2.65
material properties	Saturated volumetric water content	New Oklahoma
	Saturated hydraulic conductivity	Mesonet soil property
	Parameters for SWCC (van Genuchten fit: including α , n , m , and residual water content)	database (Scott et al. 2013)
Boundary conditions	Constant/Equilibrium suction	Equilibrium suction from curve fitting
	Evapotranspiration	Equation 4.1
	Precipitation	The Oklahoma Mesonet

Several hydraulic conductivity equations have been proposed to represent the soils' permeability function. The saturated hydraulic conductivity used in this research was from the Oklahoma Mesonet soil property database and it was determined by the van Genuchten-Mualem soil hydraulic conductivity function (Scott et al. 2013):

$$K(S_e) = K_0 S_e^L \left\{ 1 - \left[1 - S_e^{\frac{n}{n-1}} \right]^{1-\frac{1}{n}} \right\}^2 \quad (5.3)$$

where $K(S_e)$ = saturated hydraulic conductivity, cm/day

K_0 = fitting match point at saturation, cm/day

$$S_e = \text{effective saturation} = \frac{\theta - \theta_r}{\theta_s - \theta_r}$$

L = empirical parameter

n = van Genuchten SWCC parameter

Hydraulic conductivity (both saturated and unsaturated) is one of the most important soil parameters to control the moisture flow through the soil (van Genuchten 1980). Saturated hydraulic conductivity measures a saturated soil's ability to transmit water, and is a function of soil grain size, soil density, soil structure, the type of soil fluid. It also depends on the viscosity and density of the water. The saturated hydraulic conductivity can be considered as a constant for a certain type of soil. Abbaszadeh (2001) conducted tests to evaluate the effect of soil cracks on saturated hydraulic conductivity. The tests showed that the saturated hydraulic conductivity is extremely high for cracked soils, and the extremely high saturated hydraulic conductivity of cracked soils will cause an excessive wetting under the slab which can cause damage to the structure.

The saturated hydraulic conductivity varies from place to place. It varies within a wide range of several orders of magnitude, depending on the soil type. Heavy, montmorillonitic, or smectitic clay tends to have low saturated hydraulic conductivity. The saturated hydraulic conductivity from the Oklahoma Mesonet ranges from 0.1 cm/day to 532.5 cm/day, and it tended to be lower for fine textures and higher for coarse textures, with the largest difference in the loamy sand texture class (Scott et al. 2013). Figure 5.2 shows the

spatial distribution of saturated hydraulic conductivity measured at 55-cm depth. At this depth, the saturated hydraulic conductivity varies within a wide range from 0.1 cm/day to 208 cm/day. The central Oklahoma has relatively low saturated hydraulic conductivity, while the western and some parts of eastern Oklahoma have relatively high saturated hydraulic conductivity.

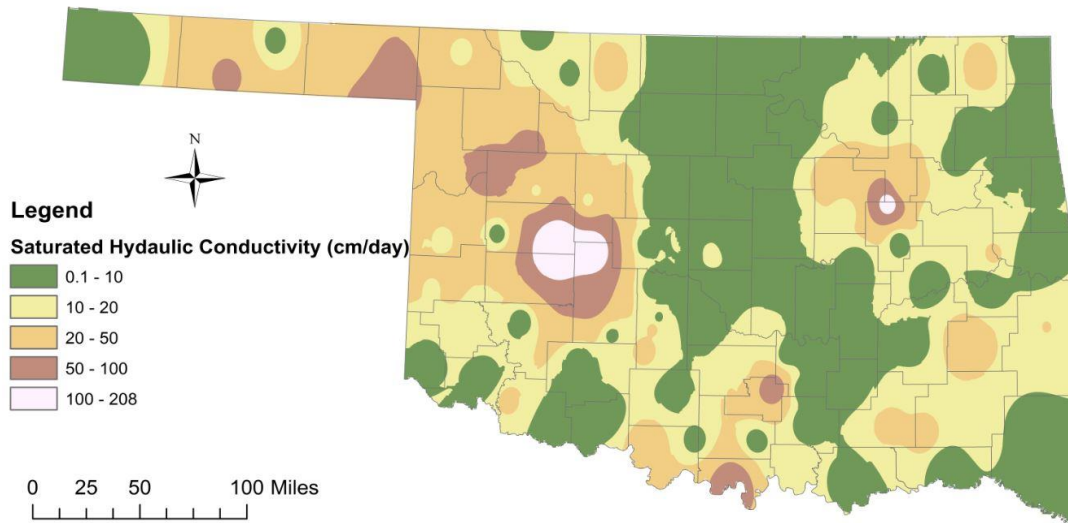


Figure 5.2 Spatial distribution of saturated hydraulic conductivity

SVFlux provides different SWCC fits for soils. In this study, the van Genuchten fit was used for all soils, since Scott et al. (2013) updated the van Genuchten parameters for the Oklahoma Mesonet. The van Genuchten equation is:

$$\Theta = \frac{1}{[1 + (\alpha \cdot \psi)^n]^m} \quad (5.4)$$

where Θ = water content

ψ = matric suction

α , n , m = van Genuchten parameters

Equation 5.2 along with 5.3 and 5.4 can be used to predict matric suction profiles at different times during a seepage process.

The boundary conditions of the model include constant suction at the bottom of the soil volume and climatic conditions, including precipitation and evapotranspiration at the soil surface. The constant suction used the equilibrium suction obtained from Equation 4.2. The daily precipitation was obtained from the Oklahoma Mesonet and the evapotranspiration was calculated by Equation 4.1.

5.2 Modeling Procedure

SVFlux can conduct the seepage analysis during either wetting or drying process. The wetting process is induced by a boundary flux of infiltration, while the drying process is induced by a boundary flux of evapotranspiration. Both wetting and drying processes include precipitation. Due to the availability of data, this research evaluated the drying process by using evapotranspiration and precipitation data. The first step is to select a starting and ending time for the model. The selection of simulation time is important to the model accuracy and stability. A larger time frame tends to give more satisfactory results than the smaller time frame (Bharadwaj 2013). Since a drying process was evaluated in the model, a two-year period of 2011-2012 was selected. The next step is to input soil properties and boundary conditions. The evapotranspiration was averaged throughout each day during a two-year period. The matric suction was converted to head of water. Detailed values of soil parameters and boundary conditions are listed in Appendix D. Then the FlexPDE turned a description of partial differential equations into a finite element model, solved the equations, and presented graphical and tabular output of the results. In order to determine the active zone depth from the numerical analysis, the plot of matric suction with

depth was established. The screenshots of a step-by-step modeling from SVFlux are shown in Appendix E.

5.3 Modeling Results

37 stations were evaluated using the numerical model. Figures 5.3 - 5.8 show the results of two-year simulation of drying process for NRMN station and GOOD station. NRMN station represents a relatively deep active zone depth and GOOD station represents a relatively shallow active zone. It can be seen from Figures 5.5 and 5.8 that changes in matric suction were found to occur at shallow depths of uncovered soil. In order to determine the active zone depth from the analysis, matric suction with depth were plotted (Figure 5.5 and 5.8). The matric suction profile with evapotranspiration and precipitation was defined based on the matric suction values at the right boundary of the soil mass and the matric suction profile with the slab was defined based on the matric suction values at the left boundary of the soil mass. Since the increment of the depth of soil was set as 0.5 m in the model, the smallest active zone depth obtained from the modeling was 0.5 m. It appears that the moisture fluctuation occurs at a point between 0 and 2-m depth for NRMN station and between 0 and 0.5-m depth for GOOD station. As a result, an active zone of 2 m and 0.5 m is defined for NRMN station and GOOD station, respectively.

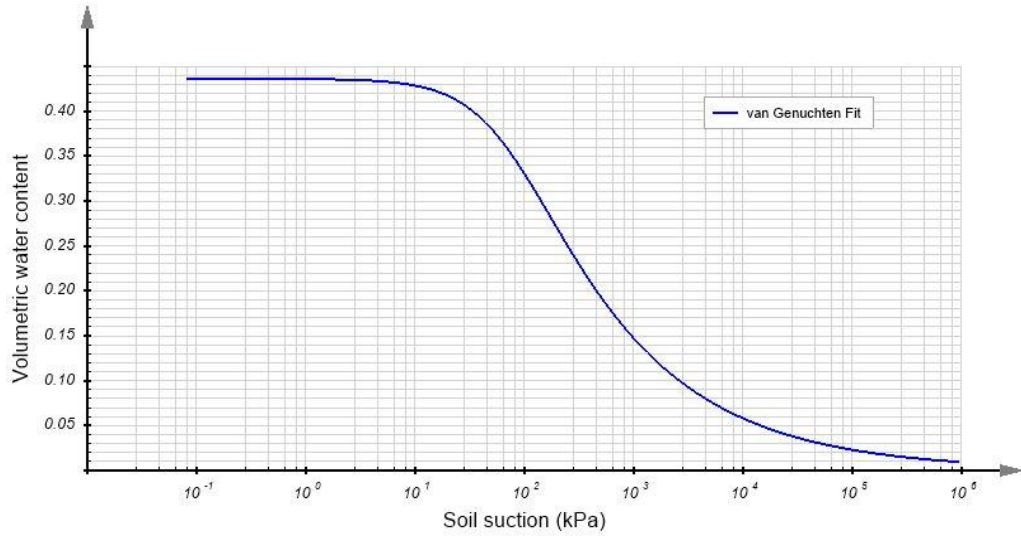


Figure 5.3 SWCC for NRMN station

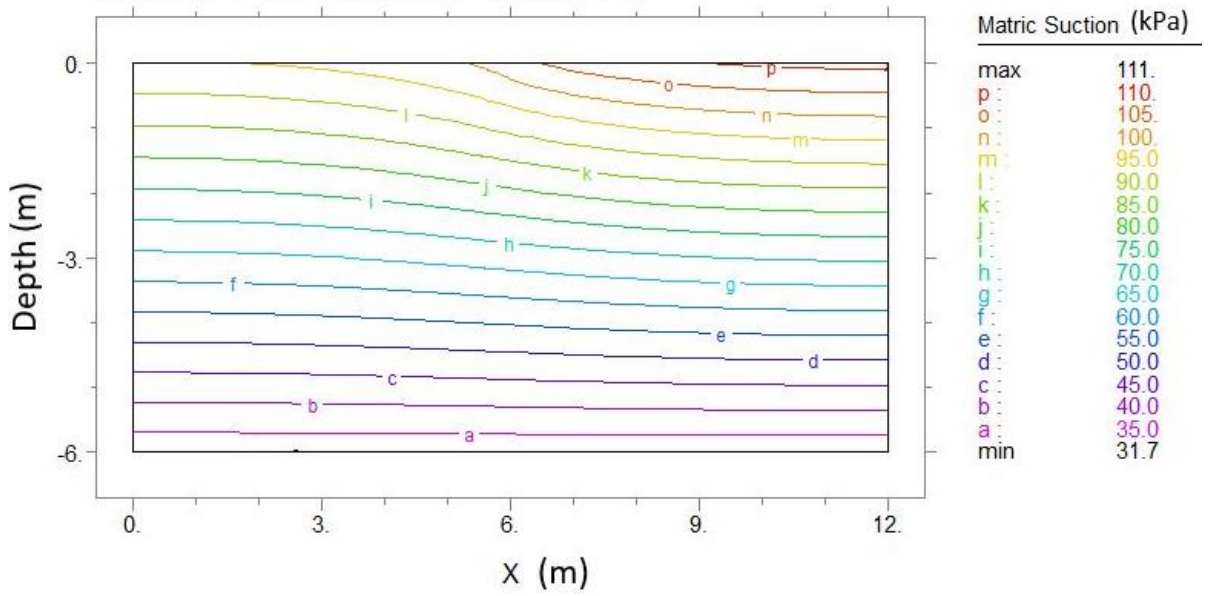


Figure 5.4 Matric suction distribution for NRMN station

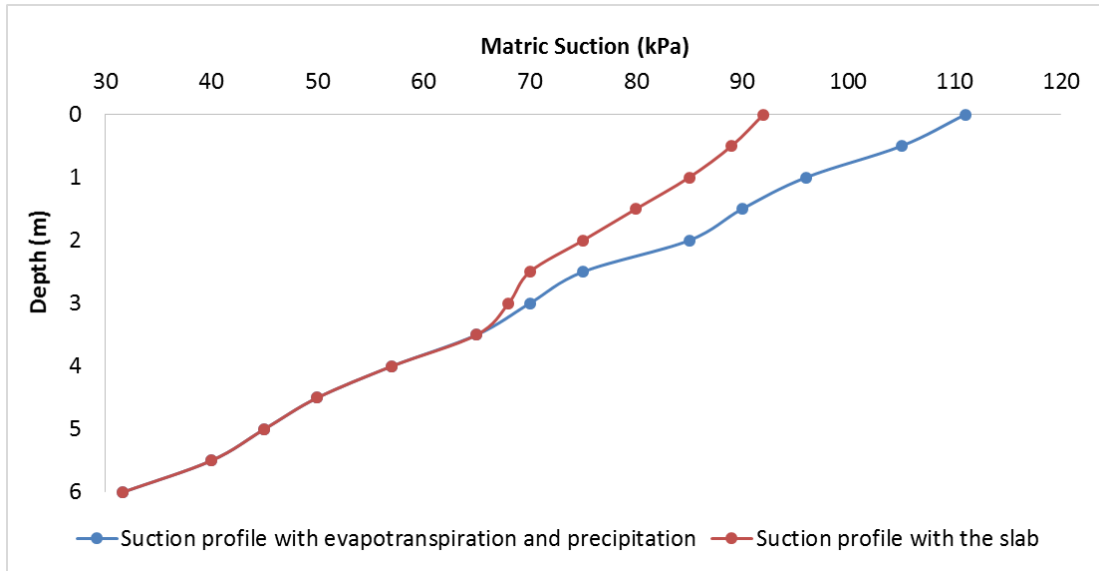


Figure 5.5 Matric suction profile for NRMN station

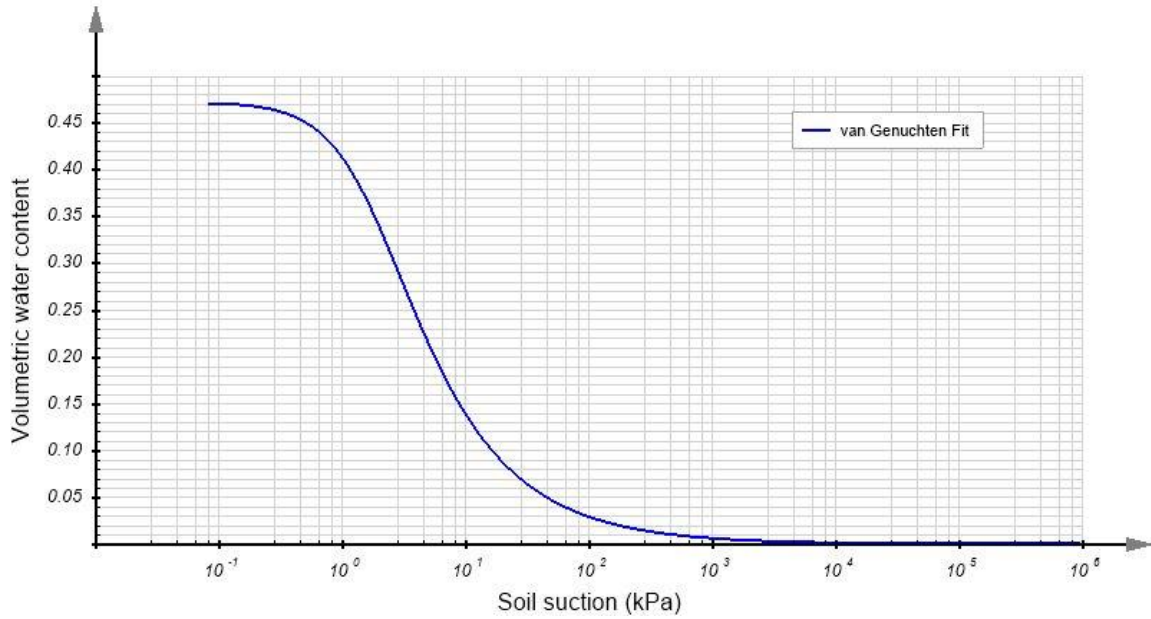


Figure 5.6 SWCC for GOOD station

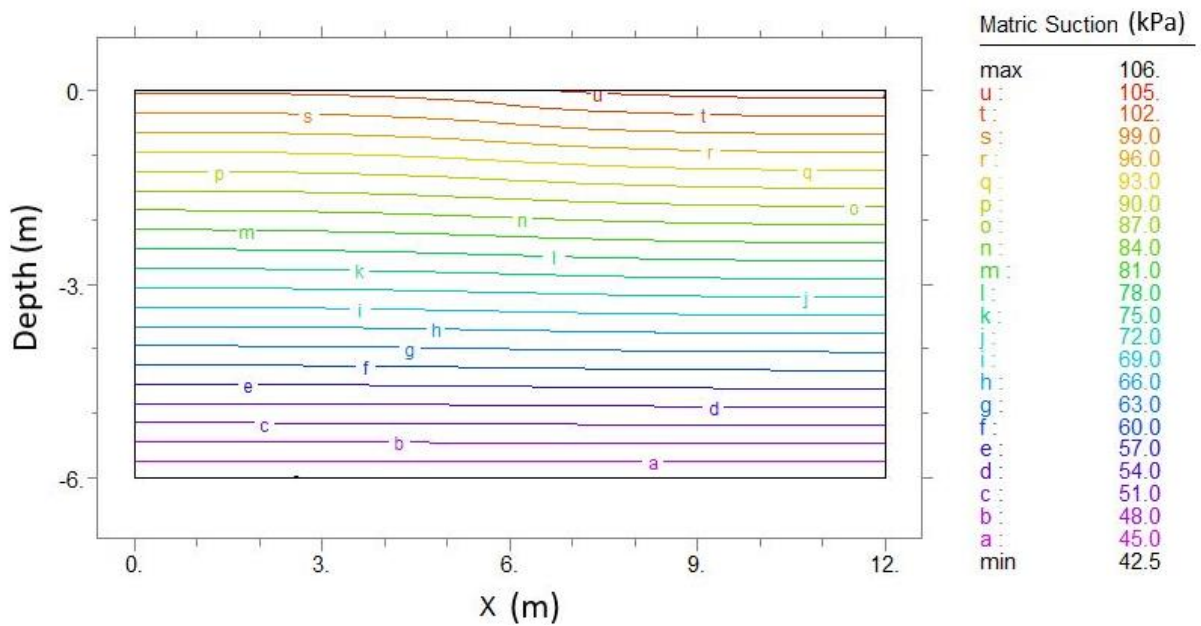


Figure 5.7 Matrix suction distribution for GOOD station

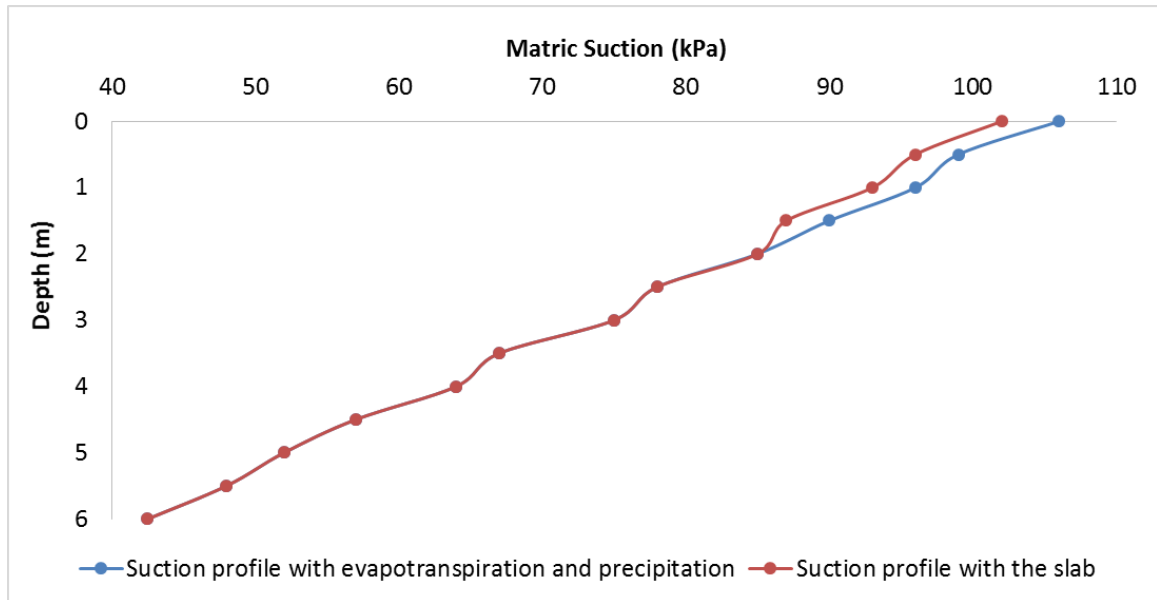


Figure 5.8 Matrix suction profile for GOOD station

Figure 5.9 shows the active zone depth of 37 stations across Oklahoma. Most of the stations had an active zoned depth ranging from 0.5 to 4 m, which is similar to the results

obtained by the empirical equation. However, the spatial distribution of active zone depth between these two methods is different. Results from the empirical equation showed eastern Oklahoma has deeper active zone than western Oklahoma, while results from the numerical model showed southwestern Oklahoma has a deeper depth than other parts of the state. It can be seen from Figure 3.7 (in Chapter 3) that soils in southern Oklahoma have a high swelling potential. The results from Figure 3.7 and Figure 5.9 may indicate a relationship between plasticity index and active zone depth, which is the larger plasticity index, the deeper the active zone depth.

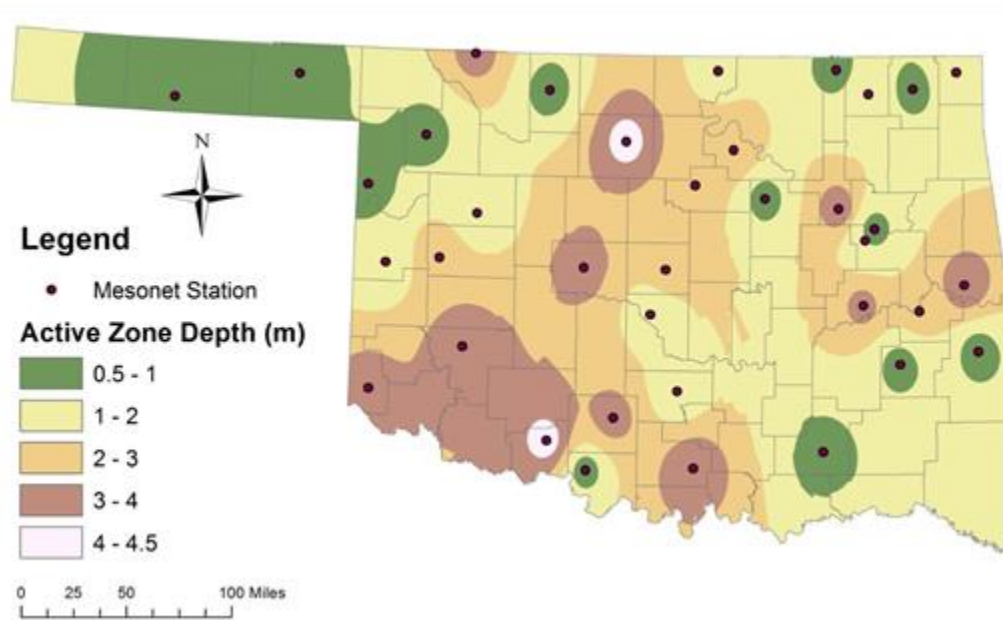


Figure 5.9 Spatial distribution of active zone depth during dry period

Table 5.2 provides reasonable estimates of the van Genuchten SWCC parameters for different soil textural groups. Carsel and Parrish (1998) obtained the data listed in Table 5.2 by analyzing a large database of SWCCs. Clayey soils generally have lower α , n , and saturated hydraulic conductivities than sandy soils because clayey soils have smaller pores than sandy soils. Soils with large continuous pores tend to have a lower resistance to flow

(and thus a higher hydraulic conductivity) than soils with small discontinuous pores. Similarly, Bharadwaj (2013) found that at low suctions near saturation, coarse-grained soils have higher hydraulic conductivity than fine-grained soils. Combined the previous literature and the results from Table 5.2, it may conclude that soils with higher clay content tend to have smaller saturated hydraulic conductivity and deeper active zone depth.

Table 5.2 Average values of van Genuchten SWCC parameters for major soil textures (Carsel and Parrish 1988)

Texture	θ_r (cm³/cm³)	θ_s (cm³/cm³)	α (1/kPa)	n	K_s (cm/day)
Sand	0.045	0.430	0.145	2.68	712.80
Loamy sand	0.057	0.410	0.124	2.28	350.20
Sandy loam	0.065	0.410	0.075	1.89	106.10
Loam	0.078	0.430	0.036	1.56	24.96
Silt	0.034	0.460	0.016	1.37	6.00
Silt loam	0.067	0.450	0.020	1.41	10.80
Sandy clay loam	0.100	0.390	0.059	1.48	31.44
Clay loam	0.095	0.410	0.019	1.31	6.24
Silty clay loam	0.089	0.430	0.010	1.23	1.68
Sandy clay	0.100	0.380	0.027	1.23	2.88
Silty clay	0.070	0.360	0.005	1.09	0.48
Clay	0.068	0.380	0.008	1.09	4.80

CHAPTER VI

RESULTS AND DISCUSSION

6.1 Comparison between Two Methodologies

By evaluating the soil properties and climatic conditions during 2011-2012, both of two methodologies reported a range of 0.5-4 m for the active zone depth for most parts of Oklahoma. This range is similar to the results reported in previous research. Typical values of active zone depths in Texas range from 1 to 5 m, although values up to 10 m have also been reported (Wray 1987, McKeen and Johnson 1990). Durkee (2000) conducted the field and laboratory tests as well as numerical modeling to evaluate the active zone depth for expansive soil test site located at Colorado State University in Fort Collins, CO. His research indicated that the active zone depth was approximately equal to the depth of soil moisture fluctuation, which ranged from 5 to 7 feet (1.5 to 2.1 m).

The spatial distributions of active zone depth obtained by the two methodologies used in this research were different. The results from the empirical equation indicated that eastern Oklahoma had the deeper active zone depth, while the numerical model showed southern Oklahoma had the deeper active zone depth. This could be due to the different types of input parameters used in the two methodologies. The empirical equation focuses

on field matric suction conditions, which are impacted by the climatic conditions. The numerical model makes use of soil types and soil's hydraulic properties. Previous research has pointed out that active zone depth is determined by a combination of soil characteristics and climatic conditions (Bell 1999, Nelson et al. 2001). This research further indicates which factors have the most significant impact on active zone depth from two different points of view.

6.2 Field Measurement for Validation

To evaluate which methodology provides a more accurate active zone depth, field measurements of matric suction were compared to the results obtained by the two methodologies. Vertical matric suction profiles were developed for selected Mesonet stations and ARM sites. The field measurements could predict the equilibrium suction and the depth to the equilibrium suction, which is the active zone depth.

6.2.1 Validation by the Data from the Oklahoma Mesonet

10 Mesonet stations with soil moisture sensors installed at 75-cm depth were selected for field validation. Figure 6.1 shows the spatial distribution of the 10 selected Mesonet stations.

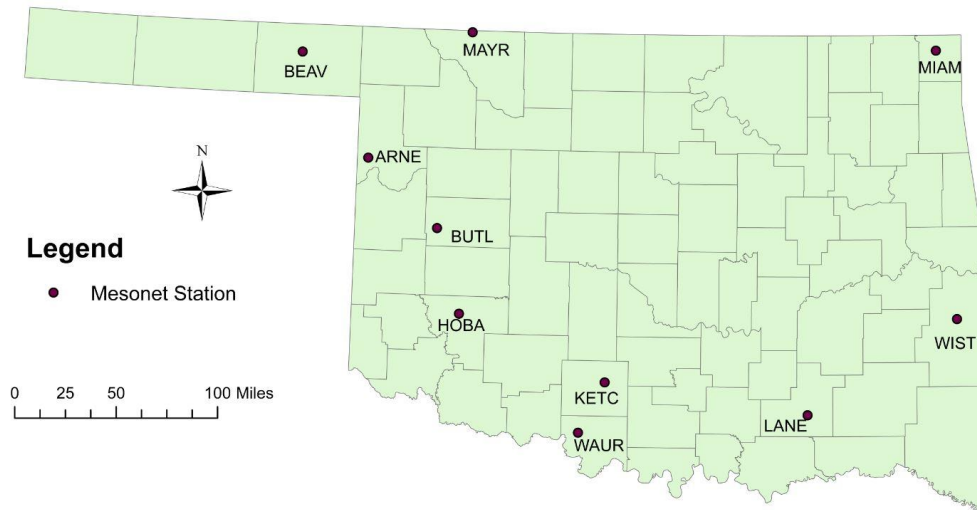
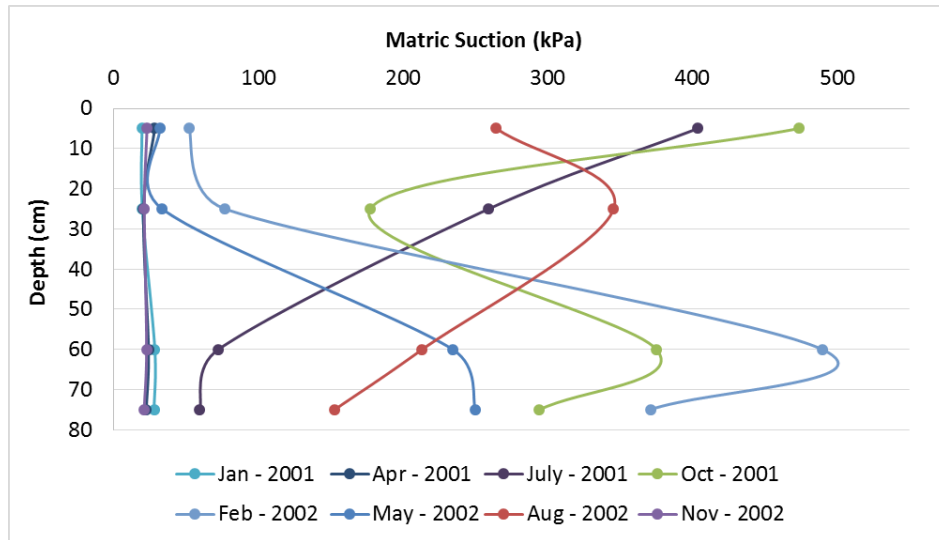
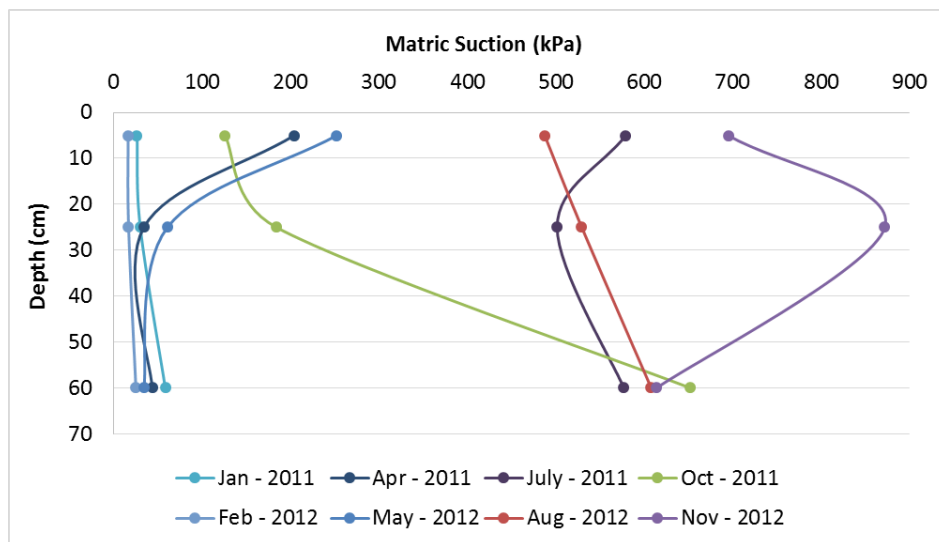


Figure 6.1 Spatial distribution of the 10 selected Mesonet stations

Figures 6.2 and 6.3 present the monthly averaged matric suction, plotted as a function of depth, for two Mesonet stations. Figure 6.2 indicates a wide range of matric suction measured at 75 cm during 2001-2002 and 60 cm during 2011-2012, which implies that even below 75 cm or 60 cm, matric suction variation is still significant. Based on Figure 6.2, the active zone depth for ARNE was greater than 75 cm during 2001-2002 and greater than 60 cm during 2011-2012. It can be seen in Figure 6.3.a and 6.3.b that the matric suction varied from 10 kPa to 50 kPa at 75 cm during 2001-2002 and 60 cm during 2007-2008. Based on the relatively small range of matric suction variation, the active zone depth for LANE station could be predicted as 75 cm during 2001-2002 and 60 cm during 2007-2008. However, in Figure 6.3.c there were large fluctuations at 75 cm, so the active zone depth for LANE during 2011-2012 was greater than 75 cm.

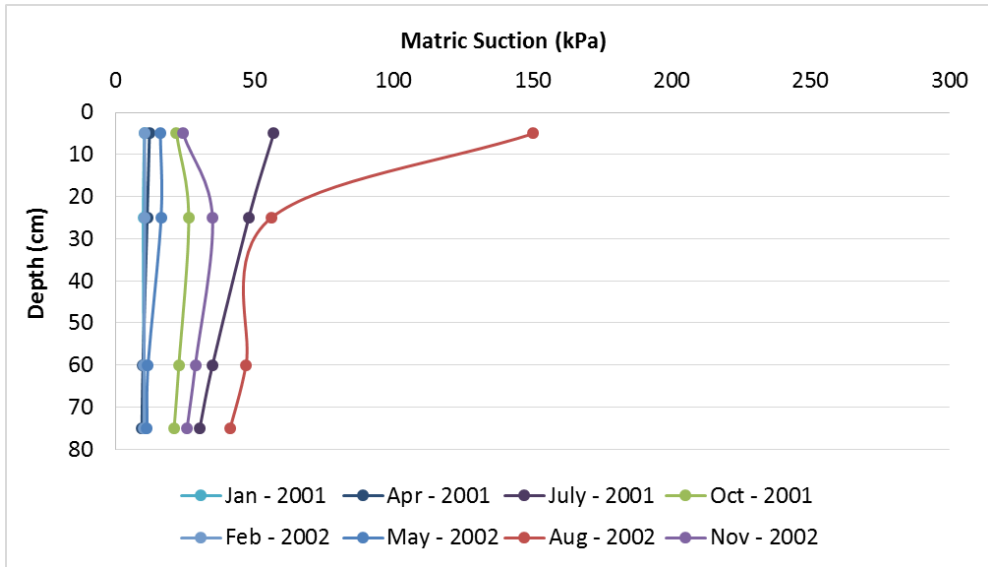


6.2.a ARNE 2001-2002

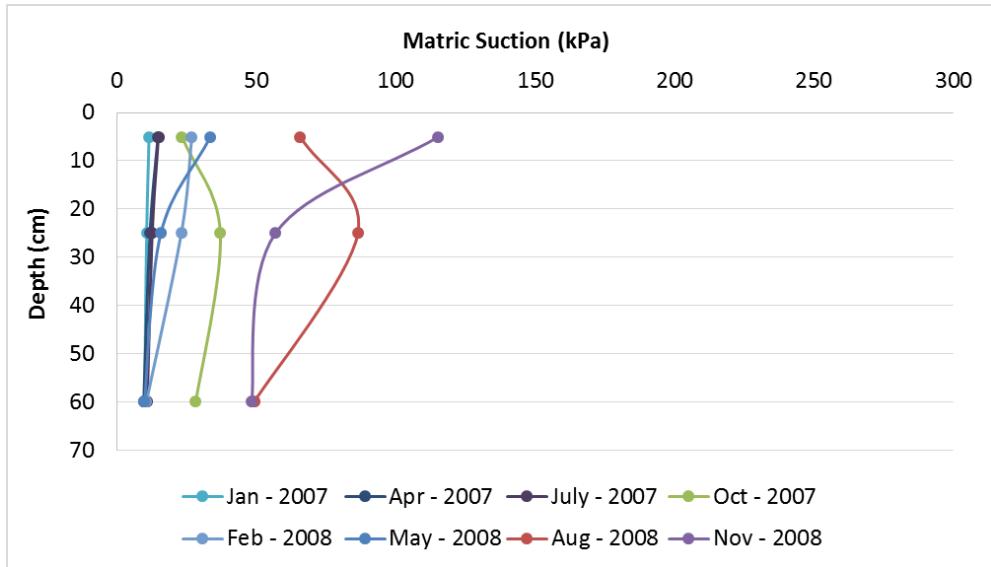


6.2.b ARNE 2011-2012

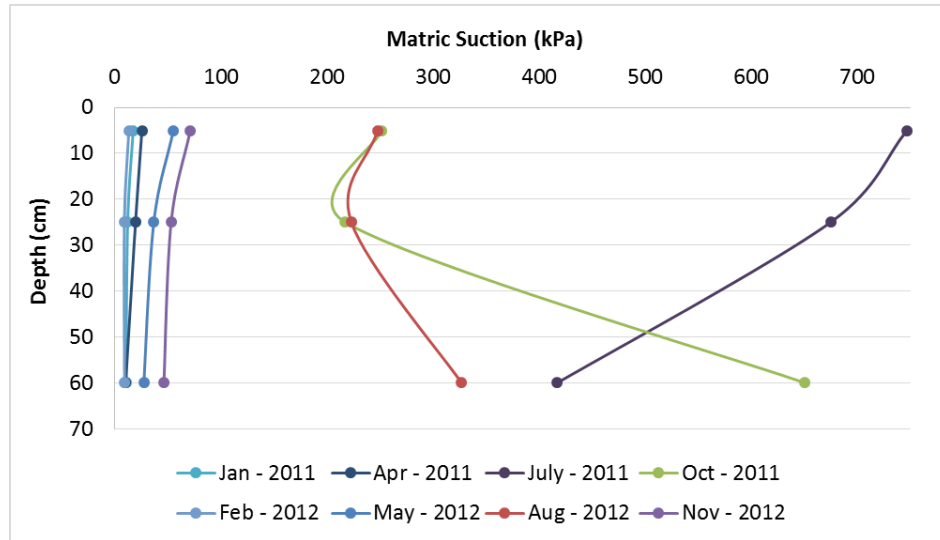
Figure 6.2 Matric suction profile for ARNE station



6.3.a LANE 2001-2002



6.3.b LANE 2007-2008



6.3.c LANE 2011-2012

Figure 6.3 Matric suction profile for LANE station

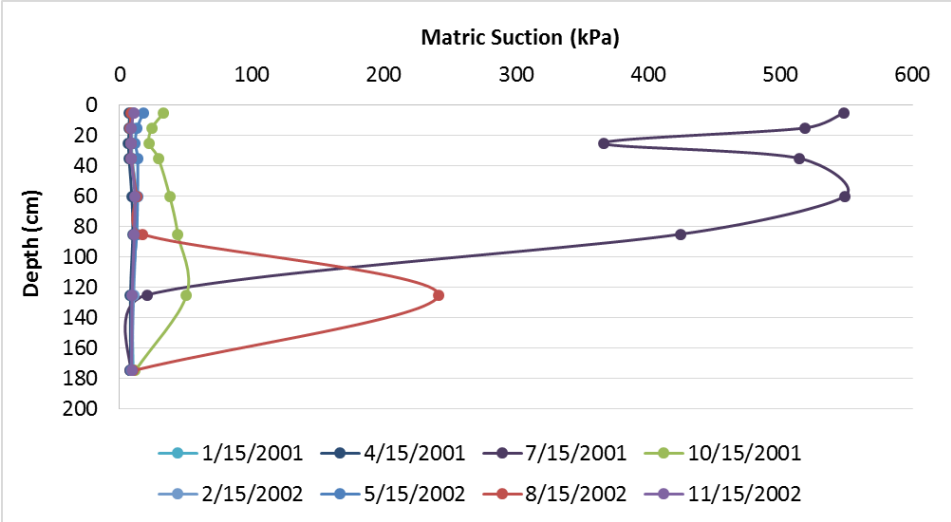
Table 6.1 summarizes the active zone depths obtained from measurements at the Oklahoma Mesonet and the two methodologies used in this research. Except for the LANE station during 2001-2002 and 2007-2008, all the other nine selected stations had significant matric suction variations at the deepest depths (either 60 cm or 75 cm) where the moisture sensors were installed. Due to the limitation of the moisture sensor depths, it is difficult to determine the active zone depth from the field measurement. Thus, it is difficult to evaluate which methodology provides the more accurate result.

Table 6.1 Active zone depth compared with the Mesonet measurement

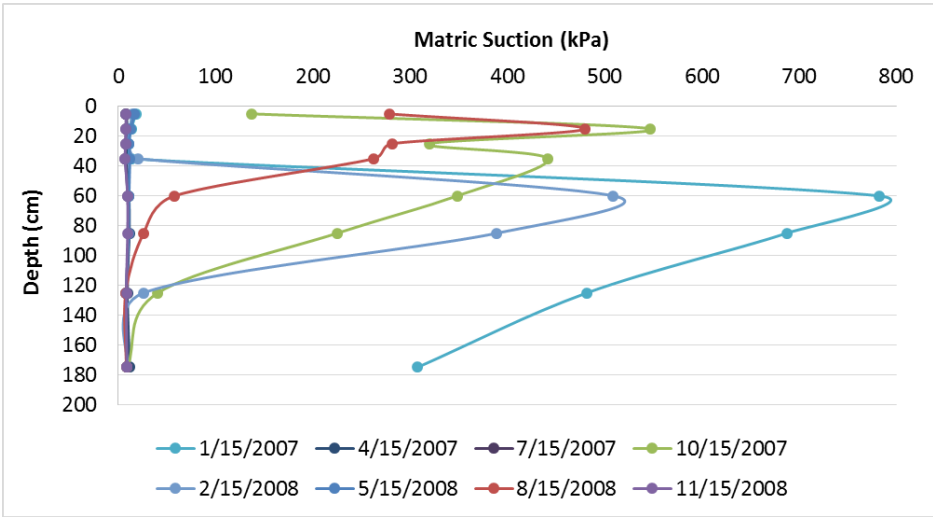
Mesonet Station	Active Zone Depth (Mesonet Measurement) (m)			Active Zone Depth (Empirical Equation) (m)			Active Zone Depth (Numerical Modeling) (m)
	2001-2002	2007-2008	2011-2012	2001-2002	2007-2008	2011-2012	2011-2012
ARNE	> 0.75	NA	> 0.6	0.7	NA	2.47	0.5
BEAV	> 0.75	NA	> 0.6	0.7	NA	0.46	0.5
BUTL	> 0.75	NA	> 0.6	1.02	NA	0.59	3.0
HOBA	> 0.75	NA	> 0.6	0.98	NA	0.99	4.0
KETC	> 0.75	> 0.6	> 0.6	1.79	1.44	0.76	3.5
LANE	0.75	0.6	> 0.6	2.55	5.41	1.13	0.5
MAYR	> 0.75	> 0.75	> 0.6	1.15	0.67	0.97	3.5
MIAM	> 0.75	NA	> 0.6	1.53	NA	0.89	2.0
WAUR	> 0.75	> 0.75	> 0.6	0.93	0.87	1.19	0.5
WIST	> 0.75	NA	> 0.6	2.67	NA	2.29	0.5

6.2.2 Validation by the Data from the ARM Network

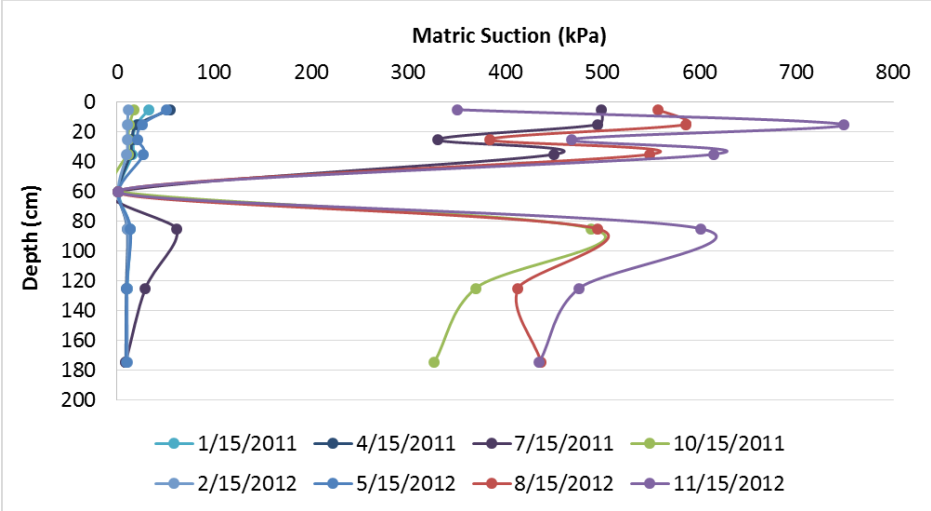
Eight ARM sites in Oklahoma (shown in Figure 3.3) have soil moisture sensors installed at depths deeper than 75 cm (85 cm, 125 cm, and 175 cm). Figures 6.4 and 6.5 present the matric suction profiles for Byron and Cordell. The matric suction profiles for all the other ARM sites are listed in Appendix F. Figures 6.4.a, 6.5.a, and 6.5.b indicate that there is a small matric suction variation at 175 cm during the specific two-year period. As a result, the active zone depths for Byron during 2001-2002 and Cordell for 2001-2002 and 2007-2008 were 175 cm.



6.4.a Byron 2001-2002

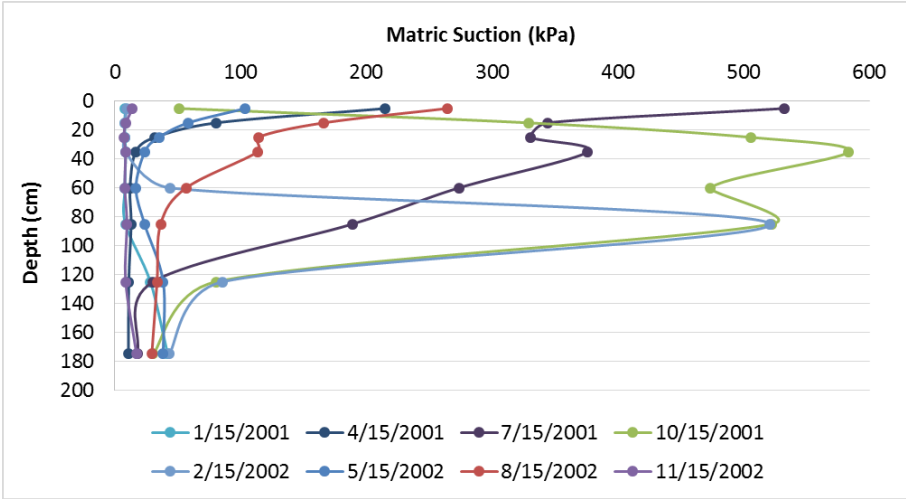


6.4.b Byron 2007-2008

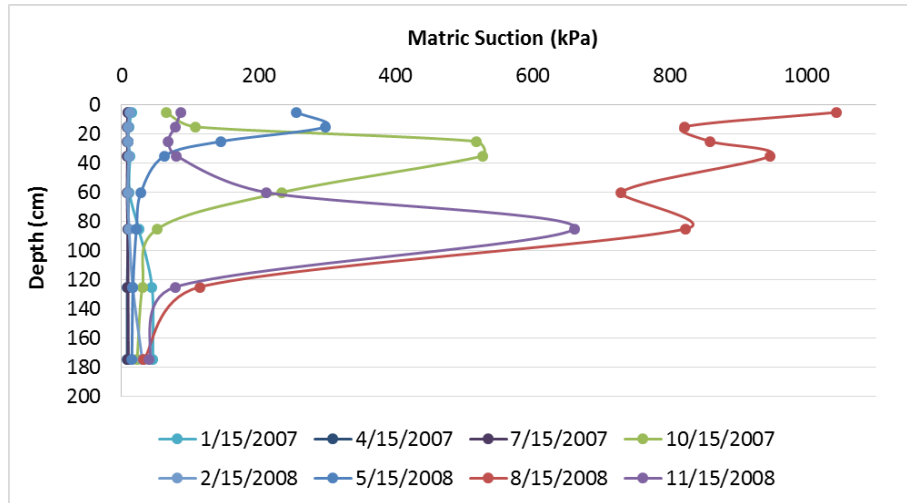


6.4.c Byron 2011-2012

Figure 6.4 Matric suction profile for Byron



6.5.a Cordell 2001-2002



6.5.b Cordell 2007-2008

Figure 6.5 Matric suction profile for Cordell

Table 6.2 lists the active zone depth obtained from the ARM sites and the two methodologies. Only Byron and El Reno sites have the matric suction data during 2011-2012. By comparing the active zone depth obtained from the three different ways, the results obtained from the empirical equation are closer to the field measurement. However, due to the limitation on spatial coverage and data availability of the ARM sites, it is still difficult to determine which methodology is more accurate in predicting the active zone depth.

Table 6.2 Active zone depth compared with the ARM measurement

Site Location	Active Zone Depth (ARM Measurement) (m)			Active Zone Depth (Empirical Equation) (m)			Active Zone Depth (Numerical Modeling) (m)
	2001-2002	2007-2008	2011-2012	2001-2002	2007-2008	2011-2012	2011-2012
Byron	1.75	1.25	> 1.75	0.5 – 1	2 – 3	0.2 – 1	1 – 2
Ringwood	1.75	1.75	NA	1 – 2	2 – 3	0.2 – 1	1 – 2
Vici	> 1.75	> 1.75	NA	1 – 2	2 – 3	1 – 2	1 – 2
El Reno	NA	NA	1.75	1 – 2	3 – 4	1 – 2	3 – 4
Cordell	1.75	1.75	NA	1 – 2	2 – 3	0.2 – 1	2 – 3
Seminole	1.25	NA	NA	1 – 2	1 – 2	1 – 2	1 – 2
Cyril	> 1.25	NA	NA	1 – 2	2 – 3	1 – 2	2 – 3
Meeker	0.85	NA	NA	1 – 2	2 – 3	1 – 2	2 – 3

CHAPTER VII

CONCLUSIONS

7.1 Summary

The performance of geotechnical structure highly depends on the soil behavior and near-surface climatic conditions. To understand the unsaturated flow properties of expansive soils, accurate field investigation is required. The Oklahoma Mesonet and the DOE ARM network provide continuous matric suction measurements by the thermal conductivity sensor. The field measurement of matric suction indicated a clear seasonal pattern of matric suction variations in response to climatic conditions, more specifically, to precipitation, evapotranspiration, and runoff. The matric suction data can be used to estimate both equilibrium suction and active zone depth. The active zone depth and the matric suction variations within this zone directly influence the shrink-swell properties of expansive soils. The realistic evaluation of the active zone is essential to prevent structures affected by soil behavior within this zone. The numerical modeling of slab-on-ground foundations built on top of the expansive soils provides a good example of applying the matric suction fluctuation and active zone depth in the geotechnical engineering practice. To reach the objectives of this research, two methodologies were

applied. The first methodology used an empirical equation, including matric suction, climate frequency, and diffusion coefficient, to determine the active zone depth. The following conclusions were drawn:

- (1) The analysis of time series plots of matric suction indicated different seasonal soil moisture trends during a year. Overall, the deeper depths (60 cm and 75 cm) had less temporal variability than those of the shallower depths (5 cm and 25 cm).
- (2) Contour maps of active zone depth indicated that the active zone depth varies year by year. However, no matter under what moisture conditions, most parts of Oklahoma have the active zone depth ranging from 0.5 m to 4 m. Eastern Oklahoma has a little deeper active zone depth than western Oklahoma due to the more frequent moisture fluctuations.
- (3) The active zone depth is highly sensitive to the diffusion coefficient. The diffusion coefficient plays a significant role in governing the rate of moisture penetration in the soil. Since the diffusion coefficient was determined by the matric suction, the active zone depth is related to the matric suction. The lower the matric suction, the higher the diffusion coefficient, the deeper the active zone depth.

The numerical modeling approach determined active zone depth by analyzing the matric suction redistribution in soil induced by evapotranspiration. Overall, the numerical models for estimating matric suction redistribution and active zone depth would be a practical tool in geotechnical engineering investigations. The results indicated that the active zone ranges from 0.5 m to 3.5 m in Oklahoma during drying periods, which are similar to the results from the numerical model. The active zone depth is highly impacted by SWCC parameters and saturated hydraulic conductivity. Both of two methodologies

used in this research prove that active zone depth is a function of soil properties and climatic conditions.

7.2 Recommendations for Future Research

Although the primary objectives of this research have been achieved, further research is necessary to improve our understanding the impact of unsaturated flow in engineering practice. Recommendations for future research are summarized below:

- (1) One limitation of this study is the shortage of field soil matric suction measured at depths greater than 75 cm. Previous research indicated that soil moisture sensors were installed up to 5-m depth for geotechnical purposes (Wray 1987, Nichol et al. 2003, Nguyen et al. 2010). As a result, matric suction measured at a deeper depth could help future research. Another limitation is that the Mitchell's matric suction prediction did not consider the groundwater table depth. The moisture conditions in unsaturated zone is often related to the depth of groundwater table (Ray et al. 2010). As a result, future research will be needed to evaluate the effect of groundwater table depth on matric suction.
- (2) Laboratory tests for the diffusion coefficient can be conducted to evaluate if the diffusion coefficient calculated from the field matric suction is accurate.
- (3) In numerical modeling, only drying process was tested by setting the evapotranspiration boundary condition. Infiltration and runoff are two important boundary variables during wetting process. By knowing these two parameters, wetting process can also be simulated in numerical modeling.
- (4) Although the models in this research were performed under two dimensions, the slab-on-ground problems can be extended to three dimensions in the future research.

The three-dimensional modeling of unsaturated flow can also help to improve the understanding of the factors that affect active zone depth.

- (5) The long-term measured matric suction can be used in slope stability analysis. In slope stability analysis, the effect of matric suction is usually ignored since matric suction will reduce with rainfall infiltration and therefore it can be assumed that matric suction does not influence the slope stability. However, in reality, the slope stability will be affected by the distribution of matric suction in soil. The slope stability increases when matric suction is taken into account.

REFERENCES

- Abbaszadeh, M. (2011). *The effect of cracks on unsaturated flow and volume change properties of expansive clays and impacts on foundation performance* (Doctoral dissertation). Retrieved from ProQuest Dissertations and Theses. (Accession Order No. 913502086).
- Aubeny, C. P., & Lytton, R. L. (2004). Shallow slides in compacted high plasticity clay slopes. *Journal of Geotechnical and Geoenvironmental Engineering*, *130*(7), 717-727.
- Aubeny, C., & Long, X. (2007). Moisture diffusion in shallow clay masses. *Journal of Geotechnical and Geoenvironmental engineering*, *133*(10), 1241-1248.
- Auvray, R., Rosin-Paumier, S., Abdallah, A., & Masrouri, F. (2014). Quantification of soft soil cracking during suction cycles by image processing. *European Journal of Environmental and Civil Engineering*, *18*(1), 11-32.
- Bai, J., Deng, W., Cui, B., & Ouyang, H. (2007). Water diffusion coefficients of horizontal soil columns from natural saline-alkaline wetlands in a semiarid area. *Eurasian Soil Science*, *40*(6), 660-664.
- Barbour, S. L., & Krahn, J. (2004). Numerical modelling—Prediction or process. *Geotechnical News*, *22*(4), 44-52.
- Basara, J. B., & Crawford, T. M. (2000). Improved installation procedures for deep-layer soil moisture measurements. *Journal of Atmospheric and Oceanic Technology*, *17*(6), 879-884.
- Beaudette, D. E., & O'Geen, A. T. (2009). Soil-Web: an online soil survey for California, Arizona, and Nevada. *Computers & Geosciences*, *35*(10), 2119-2128.
- Bell, F. G. (1999). *Geological hazards: their assessment, avoidance and mitigation*. CRC Press.

- Bharadwaj, A. (2013). *Effect of soil replacement option on surface deflections for expansive clay profiles* (Doctoral dissertation). Retrieved from ProQuest Dissertations and Theses. (Accession Order No. 3560026).
- Bobrowsky, P. T. (Ed.). (2013). *Encyclopedia of natural hazards*. Springer.
- Bond, D. (2005). Soil water and temperature system (SWATS) handbook. The U.S. Department of Energy, Office of Science, Office of Biological and Environmental Research.
- Buhler, R. L., & Cerato, A. B. (2007). Stabilization of Oklahoma expansive soils using lime and Class C fly ash. *ASCE Geotechnical Special Publication*, 162, 1-10.
- Campbell Scientific, Inc. (2009). 229 *Heat dissipation matric water potential sensor*. Instruction Manual.
- Canadian County, Oklahoma. (2013). *Multi-Jurisdictional Multi-Hazard Mitigation Plan Update*. Flanagan & Associates, LLC.
- Carsel, R. F., & Parrish, R. S. (1988). Developing joint probability distributions of soil water retention characteristics. *Water Resources Research*, 24(5), 755-769.
- Carter, B. J., & Gregory, M. S. (2008). Soil map of Oklahoma. *Erath Sciences and Mineral Resources of Oklahoma*. Educational Publication 9, Oklahoma Geological Survey.
- Chen, F. H. (2012). *Foundations on expansive soils* (Vol. 12). Elsevier.
- Childs, C. (2004). Interpolating surfaces in ArcGIS spatial analyst. *ArcUser*, July-September, 3235.
- Clarke, C., & Nevels Jr, J. (1996). Shrinkage and suction properties of Pledger-Roebuck alluvial clay. *Transportation Research Record: Journal of the Transportation Research Board*, (1546), 162-173.
- Durkee, D. B. (2000). *Active zone depth and edge moisture variation distance in expansive soils* (Doctoral dissertation). Retrieved from ProQuest Dissertations and Theses. (Accession Order No. 2000.9985540)
- El-Garhy, B. M., & Wray, W. K. (2004). Method for calculating the edge moisture variation distance. *Journal of Geotechnical and Geoenvironmental Engineering*, 130(9), 945-955.
- Farouk, A., Lamboj, L., & Kos, J. (2004). A numerical model to predict matric suction inside unsaturated soils. *Acta Polytechnica*, 44(4).
- Flanagan & Associates, LLC. (2013). Canadian County Multi-Hazard Mitigation Plan.
- Foundation Repair Guide. (2007). *Expansive Soil Problems and Solutions*. (n.d.). Retrieved April 10, 2015, from <http://www.foundation-repair-guide.com/expansive-soil.html>
- Fredlund, D. G. (1992). Background, theory, and research related to the use of thermal conductivity sensors for matric suction measurement. *Advances in Measurement of*

- Soil Physical Properties: Bringing Theory into Practice*, (advancesinmeasu), 249-261.
- Fredlund, D. G., & Xing, A. (1994). Equations for the soil-water characteristic curve. *Canadian geotechnical journal*, 31(4), 521-532.
- Fredlund, D. G., & Vu, H. Q. (2003). Numerical Modelling of Swelling and Shrinking soils around slabs-on-ground. In *Proceeding, Post-Tensioning Institute Annual Technical Conference, Huntington Beach, CA, USA*.
- Fredlund, D. G., Sheng, D., & Zhao, J. (2011). Estimation of soil suction from the soil-water characteristic curve. *Canadian geotechnical journal*, 48(2), 186-198.
- Fredlund, D. G., Rahardjo, H., & Fredlund, M. D. (2012). *Unsaturated soil mechanics in engineering practice*. John Wiley & Sons.
- Gardner, W. R. (1958). Some steady-state solutions of the unsaturated moisture flow equation with application to evaporation from a water table. *Soil science*, 85(4), 228-232.
- Gitirana Jr, G., Fredlund, M. D. & Fredlund, D. G. (2005). Infiltration-runoff boundary conditions in seepage analysis. *sat*, 1, 3.
- Guttman, N. B., & Quayle, R. G. (1996). A historical perspective of US climate divisions. *Bulletin of the American Meteorological Society*, 77(2), 293-303.
- Hillel, D. (2004). *Introduction to environmental soil physics*. Elsevier Academic Press.
- Hu L, Peron H, Hueckel T, Laloui L. (2006). Numerical and phenomenological study of desiccation of soil. *Advances in Unsaturated Soil, Seepage, and Environmental Geotechnics*. ASCE geotechnical special publication, 148, 166-173,
- Illston, B. G., Basara, J. B., & Crawford, K. C. (2004). Seasonal to interannual variations of soil moisture measured in Oklahoma. *International Journal of Climatology*, 24(15), 1883-1896.
- Illston, B. G., Basara, J. B., Fiebrich, C. A., Crawford, K. C., Hunt, E., Fisher, D. K., Ellicott, R., Fiebrich, C. A., Crawford, K. C., Humes, K. & Hunt, E. (2008). Mesoscale monitoring of soil moisture across a statewide network. *Journal of Atmospheric and Oceanic Technology*, 25(2), 167-182.
- Jensen, M. E., Burman, R. D., and Allen, R. G. (ed). (1990). *Evapotranspiration and Irrigation Water Requirements*. ASCE Manuals and Reports on Engineering Practice No.70, New York.
- Johnson, H. L. (2008). *Climate of Oklahoma. Erath Sciences and Mineral Resources of Oklahoma*. Educational Publication 9, Oklahoma Geological Survey.
- Kerrane, J. P. (2004, January 7). What Are Expansive Soils? [Web log post]. Retrieved May 15, 2015, from <http://www.bensonpc.com/blog/post/what-are-expansive-soils>

- Kirkham, M. B. (2014). *Principles of soil and plant water relations*. Academic Press.
- Kumaran, M., Mukhopadhyaya, P., & Normandin, N. (2007). Determination of equilibrium moisture content of building materials: some practical difficulties. In *Heat-Air-Moisture Transport: Measurements on Building Materials*. ASTM International.
- Luza, K. V., & Johnson, K. S. (2005). *Geologic Hazards in Oklahoma*. Oklahoma Geological Survey.
- Lytton, R. L. (1977). Foundations in expansive soils. *Numerical methods in geotechnical engineering*, 427, 457.
- Lytton, R. L. (1994). Prediction of movement in expansive clays. In *Vertical and horizontal deformations of foundations and embankments*, 1827-1845. ASCE.
- Lytton, R.L., Aubeny, C.P, and Bulut, R. (2006) Design Procedure for Expansive Soils. FHWA/TX-05/0-4518-2, Volume 2, Texas Transportation Institute, College Station, Texas.
- Mather, J. R. (1974). *Climatology: fundamentals and applications*. Macgraw hill.
- McKeen, R. G., & Johnson, L. D. (1990). Climate-controlled soil design parameters for mat foundations. *Journal of Geotechnical engineering*, 116(7), 1073-1094.
- Mitchell, P. W. (1979). The structural analysis of footings on expansive soil. *Kenneth W. G. Smith & Associates. Research Report No. I*. Webb & Son. Adelaide. Australia.
- Morris, P. H., Graham, J., & Williams, D. J. (1992). Cracking in drying soils. *Canadian Geotechnical Journal*, 29(2), 263-277.
- Mualem, Y. (1976). A new model for predicting the hydraulic conductivity of unsaturated porous media. *Water Resour. Res.*, 12(3), 513-522.
- Nelson, J. D., & Miller, D. J. (1992). *Expansive soils: problems and practice in foundation and pavement engineering*. John Wiley & Sons.
- Nelson, J. D., Overton, D. D., & Durkee, D. B. (2001). Depth of wetting and the active zone. In *Expansive Clay Soils and Vegetative Influence on Shallow Foundations*, GSP115, 95-109.
- Nelson, J. D., Chao, K. C., Overton, D. D., & Nelson, E. J. (2014). *Foundation Engineering for Expansive Soils*. John Wiley & Sons.
- Nevels, J. B. (1995). The use of soil suction in analysis of pavement cracking. In *Soil Suction Applications in Geotechnical Engineering Practice*, 14-37. ASCE.
- Nichol, C., Smith, L., & Beckie, R. (2003). Long-term measurement of matric suction using thermal conductivity sensors. *Canadian Geotechnical Journal*, 40(3), 587-597.

- Nguyen, Q., Fredlund, D. G., Samarasekera, L., & Marjerison, B. L. (2010). Seasonal pattern of matric suctions in highway subgrades. *Canadian Geotechnical Journal*, 47(3), 267-280.
- Novak, V. (1999). Soil-crack characteristics—estimation methods applied to heavy soils in the NOPEX area. *Agricultural and Forest Meteorology*, 98, 501-507.
- O'Rourke, T. D. & Bonneau, A. L. (2007). Lifeline performance under extreme loading during earthquakes. *Earthquake Geotechnical Engineering: 4th International Conference on Earthquake Geotechnical Engineering-Invited Lectures* (Vol. 6). Springer Science & Business Media.
- Perera, Y. Y., Zapata, C. E., Houston, W. N., & Houston, S. L. (2004). Long-term moisture conditions under highway pavements. *Geotechnical Engineering for Transportation Projects: Proceedings of Geo-Trans*.
- Post-Tensioning Institute. (1980). *Design and Construction of Post-Tensioned Slabs-on-Ground*. Phoenix, Arizona.
- Qiu, G. Y. and Ben-Asher, J. (2010). Experimental determination of soil evaporation stages with soil surface temperature. *Soil Science Society of America Journal* Vol. 74, No. 1: 13-22.
- Ray, R. L., Jacobs, J. M., & de Alba, P. (2010). Impacts of unsaturated zone soil moisture and groundwater table on slope instability. *Journal of geotechnical and geoenvironmental engineering*, 136(10), 1448-1458.
- Richards, L. A. (1931). Capillary conduction of liquids through porous mediums. *Journal of Applied Physics*, 1(5), 318-333.
- Richards, B. G., & Chan, C. Y. (1971). Theoretical analyses of subgrade moisture under Australian environmental conditions and their practical implications. *Australian Road Research*, 4(6).
- Ridley, A. M., Dineen, K., Burland, J. B., & Vaughan, P. R. (2003). Soil matrix suction: some examples of its measurement and application in geotechnical engineering. *Géotechnique*, 53(2), 241-253.
- Sakata, K. (1983). A study on moisture diffusion in drying and drying shrinkage of concrete. *Cement and Concrete Research*, 13(2), 216-224.
- Schaap, M. G., Leij, F. J., & van Genuchten, M. T. (2001). ROSETTA: a computer program for estimating soil hydraulic parameters with hierarchical pedotransfer functions. *Journal of hydrology*, 251(3), 163-176.
- Scott, B. L., Ochsner, T. E., Illston, B. G., Fiebrich, C. A., Basara, J. B., & Sutherland, A. J. (2013). New soil property database improves Oklahoma Mesonet soil moisture estimates*. *Journal of Atmospheric and Oceanic Technology*, 30(11), 2585-2595.

- Shi, B. X., Chen, S. S., Han, H. Q., & Zheng, C. F. (2014). Expansive Soil Crack Depth under Cumulative Damage. *The Scientific World Journal*, 2014.
- Shuai, F., Clements, C., Ryland, L., & Fredlund, D. G. (2002, March). Some factors that influence soil suction measurements using a thermal conductivity sensor. In *Unsaturated Soils: Proceedings of the 3rd International Conference on Unsaturated Soils (UNSAT 2002), Recife, Brazil*, 325-329.
- Snethen, D. R., Johnson, L. D., & Patrick, D. M. (1977). An Evaluation of Expedient Methodology for Identification of Potentially Expansive Soils. FHWA-RD-77-94. National Technical Information Service, Springfield, Virginia.
- Swenson, S., Famiglietti, J., Basara, J., & Wahr, J. (2008). Estimating profile soil moisture and groundwater variations using GRACE and Oklahoma Mesonet soil moisture data. *Water Resources Research*, 44(1).
- Tabari, H., Aeini, A., Talaei, P. H., and Some'e, B. S. (2012). Spatial distribution and temporal variation of reference evapotranspiration in arid and semi-arid regions of Iran. *Hydrological Processes* 26: 500-512.
- The Oklahoma Climatological Survey. (2002). Oklahoma Annual Climate Summary 2001.
- The Oklahoma Climatological Survey. (2011). Climate of Oklahoma [Web log post]. Retrieved January 20, 2015, from http://climate.ok.gov/index.php/site/page/climate_of_oklahoma
- The Oklahoma Climatological Survey. (2014). Map of Oklahoma climate divisions. Retrieved June 14, 2016, from http://climate.ok.gov/index.php/climate/map/map_of_oklahoma_climate_divisions/oklahoma_climate
- The Oklahoma Mesonet (2015). Mesonet Sites. Retrieved July 10, 2015, from http://www.mesonet.org/index.php/site/sites/station_names_map
- The Oklahoma Mesonet. (2016). Short Crop (Etos) ET Map. Retrieved July 5, 2016, from https://www.mesonet.org/index.php/agriculture/map/agriculture_essentials/evapotranspiration/short_crop_etos_et_map
- Thieu, N. T. M., Fredlund, M. D., Fredlund, D. G., & Vu, H. Q. (2001, October). Seepage modelling in a saturated/unsaturated soil system. In *Proceedings of the International Conference on Management of the Land and Water Resources, Hanoi, Vietnam* (pp. 20-22).
- Thode, R. (2004). SVFlux theory manual. *Soilvision Systems Ltd., Sakatchewan, Canada*.
- Thorntwaite, C. W. (1948). An approach toward a rational classification of climate. *Geographical review*, 55-94.
- U.S. Climate Data. (2010). Climate of Oklahoma. Retrieved June 14, 2016, from <http://www.usclimatedata.com/climate/oklahoma/united-states/3206>

- USDA Web soil survey. (2009). Web soil survey. Retrieved April 11, 2016, from <http://websoilsurvey.sc.egov.usda.gov>
- van Genuchten, M. T. (1980). A closed-form equation for predicting the hydraulic conductivity of unsaturated soils. *Soil science society of America journal*, 44(5), 892-898.
- Visser, A., Stuurman, R., & Bierkens, M. F. (2006). Real-time forecasting of water table depth and soil moisture profiles. *Advances in water resources*, 29(5), 692-706.
- Wilson, G. W., Fredlund, D. G., & Barbour, S. L. (1997). The effect of soil suction on evaporative fluxes from soil surfaces. *Canadian Geotechnical Journal*, 34(1), 145-155.
- Wray, W. K. (1987). Evaluation of static equilibrium soil suction envelopes for predicting climate-induced soil suction changes occurring beneath covered surfaces. In *Proc., 6th Int. Conf. on Expansive Soils* Vol. 1, 235-240.
- Zapata, C. E. (1999). *Uncertainty in soil-water-characteristic curve and impacts on unsaturated shear strength predictions*. (Doctoral dissertation). Retrieved from ProQuest Dissertations and Theses. (Accession Order No. 9950269, Arizona State University)
- Zhang, L. L., Fredlund, D. G., Zhang, L. M., & Tang, W. H. (2004). Numerical study of soil conditions under which matric suction can be maintained. *Canadian Geotechnical Journal*, 41(4), 569-582.

APPENDICES

Appendix A

Mesonet Station Information

Station ID	City	County	Soil Characteristics at 5 cm Depth			Plasticity Index (%)
ADAX	Ada	Pontotoc	Sandy loam	Sand: 61.1% Clay: 16.9%	Silt: 22%	24.5
ALTU	Altus	Jackson	Clay loam	Sand: 23.8% Clay: 36.2%	Silt: 40%	27.5
ARD2	Ardmore	Carter	Clay loam	Sand: 33.6% Clay: 32.2%	Silt: 34.1%	40
ARNE	Arnett	Ellis	Loam	Sand: 45.5% Clay: 23.4%	Silt: 31.1%	13.9
BEAV	Beaver	Beaver	Loam	Sand: 40.6% Clay: 24.3%	Silt: 35.1%	14.1
BESS	Bessie	Washita	Silt loam	Sand: 26% Clay: 23.6%	Silt: 50.5%	14
BIXB	Bixby	Tulsa	Sandy loam	Sand: 43.6% Clay: 6.9%	Silt: 49.5%	9.5
BOIS	Boise City	Cimarron	Clay	Sand: 35% Clay: 41.2%	Silt: 23.8%	27.5
BOWL	Bowlegs	Seminole	Sandy loam	Sand: 58% Clay: 13.2%	Silt: 28.8%	11.5
BREC	Breckinridge	Garfield	Silt loam	Sand: 18.8% Clay: 24.1%	Silt: 57.1%	28
BUFF	Buffalo	Harper	Loam	Sand: 31.8% Clay: 20.2%	Silt: 48%	12.5
BURN	Burneyville	Love	Silt loam	Sand: 20.1% Clay: 26%	Silt: 53.9%	2

Station ID	City	County	Soil Characteristics at 5 cm Depth		Plasticity Index (%)
BUTL	Butler	Custer	Silty clay loam	Sand: 15.6% Silt: 52% Clay: 32.3%	6
CALV	Calvin	Hughes	NA	NA (Retired in 2009)	NA
CENT	Centrahoma	Coal	Loam	Sand: 50.9% Silt: 35.9% Clay: 13.2%	10
CHAN	Chandler	Lincoln	Sandy loam	Sand: 75.5% Silt: 15.7% Clay: 8.8%	8
CHER	Cherokee	Alfalfa	Loam	Sand: 40.6% Silt: 43.6% Clay: 15.8%	14
CHEY	Cheyenne	Roger Mills	Loam	Sand: 40.3% Silt: 35.8% Clay: 23.9%	8
CLOU	Cloudy	Pushmataha	Silt loam	Sand: 36.6% Silt: 54% Clay: 9.4%	15.5
COPA	Copan	Washington	Loam	Sand: 44.6% Silt: 33.4% Clay: 22%	15.5
DURA	Durant	Bryan	Clay loam	Sand: 41.9% Silt: 30.9% Clay: 27.1%	26.5
ELRE	El Reno	Canadian	Silt loam	Sand: 16.3% Silt: 60.9% Clay: 22.8%	16
ERIC	Erick	Beckham	Sandy loam	Sand: 63.5% Silt: 22.6% Clay: 13.8%	8
EUFA	Eufaula	McIntosh	Silt loam	Sand: 36% Silt: 53.2% Clay: 10.8%	24.5
FAIR	Fairview	Major	Silty clay loam	Sand: 18.6% Silt: 51.7% Clay: 29.8%	13.7
FTCB	Fort Cobb	Caddo	Sandy loam	Sand: 78.1% Silt: 8.8% Clay: 13.1%	10.5
GOOD	Goodwell	Texas	Clay loam	Sand: 36.6% Silt: 34.6% Clay: 28.8%	16
GUTH	Guthrie	Logan	Loam	Sand: 47% Silt: 28.4% Clay: 24.6%	12.5
HASK	Haskell	Muskogee	Silt loam	Sand: 10.1% Silt: 74.2% Clay: 15.7%	13.5
HOBA	Hobart	Kiowa	Silt loam	Sand: 11% Silt: 63.5% Clay: 25.4%	27.5
HOLL	Gould	Harmon	Clay	Sand: 20.7% Silt: 35.2% Clay: 44.1%	28
HUGO	Hugo	Choctaw	Loam	Sand: 34.9% Silt: 47% Clay: 18.2%	18

Station ID	City	County	Soil Characteristics at 5 cm Depth		Plasticity Index (%)
IDAB	Idabel	McCurtain	Silty clay loam	Sand: 1.5% Silt: 67.5% Clay: 30.9%	20
INOL	Inola	Rogers	Loam	Sand: 33.4% Silt: 48.2% Clay: 18.4%	11.7
JAYX	Jay	Delaware	Silt loam	Sand: 7.4% Silt: 74.5% Clay: 18.1%	20
KETC	Ketchum Ranch	Stephens	Loam	Sand: 44.2% Silt: 33.3% Clay: 22.6%	24.5
KING	Kingfisher	Kingfisher	NA	NA (Retired in 2009)	NA
LANE	Lane	Atoka	Silt loam	Sand: 37.8% Silt: 51.5% Clay: 10.7%	12.5
MANG	Mangum	Greer	Loamy sand	Sand: 88.7% Silt: 2.9% Clay: 8.4%	10
MAYR	May Ranch	Woods	Loam	Sand: 44.2% Silt: 34.3% Clay: 21.6%	13
MCAL	McAlester	Pittsburg	Sandy loam	Sand: 66.2% Silt: 25% Clay: 8.8%	13.5
MEDI	Medicine Park	Comanche	Sandy loam	Sand: 63.6% Silt: 18.9% Clay: 17.6%	26.5
MIAM	Miami	Ottawa	Silt loam	Sand: 15.6% Silt: 60.5% Clay: 23.9%	24.5
MINC	Minco	Grady	Silt loam	Sand: 18.7% Silt: 61.1% Clay: 20.2%	16
NEWK	Newkirk	Kay	Silty clay loam	Sand: 13.6% Silt: 56.6% Clay: 29.9%	24.5
NOWA	Delaware	Nowata	Silt loam	Sand: 22% Silt: 59.2% Clay: 18.9%	24.5
NRMN	Norman	Cleveland	Silt clay	Sand: 8.3% Silt: 49% Clay: 42.7%	28
OILT	Oilton	Creek	Loam	Sand: 45.8% Silt: 40.3% Clay: 13.9%	14
OKEM	Okemah	Okfuskee	Loam	Sand: 27.3% Silt: 49.3% Clay: 23.4%	24.5
OKMU	Morris	Okmulgee	Silt loam	Sand: 15.9% Silt: 66.5% Clay: 17.6%	21.7
PAUL	Pauls Valley	Garvin	Silt loam	Sand: 23.3% Silt: 60.4% Clay: 16.3%	24.5
PAWN	Pawnee	Pawnee	Silty clay loam	Sand: 11.2% Silt: 50.5% Clay: 38.2%	11.5

Station ID	City	County	Soil Characteristics at 5 cm Depth			Plasticity Index (%)
			Soil Type	Sand	Silt	
PORT	Clarksville	Wagoner	Sandy loam	Sand: 53.1% Clay: 12.8%	Silt: 34.1%	12.5
PRYO	Adair	Mayes	Silt loam	Sand: 14.9% Clay: 18.9%	Silt: 66.2%	15.5
PUTN	Putnam	Dewey	Loam	Sand: 31.6% Clay: 24.1%	Silt: 44.3%	16
REDR	Red Rock	Noble	Clay loam	Sand: 28.7% Clay: 29%	Silt: 42.3%	24.5
SALL	Sallisaw	Sequoyah	Silt loam	Sand: 22.9% Clay: 15.7%	Silt: 61.4%	26.5
SHAW	Shawnee	Pottawatomie	Silt loam	Sand: 23.2% Clay: 18.9%	Silt: 57.9%	26.5
SPEN	Spencer	Oklahoma	Sandy loam	Sand: 74.2% Clay: 16.4%	Silt: 9.4%	11.5
STIG	Stigler	Haskell	Silt loam	Sand: 21.9% Clay: 12.6%	Silt: 65.5%	26.5
STIL	Stillwater	Payne	Silty clay loam	Sand: 15.7% Clay: 34.8%	Silt: 49.6%	16
TAHL	Tahlequah	Cherokee	Silt loam	Sand: 25.8% Clay: 12.6%	Silt: 61.6%	15
TIPT	Tipton	Tillman	Loam	Sand: 42.6% Clay: 15.8%	Silt: 41.6%	31
TISH	Tishomingo	Johnston	Silt loam	Sand: 32% Clay: 17.6%	Silt: 50.4%	31
VINI	Vinita	Craig	Silt loam	Sand: 15.6% Clay: 20.3%	Silt: 64.1%	24.5
WALT	Walters	Cotton	Silty clay loam	Sand: 17.8% Clay: 31.8%	Silt: 50.3%	12.5
WASH	Washington	McClain	Loam	Sand: 41.2% Clay: 21.5%	Silt: 37.3%	12.6
WATO	Watonga	Blaine	Loam	Sand: 33.7% Clay: 22.5%	Silt: 43.9%	15.7
WAUR	Waurika	Jefferson	Sandy loam	Sand: 66.1% Clay: 13.2%	Silt: 20.7%	12.5
WEST	Westville	Adair	Silt loam	Sand: 18.8% Clay: 13.3%	Silt: 67.9%	14

Station ID	City	County	Soil Characteristics at 5 cm Depth			Plasticity Index (%)
WILB	Wilburton	Latimer	Silt loam	Sand: 33.1% Clay: 15.1%	Silt: 51.7%	26.5
WIST	Wister	LeFlore	Silt loam	Sand: 17.5% Clay: 20.8%	Silt: 61.8%	26
WOOD	Woodward	Woodward	Clay loam	Sand: 35.3% Clay: 28.6%	Silt: 36.2%	12.5
WYNO	Wynona	Osage	Loam	Sand: 25.4% Clay: 26.3%	Silt: 48.3%	30

Appendix B

Detailed calculation of Equation 4.1:

$$ET_{SZ} = \frac{0.408 \Delta (R_n - G) + \gamma c_n u_2 (e_s - e_a) / (T + 273)}{\Delta + \gamma (1 + C_d u_2)}$$

where ET_{SZ} = standardized reference crop evapotranspiration (mm/day);

$$\Delta = \text{slope of the vapor pressure-temperature curve (kPa/}^\circ\text{C)} = \frac{2503 \exp\left(\frac{17.27 T}{T + 237.3}\right)}{(T + 237.3)^2},$$

$$T = \text{mean daily air temperature at 1.5 to 2.5-m height (}^\circ\text{C)} = \frac{T_{\max} + T_{\min}}{2},$$

T_{\max} = daily maximum air temperature ($^\circ\text{C}$);

T_{\min} = daily minimum air temperature ($^\circ\text{C}$);

R_n = net radiation at the crop surface ($\text{MJ/m}^2/\text{day}$) = $R_{ns} - R_{nl}$;

R_{ns} = net solar or short-wave radiation ($\text{MJ/m}^2/\text{day}$) = $(1 - \alpha) R_s$;

α = albedo or canopy reflection coefficient, is set as 0.23 for the standardized short and tall reference surfaces;

R_s = the incoming solar radiation ($\text{MJ/m}^2/\text{day}$);

R_{nl} = net outgoing long-wave radiation ($\text{MJ/m}^2/\text{day}$) = $\sigma f_{cd} (0.34 - 0.14\sqrt{e_a}) T_k^4$;

σ = Stefan-Boltzmann constant = 4.901×10^{-9} ($\text{MJ/K}^4/\text{m}^2/\text{day}$);

e_a = actual vapor pressure (kPa) = $0.6108 \exp\left(\frac{17.27 T_{\text{dew}}}{T_{\text{dew}} + 237.3}\right)$;

e_s = mean saturation vapor pressure at 1.5 to 2.5-m height (kPa) =
 $\frac{e^o(T_{\max}) + e^o(T_{\min})}{2}$;

$e^o(T)$ = saturation vapor pressure function = $0.6108 \exp\left(\frac{17.27 T}{T+237.3}\right)$;

T_{dew} = daily dew point temperature ($^{\circ}\text{C}$);

T_k = mean absolute temperature (K) = $T + 273.16$;

f_{cd} = cloudiness function = $1.35 \frac{R_s}{R_{s0}} - 0.35$ (dimensionless, limited to $0.05 \leq f_{\text{cd}} \leq 1.0$);

R_{s0} = clear-sky solar radiation ($\text{MJ}/\text{m}^2/\text{day}$) = $(0.75 + 2 \times 10^{-5} Z) R_a$;

Z = weather station elevation above sea level (m);

R_a = extraterrestrial radiation ($\text{MJ}/\text{m}^2/\text{day}$);

$$= \frac{24}{\pi} G_{\text{sc}} d_r [\omega_s \sin(\phi) \sin(\delta) + \cos(\phi) \cos(\delta) \sin(\omega_s)];$$

G_{sc} = solar constant = $4.94 \text{ [MJ//m}^2/\text{h]}$;

d_r = inverse relative distance factor for earth-sun = $1 + 0.33 \cos\left(\frac{2\pi J}{365}\right)$;

J = number of the day in the year between 1 (January 1) and 365 or 366 (December 31);

ω_s = sunset hour angle = $\arcsin[-\tan(\phi) \tan(\delta)]$;

ϕ = weather station latitude;

δ = solar declination = $0.409 \sin\left(\frac{2\pi}{365}J - 1.39\right)$;

G = soil heat flux density at the soil surface (MJ/m²/day); compared to R_n , G is very small, so G is set as 0 in this equation;

γ = psychrometric constant (kPa/°C);

u_2 = mean daily wind speed at 2-m height (m/s);

C_n = numerator constant for reference type (900 for short reference crop);

C_d = denominator constant for reference type (0.34 for short reference crop).

Appendix C

Fitting Parameters and Active Zone Depth for Dry Period

Station ID	R Square of Fitting	U _e (pF)	U ₀ (pF)	n (cycles/year)	α (cm ² /day)	Active Zone Depth (m)
ARD2	0.66	2.89	0.91	0.89	75	0.81
ARNE	0.83	3.28	0.75	0.94	765	2.47
BEAV	0.89	3.27	0.70	0.81	32	0.46
BIXB	0.68	2.76	0.83	0.98	62	0.75
BREC	0.54	2.92	0.74	0.99	45	0.62
BUTL	0.79	3.19	0.78	0.96	41	0.59
CENT	0.69	2.60	0.55	0.95	41	0.51
CHER	0.87	3.18	0.82	0.93	13	0.33
CHEY	0.64	3.33	0.62	1.13	7	0.24
COPA	0.79	2.94	1.08	0.99	74	0.89
ELRE	0.58	2.93	0.74	0.77	40	0.51
EUFA	0.67	2.92	0.99	0.97	251	1.59
GOOD	0.64	3.01	0.83	0.15	67	0.31
HASK	0.59	2.96	0.93	1.03	340	1.86
HOBA	0.73	3.04	0.82	0.65	168	0.99
HOLL	0.73	2.88	0.84	0.89	74	0.78
KETC	0.70	3.06	0.87	0.68	90	0.76
LANE	0.77	2.63	0.85	1.02	135	1.13
MAYR	0.86	3.14	0.90	0.96	101	0.97
MIAM	0.78	2.84	0.92	1.02	78	0.89
NEWK	0.65	2.81	0.74	1.04	3747	5.74
NOWA	0.82	3.06	0.91	0.99	989	3.09
NRMN	0.66	2.97	0.88	0.67	2089	3.67
OILT	0.73	2.54	0.47	1.11	141	0.96
PAUL	0.53	2.62	0.60	1.06	2074	3.97
PAWN	0.68	2.61	0.68	0.93	31	0.48
PORT	0.74	2.80	0.99	0.95	114	1.06
PUTN	0.87	2.97	0.93	0.95	36	0.58
SALL	0.63	2.49	0.71	1.12	174	1.13
SPEN	0.56	2.63	0.71	1.19	82	0.89
STIG	0.78	2.51	0.64	1.19	816	2.71
STIL	0.80	2.85	0.93	0.96	216	1.43
VINI	0.71	2.50	0.74	0.96	187	1.23
WALT	0.67	3.23	0.78	1.82	86	1.17
WAUR	0.62	2.76	0.82	0.90	174	1.19
WILB	0.63	3.02	1.02	1.02	2153	4.82
WIST	0.62	3.13	0.87	1.03	1360	3.66
WOOD	0.82	3.25	0.88	0.96	573	2.29

Fitting Parameters and Active Zone Depth for Wet Period

Station ID	R Square of Fitting	U_e (pF)	U₀ (pF)	n (cycles/year)	α (cm²/day)	Active Zone Depth (m)
ARD2	0.66	2.71	0.75	0.99	0.6	0.22
BOIS	0.54	3.28	0.58	0.56	0.8	0.31
BOWL	0.50	2.60	0.67	0.95	5.4	0.67
BREC	0.55	2.77	0.71	1.17	7.7	0.73
BURN	0.58	2.79	0.72	0.99	0.7	0.24
CENT	0.72	2.28	0.31	1.00	43.3	1.30
DURA	0.57	2.70	0.73	0.98	8.5	0.85
FAIR	0.59	2.67	0.67	1.35	3.2	0.43
GOOD	0.83	2.57	1.43	0.32	2.8	1.06
KETC	0.53	2.62	0.76	1.00	18.7	1.27
KING	0.77	3.26	1.40	0.29	0.3	0.34
LANE	0.62	2.24	0.32	0.98	284.9	3.42
MAYR	0.56	2.82	0.71	1.28	7.7	0.70
PAUL	0.72	2.39	0.49	0.98	11.2	0.83
WASH	0.55	2.32	0.30	0.95	100.9	1.99
WAUR	0.61	2.70	0.74	0.72	1.2	0.37
WOOD	0.62	2.81	0.68	1.17	0.2	0.11

Fitting Parameters and Active Zone Depth for Average Period

Station ID	R Square of Fitting	U _e (pF)	U ₀ (pF)	n (cycles/year)	α (cm ² /day)	Active Zone Depth (m)
ARD2	0.56	2.49	0.67	1.00	20	1.26
ARNE	0.71	2.08	0.70	0.50	3	0.70
BEAV	0.57	3.32	0.55	0.53	4	0.74
BOIS	0.76	1.84	2.09	0.19	15	3.63
BOWL	0.56	2.43	0.57	0.97	29	1.42
BREC	0.55	2.77	0.56	1.10	16	1.01
BUTL	0.77	1.86	1.15	0.38	3	1.02
CHER	0.86	3.21	0.83	0.51	1	0.51
CHEY	0.82	3.61	1.26	0.39	1	1.29
DURA	0.68	2.50	0.66	1.02	25	1.36
ELRE	0.52	2.48	0.55	1.10	40	1.55
ERIC	0.75	3.05	0.96	0.43	20	2.15
FTCB	0.52	2.86	0.82	1.07	22	1.36
HOBA	0.65	3.06	0.63	1.12	15	0.98
HOLL	0.68	2.83	0.85	1.08	64	2.36
KETC	0.61	2.48	0.69	1.02	18	1.18
KING	0.64	2.68	0.65	1.13	132	2.99
LANE	0.67	2.32	0.44	0.96	112	2.55
MAYR	0.76	2.88	0.97	0.43	6	1.15
MIAM	0.66	2.47	0.69	0.87	26	1.53
NEWK	0.61	3.10	0.82	0.67	79	3.26
NOWA	0.69	2.93	0.73	0.88	32	1.74
OILT	0.58	2.60	0.57	1.07	11	0.84
SHAW	0.71	2.60	0.82	0.99	29	1.63
STIG	0.61	2.57	0.49	0.96	112	2.65
TIPT	0.70	2.94	0.64	1.08	16	1.06
VINI	0.71	2.57	0.79	0.79	16	1.34
WAUR	0.55	2.42	0.64	1.01	11	0.93
WIST	0.78	2.63	0.78	0.91	74	2.67

Appendix D

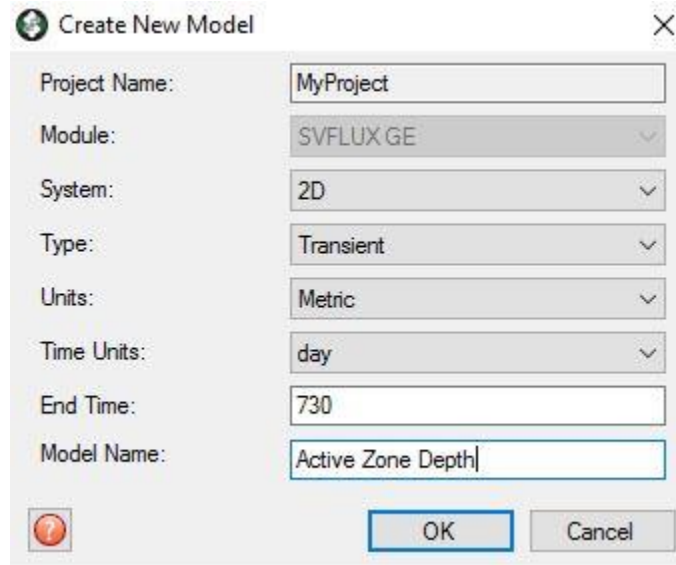
Input Parameters in SVFlux and Active Zone Depth for Dry Period

Station ID	θ_r	θ_s	α	n	K_s (cm/day)	Constant Head (m)	ET (mm/day)	Depth (m)
ARD2	0.065	0.424	0.072	1.22	1.9	7.84	4.08	4
ARNE	0.055	0.406	0.333	1.36	36.2	18.95	4.75	0.5
BEAV	0.079	0.406	0.48	1.45	29.3	18.57	5.34	0.5
BIXB	0.031	0.356	0.082	1.46	21.2	5.72	3.42	4
BREC	0.075	0.443	0.151	1.16	1.3	8.23	4.47	4.5
BUTL	0.073	0.417	0.154	1.22	3.4	15.58	5.11	3
CHER	0.03	0.401	0.343	1.38	28.8	15.23	4.30	0.5
CHEY	0.066	0.424	0.199	1.32	17.4	21.15	5.33	1
COPA	0.054	0.417	0.132	1.34	30.2	8.79	3.75	0.5
ELRE	0.073	0.401	0.202	1.21	3.6	8.43	4.49	3.5
EUFA	0.06	0.382	0.178	1.13	0.3	8.38	3.78	3.5
GOOD	0.075	0.471	0.58	1.69	54.9	10.33	5.50	0.5
HASK	0.061	0.423	0.093	1.39	11.1	9.05	3.50	1
HOBA	0.083	0.401	0.322	1.16	1.8	10.97	5.34	4
HOLL	0.072	0.414	0.175	1.19	4.7	7.51	5.01	3.5
KETC	0.061	0.411	0.069	1.23	2.2	11.39	4.65	3.5
LANE	0.018	0.339	0.108	1.45	25.2	4.28	3.53	0.5
MAYR	0.073	0.425	0.145	1.21	3.4	13.81	4.91	3.5
MIAM	0.081	0.509	0.028	1.35	5.6	6.97	3.45	2
NEWK	0.07	0.445	0.072	1.41	9	6.48	4.11	1.5
NOWA	0.072	0.448	0.057	1.39	6.5	11.49	3.54	2
NRMN	0.07	0.436	0.014	1.41	0.1	9.23	4.23	2
OILT	0.036	0.371	0.241	1.35	27.2	3.45	3.56	0.5
PAUL	0.041	0.386	0.1	1.42	14.8	4.21	3.85	1
PAWN	0.076	0.47	0.081	1.23	4.5	4.12	4.09	3
PORT	0.043	0.364	0.202	1.33	15.6	6.32	3.66	0.5
PUTN	0.043	0.419	0.109	1.43	16.8	9.28	4.91	1
SALL	0.064	0.403	0.019	1.64	1.6	3.09	3.26	4
SPEN	0.048	0.357	0.125	1.25	6.4	4.31	4.10	2.5
STIG	0.051	0.358	0.028	1.4	0.4	3.23	3.43	2.5
STIL	0.052	0.381	0.095	1.36	6.2	7.12	3.75	2.5
VINI	0.101	0.481	0.305	1.23	30.5	3.16	3.64	0.5
WALT	0.058	0.387	0.067	1.26	1	16.82	4.84	4.5
WAUR	0.034	0.351	0.318	1.35	34.3	5.75	4.45	0.5
WILB	0.094	0.513	0.232	1.23	40.2	10.36	3.62	0.5
WIST	0.082	0.514	0.111	1.22	20.3	13.53	3.19	0.5
WOOD	0.026	0.411	0.331	1.38	36.4	17.86	4.99	0.5

Appendix E

Screenshots of modeling steps:

1. Create the model

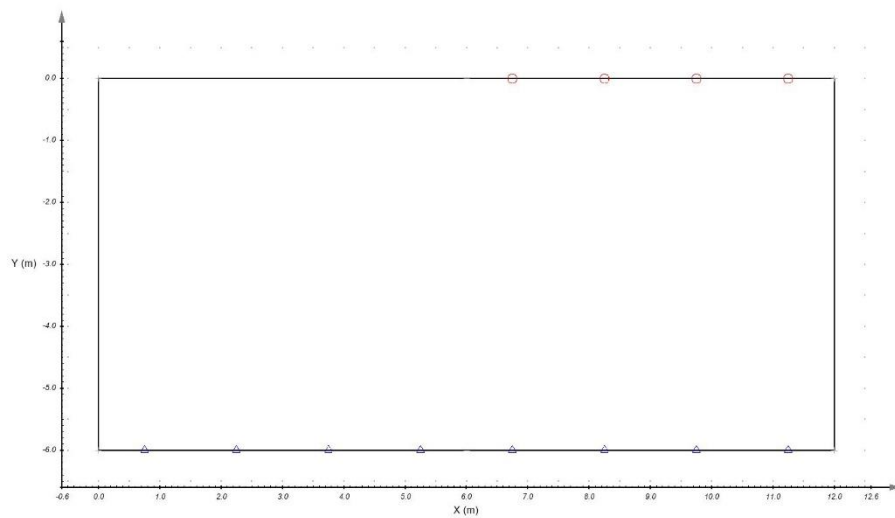


The screenshot shows a dialog box titled "Create New Model" with a close button (X) in the top right corner. The dialog contains several input fields and dropdown menus:

- Project Name: MyProject
- Module: SVFLUX GE
- System: 2D
- Type: Transient
- Units: Metric
- Time Units: day
- End Time: 730
- Model Name: Active Zone Depth

At the bottom left, there is a help icon (a red circle with a question mark). At the bottom right, there are two buttons: "OK" and "Cancel".

2. Define model geometry



3. Define material/soil properties

Material Properties: Unsaturated [X]

Material Name: Fill:

Volumetric Water Content | Hydraulic Conductivity

Saturated Conditions

Parameter	Value	Units
Saturated VWC:	0.351	
Specific Gravity, Gs:	2.650	

SWCC

Advanced

4. Define initial conditions

Initial Conditions - Head [X]

Scope:

Variable: kPa

Type:

Per Region

Constant

PWP: kPa

5. Define boundary conditions

Boundary Conditions [Close]

Region Name:

Boundary Conditions

	X	Y	Boundary Condition	Description	Boundary Name
▶	0.000	-6.000	Head Constant	-2.606 (m)	BN453573
	6.000	-6.000	Continue		
	12.000	-6.000	Zero Flux		BN409878
	12.000	0.000	Normal Flux Constant	-0.035 (m ³ /day/m ²)	BN195621
	6.000	0.000	Zero Flux		BN854143

Update Selected Segment (length = 6.000 m)

Boundary Condition:

Constant: Units: (m)

Boundary Name:

Show Boundary Condition Legend

6. Define model output

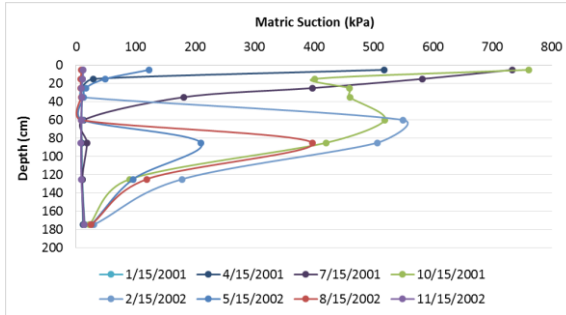
FlexPDE Plot Manager [Min] [Max] [Close]

Plots

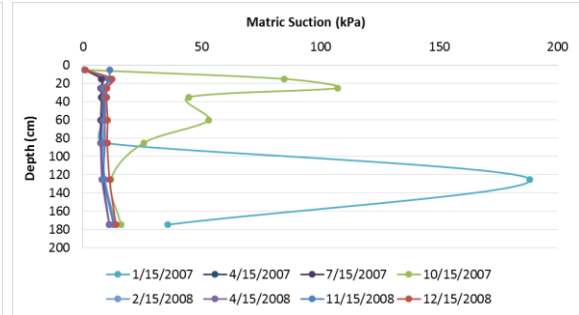
	Title	Variable	Restriction	Update Method	Solver Option	Group
	PWP	uw		t = from 0 by 73 to 730	Display	
	Matric Suction	um		t = from 0 by 73 to 730	Display	
	Pressure Head	hp		t = from 0 by 73 to 730	Display	
	Fluxes	flux,fluxy		t = from 0 by 73 to 730	Display	
	Initial PWP	uw0		at t = 0	Display	
	Initial Head	h0		at t = 0	Display	
	vwc	vwc		t = from 0 by 73 to 730	Display	
	XY Flux	flux,fluxy		t = from 0 by 73 to 730	Display	

Appendix F

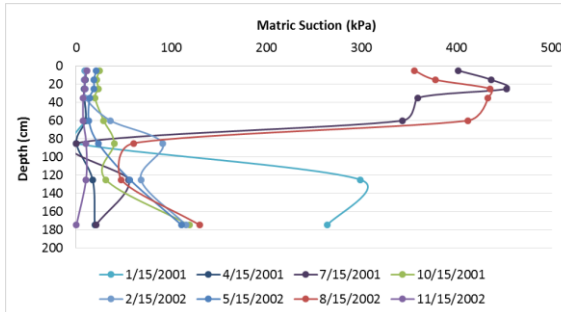
Matric suction profile for the ARM sites:



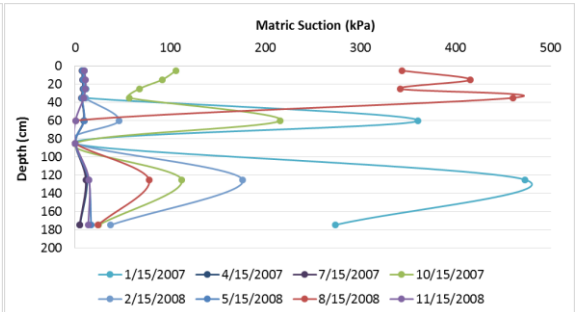
Ringwood 2001-2002



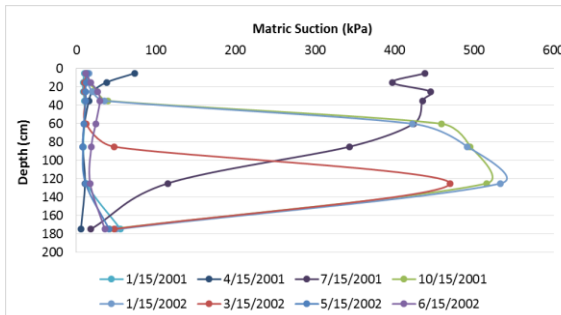
Ringwood 2007-2008



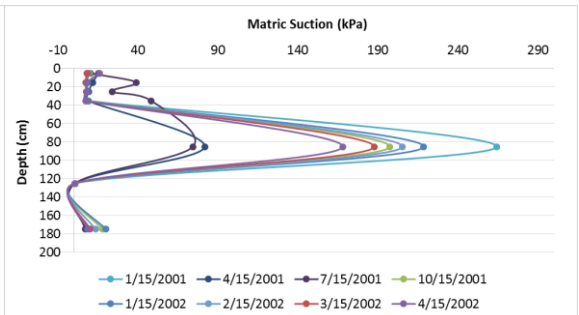
Vici 2001-2002



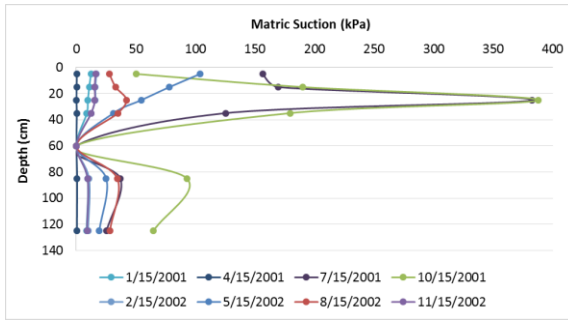
Vici 2007-2008



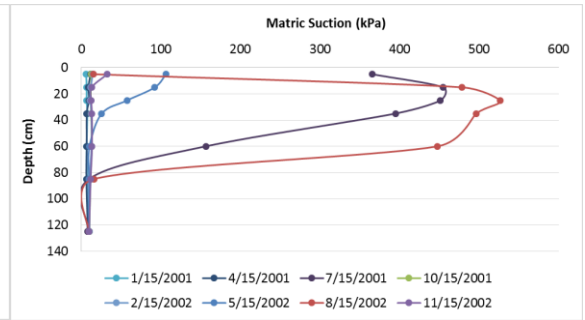
El Reno 2001-2002



Seminole 2001-2002



Cyril 2001-2002



Meeker 2001-2002

VITA

Er Yue

Candidate for the Degree of

Doctor of Philosophy

Thesis: SOIL MATRIC SUCTION AND ACTIVE ZONE DEPTH IN OKLAHOMA

Major Field: Civil Engineering

Biographical:

Education:

Completed the requirements for the Doctor of Philosophy in Civil Engineering at Oklahoma State University, Stillwater, Oklahoma in December 2016.

Completed the requirements for the Master of Science in Geography at Oklahoma State University, Stillwater, Oklahoma in December 2011.

Completed the requirements for the Bachelor of Science in Meteorology at Nanjing University of Information Science and Technology, Nanjing, Jiangsu, China in 2009.